宮 崎 大 学 大 学 院

博 士 学 位 論 文

Development of food functionality evaluation system and its applications

(食品機能性評価法の開発とその応用)

2015 年 3 月

宮崎大学大学院農学工学総合研究科

生物機能応用科学専攻

永濵　　清子

Table of Contents

Acknowledgements

I would like to express my sincere gratitude to my supervisor, Professor Masahito Suiko at University of Miyazaki for providing me this precious study opportunity, a valuable knowledge, guidance, continuous support, and warm encouragement throughout the study for my dissertation.

I especially would like to express my deepest appreciation to my supervisor, Associate Professor Nozomu Eto at University of Miyazaki for his elaborated guidance, considerable encouragement and invaluable discussion that make my research of great achievement and my study life unforgettable.

I wish to express my gratitude and appreciation to Professor Kunihito Yamamori at University of Miyazaki for providing computer program of artificial neural network, his valuable guidance and warm encouragement for my dissertation.

I wish to express great appreciation Professor Yoichi Sakakibara at University of Miyazaki for his valuable guidance and warm encouragement for my dissertation.

I am also grateful to Associate Professor Kazuo Nishiyama and Professor Emeritus Ikuo Yoshihara at University of Miyazaki for food functionality evaluation system study, Professor Yoh-ichi Matsushita and Associate Professor Kazuhiro Sugamoto at University of Miyazaki for analysis and fractionation of blueberry leaf, Professor Kazuhiro Morishita at University of Miyazaki for

providing HTLV-1-associated cell lines, Associate Professor Masao Yamasaki at University of Miyazaki for his expertise in flow cytometric analysis, Professor Noboru Murakami and Associate Professor Keiko Nakahara for animal experiment, Dr. Keiichi Fukui and Mr. Tomomi Kondoh at Miyazaki JA Food Research & Development Inc. for providing a lyophilized powder of Tamatama kumquat pericarp, and Dr. Takashi Ando and Ms. Miwa Satoh at Miyazaki Agricultural Research Institute for analysis of carotenoids.

I am very grateful to Dr. Asuka Uchida, Ms. Takako Taniguchi, Dr. Shohei Miyamoto, and Dr. Harish Kumar Madhyastha for their valuable cooperation in my experiments for food functionality evaluation system study and Mr. Tomofumi Shimojyo for study of kumquat pericarp *in vivo*.

I thank Dr. Michinori Kohara (The Tokyo Metropolitan Institute of Medical Science) for providing HCV replicon cells and Dr. Michiyuki Maeda (Kyoto University) and Dr. Naomichi Arima (Kagoshima University) for providing HTLV-1-associated cell lines.

This work was supported in part by Grant-in-Aid for Scientific Research of Priority Area from the Ministry of Education, Culture, Sports, Science and Technology of Japan, by a research fund from the Miyazaki Prefecture Collaboration of Regional Entities for the Advancement of Technological Excellence, JST, and by Miyazaki JA Food Research & Development Inc..

Finally, I am thankful to members of Eto laboratory at University of Miyazaki for their kind helps and encouragements during the doctoral course.

1

Abbreviations

ANN	: artificial neural network
ANOVA	: one-way analysis of variance
ARE	: antioxidant response element
ATLL	: adult T-cell leukemia/lymphoma
BBL	: blueberry leaf
BBL-HWE	: blueberry leaf hot water extracts
Bcl-2	: B-cell lymphoma 2
BITC	: benzyl isothiocyanate
*c*9, *t*11-CLA	: *cis*-9, *trans*-11 conjugated linoleic acid
calcein-AM	: calcein-acetoxymethyl
CDKs	: cyclin-dependent kinases
CLA	: conjugated linoleic acid
Conc.	: concentration
DHA	: docosahexaenoic acid
DMEM	: Dulbecco's modified Eagle's medium
DR	: death receptor
EGC	: epigallocatechin
EGCG	: epigallocatechin-3-gallate
ELISA	: enzyme-linked immunosorbent assay
ERK2	: extracellular signal-regulated kinase 2

EtOAc : ethyl acetate

FADD : Fas-associated death domain protein

FCS : fetal calf serum

GABA : gamma-aminobutyric acid

GAPDH : glyceraldehyde-3-phosphate dehydrogenase

HCC : hepatocellular carcinoma

HCV : hepatitis C virus

HPLC : high-performance liquid chromatography

Hsp70 : heat shock protein 70

Hsp90 : heat shock protein 90

HTLV-1 : human T-cell lymphotropic virus type 1

HW : hot water extract

IC50 : 50% inhibitory concentration

IFN : interferon

ILs : interleukins

KP : kumquat pericarp

KP-AF : kumquat pericarp acetone fraction

LU : lytic units

MAb : monoclonal antibody

MLR : multiple linear regression

MxA : IFN-inducible antiviral protein Mx

NK : natural killer

NQO1 : NAD(P)H dehydrogenase [quinone] 1

Nrf2 : nuclear factor erythroid 2-related factor 2

NT : not tested

OPA : oligomeric proanthocyanidin

p53 : tumor suppressor p53

PAb : polyclonal antibody

PARP : poly (ADP-ribose) polymerase

PBS : phosphate buffered saline

PSA : prostate-specific antigen

PUFA : polyunsaturated fatty acids

QSAR : quantitative structure-activity relationships

R^2 : coefficient of determination

RMSE : root mean square error

SD : standard deviation

SE : standard error

SLR : single linear regression

*t*10, *c*12-CLA : *trans*-10, *cis*-12 conjugated linoleic acid

tNOX : tumor-associated hydroquinone oxidase

TRAIL : tumor necrosis factor-related apoptosis-inducing ligand

TXNRD1 : thioredoxin reductase 1

XIAP : X-linked inhibitor of apoptosis protein

Abstract

Food functionalities have recently attracted the attention of researchers because foods have the potential to prevent disease and promote health. However, the evaluation of the numerous food functionalities consumes much time because it is necessary to conduct many individual experiments. To achieve this rapidly and cost effectively, the author has attempted to develop a new food functionality evaluation system that allows for simultaneous estimation of the multiple food functionalities from expression data of intracellular marker proteins using informatics.

To estimate three food functionalities, namely cancer cell growth suppression activity, antiviral activity, and antioxidative stress activity, each model was constructed using expression data of marker proteins as input data, and food functionalities as the output value. When prediction performances of three types of mathematical models constructed by simple, multiple regressions, or artificial neural network (ANN) were compared, the most adequate model was the one constructed using an ANN. There were no statistically significant differences between the actual data and estimated values calculated by the ANN models. Moreover, the author attempted to build the new ANN models for two food functionalities including human T-cell lymphotropic virus type 1 (HTLV-1)-infected cell growth suppression activity, and natural killer (NK) cell activation activity. As a result, there was no significant evidence to conclude that the actual data and the data from the ANN models differ. The ANN models could also estimate HTLV-1-infected cell growth suppression activity and NK cell activation activity with reasonable accuracy. Next, the author evaluated various natural products using our system as a first screening. Blueberry leaf (BBL) was found to have two food functionalities such as antiviral activity and HTLV-1-infected cell growth

suppression activity by the system at same time. In addition, the pericarp extracts of three citruses, such as bitter orange, hyuganatsu, and kumquat, were estimated to have NK cell activation activity. Among them, kumquat pericarp (KP) extracts had a strong NK cell activation activity. As applied examples, this study further focused on HTLV-1-infected cell growth suppression activity by BBL and NK cell activation activity by KP.

To clarify the active components responsible for the HTLV-1-infected cell growth suppression activity of BBL and the mechanism of action *in vitro*, BBL extract was fractionated into eight distinct fractions by Sephadex LH-20 column chromatography. Then, the author examined antiproliferative effect of each fraction on HTLV-1-infected cells MT2 and performed chemical analyses of the fractions. Moreover, effect of the most effective fraction on MT2 cells was analyzed by flow cytometry and Western blotting. The fraction contained highly oligomeric proanthocyanidin (OPA) with a mean degree of polymerization of 3.1. Cell growth suppression by the OPA fraction was significantly higher in all HTLV-1-infected cell lines than in MOLT-4, HTLV-1 negative T cell line. It inhibited the growth of MT2 cells by inducing caspase-dependent apoptosis through a death receptor-mediated pathway and G_2/M cell cycle arrest along with the down-regulation of cyclin B1 and cdc2. The BBL OPA fraction may be a source of novel compounds for reducing the risk of developing adult T-cell leukemia.

NK cell activation potential of KP and their constituents are not well characterized and the effect has not yet been verified *in vivo*. Therefore, the author attempted to validate the NK cell activation potential of KP *in vitro* and *in vivo*. The author first separated various fractions from KP using extraction with the pH-dependent organic solvent. Then, the effect of the KP fractions on NK cell activation was determined by the amount of IFN-γ production using human NK cell line, KHYG-1. Acetone fraction from KP (KP-AF) was found to have the strongest NK cell activation

activity and the thermolability. KP has shown to contain carotenoids, essential oil, and flavonoids. Among tested seven compounds, only β-cryptoxanthin exhibited the enhancement of IFN-γ production in KHYG-1. These results suggest that the NK cell activation effects of KP-AF from kumquat may be caused by carotenoids such as β-cryptoxanthin. The author examined whether orally administered KP-AF also enhanced the NK cell activation of restraint stress mice. Oral administration of KP-AF significantly improved the suppressed NK cytotoxic activity per a splenocyte in restraint stressed mice. These results suggest that oral administration of KP-AF enhance NK cytotoxic activity of splenocyte. NK cell activation effects of KP-AF were confirmed by both *in vivo* and *in vitro*.

In conclusion, the author developed a new food functionality evaluation system. The system was helpful in clarifying the active components and the mechanism of action *in vitro*. Additionally, estimated effects by the system were confirmed by *in vivo*. Furthermore, if more food functionalities can be presumed from the expression data of the marker proteins at the same time, it will be useful as a first screening method of food constituents for various beneficial purposes.

Introduction

Since ancient times, food has been known to be closely associated with medicine, appropriately summarized by the ancient Chinese saying "Medicine and food are isogenic".[1] Similarly, "Let food be thy medicine and medicine be thy food" is a well-known doctrine of Hippocrates (460–377 B.C.).[2] These ideas serve as the foundation for functional foods nowadays. Generally, food serves not only primary (nutritional) and secondary (sensory) functions such as providing taste, flavor, and texture but also serve tertiary (physiological) functions such as disease prevention and health promotion. However, the tertiary function of food (food functionality) has only recently attracted researchers' attention.

The potential of food for disease prevention is supported by several reports including a prospective cohort study in Japan, where the consumption of fruits was associated with a lower risk of cardiovascular disease[3] and a higher intake of fruits and vegetables was associated with a dose-dependent decrease in the risk of esophageal squamous cell carcinoma.[4] In another epidemiologic study, the effect of the intake of fruit and vegetables on cancer risk was assessed using a meta-analytic approach to evaluate evidence from a case-control and a prospective study, which suggested a protective effect of both fruits and vegetables towards reducing the risk of cancer.[5] Moreover, fruits and vegetables are rich in polyphenols, and their effects on the prevention of various diseases are widely supported by the findings of epidemiological studies, experimental studies on animals or cultured human cell lines, and clinical studies.[6]

Several functions of food should be evaluated, for example, antioxidative activity,[7, 8] antimutagenic activity,[9-11] and cancer cell growth suppression activity.[12-14] In addition, some natural products have multiple functions. For instance, catechins contained in tea are known to possess

multiple functions including prevention of cancer[15] and cardiovascular disease,[16] antioxidant or pro-oxidant activities,[17] and anti-obesity, antidiabetic,[18] and anti-inflammatory effects.[19] Thus, while investigating food constituents for their potential functional effects, optimal approaches should include the ability to screen multiple effects simultaneously, thus saving both time and labor. Moreover, the use of such approaches might reduce the risk of overlooking these different useful effects due to screening methods that assess only a specific food functionality.

In drug discovery, identification of new drug candidates employs the use of *in vitro* assays such as cell-based assays,[20] as well as *in silico* assays such as computational methods.[21-24] *In silico* assays are useful for the assessment of pharmacokinetics, toxicity, and pharmacological effects. They are also beneficial in shortlisting the number of compounds that need to be subjected to chemical assays, thus saving time and money. Computational approaches such as analysis of quantitative structure-activity relationships (QSAR)[25, 26] and artificial neural networks (ANN)[27, 28] have been applied to identify foods with a single functionality on a specific target molecule. Therefore, *in silico* assays such as computational mathematical models might also be applied for the evaluation of food functionalities in food science. Moreover, the assays might increase the efficiency of functional food development and food science research.

In this study, we have attempted to evaluate multiple food functionalities by a unified experimental system using a computational method. A conceptual diagram of the unified experimental system is shown in **Figure 1**. Computational mathematical models need information to express some characteristics of the test compound, namely, a feature quantity. In our concept, food functionality data (e.g., direct data on the suppression of hepatitis C virus (HCV) replication) was mathematized into an equation using the feature quantity. Similarly, another set of food functionality data (e.g., direct data on the enhancement of cellular cytotoxicity) was also

mathematized into an equation by using the same feature quantity. Additionally, when the feature quantity can be used as common data among multiple food functionalities, activities of the food functionalities can be estimated simultaneously, using the same feature quantity. In the QSAR model, biological activity is mathematized into an equation by quantitative correlation with the chemical structure. However, it is impossible to estimate the food functionalities of natural food products by evaluating the chemical structure because these products contain a mixture of numerous food constituents. Therefore, the expression data of marker proteins in the cell that responded to stimulation by a compound were utilized as the feature quantity in this study. Even if the information about the chemical structure of the compound is unclear, the expression data of marker proteins in the cells can be quantified by the information of a compound influencing the cells.

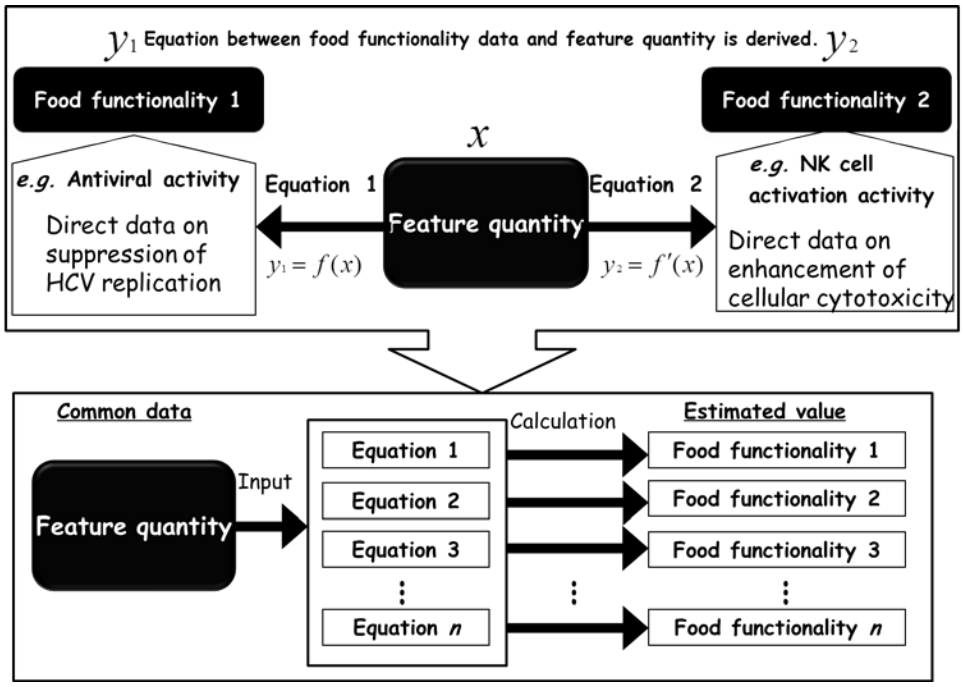

Figure1. Conceptual diagram of the unified experimental system for the estimation of food functionality.

Our food functionality evaluation system enabled us to estimate five food functionalities (e.g., cancer cell growth suppression activity, antiviral activity, antioxidative stress activity, human T-cell lymphotropic virus type 1 (HTLV-1)-infected cell growth suppression activity, and natural killer (NK) cell activation activity) simultaneously.

Cancer cell growth suppression activity was evaluated by a cell proliferation assay using the human hepatocellular carcinoma cell line HepG2. According to the World Health Organization, liver cancer is one of the major causes of death worldwide, accounting for 746,000 deaths per year in 2012 (http://globocan.iarc.fr/Pages/fact_sheets_cancer.aspx). Hepatocellular carcinoma (HCC) is the most common type of primary liver cancer. The main risk factors are hepatic viral infection (e.g., hepatitis B and C virus), aflatoxin exposure, tobacco smoking, alcohol consumption, obesity, and diabetes.[29] Chemopreventive properties of natural products and food constituents against liver cancer or HCC have been reported in a vast number of studies. In Japan, Public Health Center-based prospective study reported that high consumption of n-3 polyunsaturated fatty acids (PUFAs) found in fish,[30] coffee,[31] and vegetables containing α- and β-carotene[32] is positively associated with reduced risk of liver cancer. Moreover, many phytochemicals such as plant polyphenols and dietary antioxidants have shown chemopreventive properties against HCC or liver cancer in several *in vitro*[33-36] and *in vivo* studies.[34, 36, 37]

Antiviral activity was determined by measuring the impact on suppression of HCV replication using a HCV subgenomic replicon system.[38] HCV, a member of the *Flaviviridae* family of enveloped positive-strand RNA viruses, is the main cause of liver fibrosis and cirrhosis, which in turn results in HCC in a significant number of patients.[39] Approximately 130-170 million people worldwide are chronically infected with HCV.[39] Until a HCV subgenomic replicon system was developed in 1999,[40] the development of anti-HCV reagents was hampered for lack of an efficient

cell culture system to evaluate HCV RNA replication. Recent studies have reported that HCV RNA replication was inhibited by some constituents or extracts of natural products, such as β-carotene,[41] vitamin D_2,[41] linoleic acid,[41] curcumin,[42] silibinin A and B,[43] quercetin,[44] (+)-epicatechin,[45] (-)-epicatechin,[45] caffeic acid n-octyl ester,[46] arachidonic acid,[47] docosahexaenoic acid,[47] eicosapentaenoic acid,[47] procyanidin B1 from Cinnamomi cortex,[48] proanthocyanidin from rabbit-eye blueberry leaves,[49] pheophorbide a and pyropheophorbide a from *Morinda citrifolia* leaves,[50] and lucidone from *Lindera erythrocarpa* Makino fruits.[51]

Antioxidative stress activity was evaluated based on induction of antioxidant response element (ARE)-mediated gene expression using a reporter assay.[52] The nuclear factor erythroid 2-related factor 2 (Nrf2)/ARE pathway plays an important role in the cellular antioxidant defense against endogenous and exogenous stresses caused by reactive oxygen species and electrophiles.[53] The transcription factor Nrf2 induces the expression of antioxidant and phase II enzymes that protect the cell from oxidative damage (e.g., heme oxygenase1, NAD(P)H:quinone oxidoreductase-1, and glutathione S-transferases) by binding to the ARE region of the gene promoter.[53] Recent studies using the ARE-luciferase reporter cells have reported that ARE-mediated gene expression was induced by food constituents and extracts such as benzyl isothiocyanate,[52] quercetin,[52, 54] kaempferol,[52, 54] fisetin,[52] luteolin,[52] myricetin,[52] naringenin,[54] (−)-epigallocatechin-3-gallate,[55] (−)-epicatechin-3-gallate,[55] cafestol,[56] and tomato extracts.[54]

HTLV-1-infected cell growth suppression activity was evaluated by a cell proliferation assay using HTLV-1-infected T-cells MT2. Adult T-cell leukemia/lymphoma (ATLL) is an aggressive malignant disease caused by clonal proliferation of HTLV-1-infected mature $CD4^+$ cells.[57] Currently, an estimated 10-20 million people worldwide are infected with HTLV-1. The vast majority of these infected people remain clinically asymptomatic, whereas 2–5% of the infected

patients develop ATLL after a very long latency period, lasting at least 20–30 years.[57] Despite the availability of various combination chemotherapy regimens, patients with aggressive ATLL such as those with acute lymphoma, have a poor prognosis after ATLL development, with a median survival time of less than 13 months. Currently, the known therapies for ATLL are not very effective. Therefore, it is important to identify appropriate therapies that are more effective in preventing the development of ATLL and/or prolonging the patient's survival after ATLL development. As ATLL develops over time, daily diet might play an important role in ATLL development. Natural products, including some foods and herbal medicines, have recently attracted attention as potential therapeutics because of their general benefits including lower toxicities and lower costs compared with those of regular drugs. Epidemiological studies suggest dietary intake of flavonoids, compounds naturally present in many foods, might reduce the risk of tumors of the breast, colon, lung, prostate, and pancreas.[58] Recent studies have reported that proliferation of HTLV-1-associated cell lines was inhibited by some constituents and extracts of natural products, such as curcumin,[59] genistein,[60] soy-isoflavones,[61] brown algae fucoxanthin,[62] fucoidan extracts,[63] and *Bidens pilosa*.[64]

NK cell activation activity was determined by interferon (IFN)-γ production using human NK cell line, KHYG-1. NK cells play an important role in innate immune response, such as preventing growth of certain virally-infected cells in the early stage of host defense, and elimination of tumor target cells.[65, 66] NK cells are activated by both direct and indirect modulation of cytokines, such as IFN and interleukins (ILs), to kill the target cells.[67] Decrease in NK activity is likely to be associated with increased cancer risk[68] and certain infectious disease outcomes,[69] therefore enhanced NK activity is beneficial for maintaining good health. Probiotics,[70] ginseng polysaccharide,[71] β-carotene[72] and oligonol[73] have all been shown to enhance NK activity in human

subjects. *In vivo* experiments with various foods (*e.g.*, *Lactobacillus acidophilus*[74] and β-glucan from maitake mushrooms[75]) on viral infection and tumor-bearing mouse models have shown reduced disease risk by enhancing NK activity.

In chapter I, the author has explained the development of the food functionality evaluation system for five food functionalities. In chapter II, the author has focused on the molecular mechanism responsible for the antiproliferative effect of blueberry leaf constituents on HTLV-1-infected cells. Finally, the effects of kumquat pericarp on NK cell activity *in vitro* and *in vivo* are discussed in chapter III.

Chapter I

An efficient approach for simultaneous estimation of the multiple food functionalities

Food functionalities are being evaluated actively in the recent decade. The method to evaluate food functionality has three steps. The first step is *in vitro* assay using cultured cell lines. The second step is *in vivo* assay using mice or rats. The third step is a clinical trial to demonstrate the effect in human. Generally, as for first screening, *in vitro* assay by cells is often chosen. However, the evaluation of the numerous food functionalities consumes much time because it is necessary to conduct many individual experiments. To achieve this rapidly and cost effectively, a new screening system using an *in silico* assay is proposed to evaluate multiple food functionality simultaneously.

Experimental Procedures

Food constituents, drugs, and food extracts. The tested food constituents were as follows: lipoic acid, curcumin, resveratrol, epigallocatechin-3-gallate (EGCG), arachidonic acid, epigallocatechin (EGC), kaempferol, chlorogenic acid, galangin, linoleic acid, and astaxanthin (Sigma-Aldrich Co., St. Louis, MO), glycitein, quercetin, gamma-aminobutyric acid (GABA), and capsaicin (Wako Pure Chemical Industries, Ltd., Osaka, Japan), *cis*-9, *trans*-11 conjugated linoleic acid (CLA), and *trans*-10, *cis*-12 CLA (Cayman Chemical Co., Ann Arbor, MI), cyanidin, pelargonidin, and delphinidin (Extrasynthèse, Genay, France), genistein (Wako Chemicals, USA, Inc., Dallas, TX), daidzein (Fujicco Co., Ltd., Kobe, Japan), rosmarinic acid (MP Biomedicals, Inc., Irvine, CA), benzyl isothiocyanate (BITC) (Tokyo Chemical Industry Co., Ltd., Tokyo, Japan), beta-carotene and *dl*-alpha-tocopherol (LKT Laboratories, St. Paul, MN), docosahexaenoic acid (DHA) (Nu-Chek-Prep, Elysian, MN), and caffeine (Latoxan, Rosans, France). The tested drugs were as follows: simvastatin, lovastatin, and pravastatin (Wako Pure Chemical Industries, Ltd.), fluvastatin, and atorvastatin (Toronto Research Chemicals, Inc., North York, Canada), ribavirin (MP Biomedicals, Inc.), and interferon-alpha 2b (Prospec-Tany Technogene Ltd, Rehovot, Israel). Edible plants collected in Miyazaki, Japan were as follows: leaves and roots of Japanese radish (*Raphanus sativus*), roots of burdock (*Arctium lappa*), leaves of carrot (*Daucus carota*), onion (*Allium cepa* L.), komatsuna (*Brassica rapa* L var. peruviridis), suioh (*Ipomoea batatas* L.), spearmint (*Mentha spicata*), rosemary (*Rosmarinus officinalis*), lemon balm (*Melissa officinalis*), stevia (*Stevia rebaudiana*), sweet basil (*Ocimum basilicum*), green tea (*Camellia sinensis*), and blueberry (*Vaccinium virgatum*), placenta of bitter gourd (*Momordica charantia* L.), whole beans of soybean

(*Glycine max*), flower of chamomile (*Chamaemelum nobile*), bitter orange (*Citrus aurantium*), hyuganatsu (*Citrus tamurana* hort. ex Tanaka), and kumquat (*Fortunella crassifolia*). Each sample of lyophilized powder (1 g) was extracted by vortexing for 30 seconds with 80% ethanol (30 mL), whereas blueberry leaves powder was extracted with 80% ethanol or hot water. The extracts were filtered through filter paper (filter paper No. 2, Toyo, Tokyo, Japan), concentrated with a vacuum evaporator, and completely dried with a freeze drier. The lyophilized extracts were redissolved in dimethyl sulfoxide.

Cells. The human hepatocellular carcinoma cells HepG2 (purchased from the Japan Cancer Research Resources Bank, Osaka, Japan) were maintained in Dulbecco's modified Eagle's medium (DMEM) (Sigma-Aldrich Co.) supplemented with 10% fetal calf serum (FCS) and penicillin-streptomycin (100 U/mL penicillin and 100 μg/mL streptomycin) (Sigma-Aldrich Co.). HCV replicon cells (kindly provided by Dr. Michinori Kohara, Tokyo Metropolitan Institute of Medical Science, Japan), human hepatoma HuH-7 cells carrying a HCV subgenomic replicon derived from the genotype 1b isolate Con1,[38] were maintained in DMEM supplemented with Glutamax (Invitrogen, Carlsbad, CA), 10% FCS, penicillin-streptomycin (100 U/mL penicillin and 100 μg/mL streptomycin) (Invitrogen) and 500 μg/ml of G418 (Invitrogen). HepG2/ARE cells, in which a luciferase-based ARE reporter construct derived from human NAD(P)H dehydrogenase [quinone] 1 (NQO1) was stably transfected, were established by modifications of the method of Boerboom et al..[52] The cells were maintained in DMEM (Sigma-Aldrich Co.) supplemented with 10% FCS, penicillin-streptomycin (100 U/mL penicillin and 100 μg/mL streptomycin) (Sigma-Aldrich Co.), and 500 μg/mL of G418 (Sigma-Aldrich Co.). HTLV-1-infected T-cells MT2 (obtained from the Fujisaki Cell Center, Hayashibara Biochemical Laboratories, Okayama, Japan) were established from HTLV-1-transformed umbilical cord blood T-cell lines.[76] MT2 cells were cultured in RPMI

1640 medium (Sigma-Aldrich Co.) supplemented with 10% fetal calf serum and penicillin-streptomycin (100 U/mL penicillin and 100 μg/mL streptomycin) (Sigma-Aldrich Co.). The human natural killer cells KHYG-1 were obtained from the Japanese Collection of Research Bioresources (JCRB, Osaka, Japan) and maintained in RPMI 1640 medium (Wako) supplemented with 10% fetal calf serum, penicillin-streptomycin (100 U/mL penicillin and 100 μg/mL streptomycin) (Wako), and 100 U/mL interleukin-2 (Wako). All cells were maintained in a humidified atmosphere containing 5% CO_2 at 37°C.

Measurement of the expression levels of marker proteins. HepG2 cells were seeded into 100 mm tissue culture dishes at 3×10^6 cells/dish and incubated for 24 h. Subsequently, the medium was replaced with one containing a food constituent or extract. After exposure for 24 h, cells were washed with cold phosphate buffered saline (PBS), solubilized with ice-cold lysis buffer (1 m mol/L EDTA, 0.005% Tween 20 and 0.5% Triton-X-100 in PBS) containing protease inhibitor cocktail (Roche, Basel, Switzerland). The protein concentrations of the cell lysates were measured by DC protein assay (Bio-Rad Laboratories, Hercules, CA) and then the sample was set to 1 mg/mL. Then, the fourteen kinds of marker proteins were measured by sandwich enzyme-linked immunosorbent assay (ELISA) to detect the intracellular response generated by the food constituent or extract. Measured proteins were as follows: thioredoxin, survivin, heat shock protein 70 (Hsp70), X-linked inhibitor of apoptosis protein (XIAP), Fas-associated death domain protein (FADD), thioredoxin reductase 1 (TXNRD1), heat shock protein 90 (Hsp90), IFN-inducible antiviral protein Mx (MxA), tumor-associated hydroquinone oxidase (tNOX), NQO1, tumor suppressor p53 (p53), extracellular signal-regulated kinase 2 (ERK2), B-cell lymphoma 2 (Bcl-2), and glyceraldehyde-3-phosphate dehydrogenase (GAPDH). **Table I-1** shows the kits or combinations of antibodies used in sandwich ELISA to detect each marker protein. Microtiter plates (96 well) were coated with 100

μL of capture antibody in 50 mmol/L carbonate buffer (pH 9.6) and incubated overnight at 4°C. The plates were blocked with 300 μL of 5% skim milk in PBS and incubated overnight at 4°C. Subsequently, the cell lysates (100 μL) were added into each well and incubated for 2 h at 37°C. All of the cell lysates were analyzed in duplicate. The plates were incubated with 100 μL of detection antibody for 1 h at 37°C, followed by incubation with a secondary antibody. The peroxidase reaction was initiated by the addition of 100 μL of substrate solution, [0.1 mol/L citrate buffer (pH 4.0) containing 0.03% H_2O_2, and 0.3 mg/mL 2,2'-azino-bis(3-ethylbenzothiazoline-6-sulfonic acid) (Wako)]. After 10 min, the absorbance was measured at 405 and 490 nm with a multichannel microtiter plate reader (Vmax; Molecular Devices, Redwood City, CA). ELISA data were normalized by comparison with the absorbance of GAPDH. The relative marker protein expression level was represented by a relative value in comparison with the control.

Table I-1. List of Antibodies used for ELISA

Marker Protein	Capture Antibody	Detection Antibody	Secondary Antibody
thioredoxin	mouse MAb[a] (Serotec, Oxford, UK)	goat PAb[b] (R&D systems Inc., Minneapolis, MN)	mouse PAb, peroxidase conjugated (Pierce, Rockford, IL)
survivin	mouse MAb (established)	goat PAb (R&D systems Inc.)	mouse PAb, peroxidase conjugated (Pierce)
FADD	rabbit PAb (USBiological, Swampscott, MA)	mouse MAb (BD Transduction Lab.)	goat PAb, peroxidase conjugated (ICN Pharmaceuticals Inc., Aurora, Oh.)
TXNRD1	rabbit PAb (LabFrontier, Seoul, Korea)	mouse MAb (Abcam Ltd., Cambridge, UK)	goat PAb, peroxidase conjugated (ICN Pharmaceuticals Inc.)
Hsp90	mouse MAb (BD Transduction Lab., San Diego, Calif.)	goat PAb (Santa Cruz Biotechnology, Santa Cruz, CA)	mouse PAb, peroxidase conjugated (Pierce)
MxA	mouse MAb (KYOWA MEDEX Co.,Ltd., Tokyo, Japan)	biotinylated mouse MAb (established)	streptavidin, peroxidase conjugated (GE Healthcare Biosciences, Little Chalfont, UK)
tNOX	mouse MAb (established)	biotinylated mouse MAb (established)	streptavidin, peroxidase conjugated (GE Healthcare Biosciences)
NQO1	mouse MAb (Abnova, Taipei, Taiwan)	goat PAb (IMGENEX Co., San. Diego, CA)	mouse PAb, peroxidase conjugated (Pierce)
Hsp70	Duoset IC kit (R&D systems Inc.)		
XIAP	Duoset IC kit (R&D systems Inc.)		
ERK2	Duoset IC kit (R&D systems Inc.)		
p53	Duoset IC kit (R&D systems Inc.)		
Bcl-2	Duoset IC kit (R&D systems Inc.)		
GAPDH	Whole-cell Normalization kit (Active Motif, Carlsbad, CA)		

[a] Mab, monoclonal antibody. [b] PAb, polyclonal antibody. This table was cited from previously described study.[77]

Determination of cancer cell growth suppression activity. Cancer cell growth suppression activities for food constituents and extracts were determined by a cell proliferation assay. HepG2

cells were inoculated into a 96-well microtiter plate (Corning) at 1×10^4 cells/well, and cultured for 24 h. The cells were incubated in the presence or absence of food constituents or extracts. After 48 h of incubation, the cell survival rate was measured by the WST-8 [2-(2-methoxy-4-nitrophenyl)-3-(4-nitrophenyl)-5-(2,4-disulfophenyl)-2H-tetrazolium, monosodium salt] cell-counting kit (Dojindo, Kumamoto, Japan) according to the manufacturer's protocol. The WST-8 assay is based on a water soluble formazan reaction occurred only in viable cells.[78] Cancer cell growth suppression activity was calculated by using the following equation: Cancer cell proliferation rate = (absorbance of test)/(absorbance of control). The absorbance in the microplate wells was measured at 450 nm with a multichannel microtiter plate reader (Vmax; Molecular Devices).

Measurement of antiviral activity. Antiviral activity was evaluated by measuring the impact on suppression of HCV replication using a HCV subgenomic replicon system.[38] The HCV replicon cells in DMEM supplemented with Glutamax and 5% FCS (5×10^3 cells/well) were plated in 96-well plates and were cultured for 24 h. Then, the cells were treated with each food constituent or extract for 72 h. HCV replicon levels were determined by the luciferase reporter assay and cell proliferation rate were determined by the WST-8 assay. The luciferase activity was quantified using the Steady-Glo luciferase assay system (Promega, Madison, WI) according to the manufacturer's protocol, and the luminescence was measured by the DTX 800 Multimode Detector (Beckman Coulter, Fullerton, CA). The relative luciferase activity was represented by the relative value in comparison with the control. Antiviral activity was defined as follows: Viral replication rate = (relative luciferase activity)/(cell proliferation rate).

Determination of antioxidative stress activity. Antioxidative stress activity was evaluated by induction of ARE-mediated gene expression using a reporter assay.[52] The HepG2/ARE cells were inoculated into 96-well plates at 4×10^4 cells/well. After 24 h incubation, the cells were treated with

each food constituent or extract for 24 h. The luciferase activity was quantified using the Bright-Glo luciferase assay system (Promega) according to the manufacturer's protocol, and the luminescence was measured by using a multiplate reader (GENios, Tecan Japan Co. Ltd., Japan). Luciferase activity and cell proliferation rate were calculated by the same method as for antiviral activity. Antioxidative stress activity was calculated as follows: ARE-luciferase activity rate = (relative luciferase activity)/(cell proliferation rate).

Determination of HTLV-1-infected cell growth suppression activity. HTLV-1-infected cell growth suppression activity was determined by a cell proliferation assay using HTLV-1-infected cells MT2. The effect of food constituents and extracts on cell growth was also examined by the WST-8 cell-counting kit (Dojindo). Briefly, cells were inoculated into a 96-well microtiter plate at 9×10^3 cells/well, and cultured for 24 h. The cells were treated with various concentrations of food constituents or extracts or vehicle control (dimethyl sulfoxide). After 72 h of incubation, WST-8 (10 μL) was added for 4 h of incubation, and the absorbance was measured at 450 nm with a reference wavelength of 650 nm using a multichannel microtiter plate reader (Emax; Molecular Devices, Redwood City, CA, USA). HTLV-1-infected cell growth suppression activity was calculated by using the following equation: MT2 cell proliferation rate = (absorbance of test)/(absorbance of control).

Determination of NK cell activation activity. NK cell activation activities for food constituents and extracts were determined by the amount of IFN-γ production using human NK cell line, KHYG-1 cells. Cells were inoculated into a 48-well microtiter plate at 6×10^4 cells/well, and treated with each food constituent or extract or vehicle control (dimethyl sulfoxide). After 24 h of incubation, the culture medium was centrifuged at 180 × *g* for 5 min to remove the cells. IFN-γ levels in the

supernatants were determined by Human IFN- γ ELISA Development Kit (PeproTech, Rocky Hill, NJ, USA) according to the manufacturer's instructions. NK cell activation activity was calculated by using the following equation: relative IFN-γ production = (amount of IFN-γ production for test)/(amount of IFN-γ production for control).

Design of the evaluation system. A conceptual diagram of the evaluation system is shown in **Figure I-1**. Three effects were chosen to estimate three food functionalities of the food constituents, namely cancer cell growth suppression activity, antiviral activity, and antioxidative stress activity. Mathematically, these estimations were carried out by single linear regression (SLR), multiple linear regression (MLR), or using an ANN as the non-linear model.

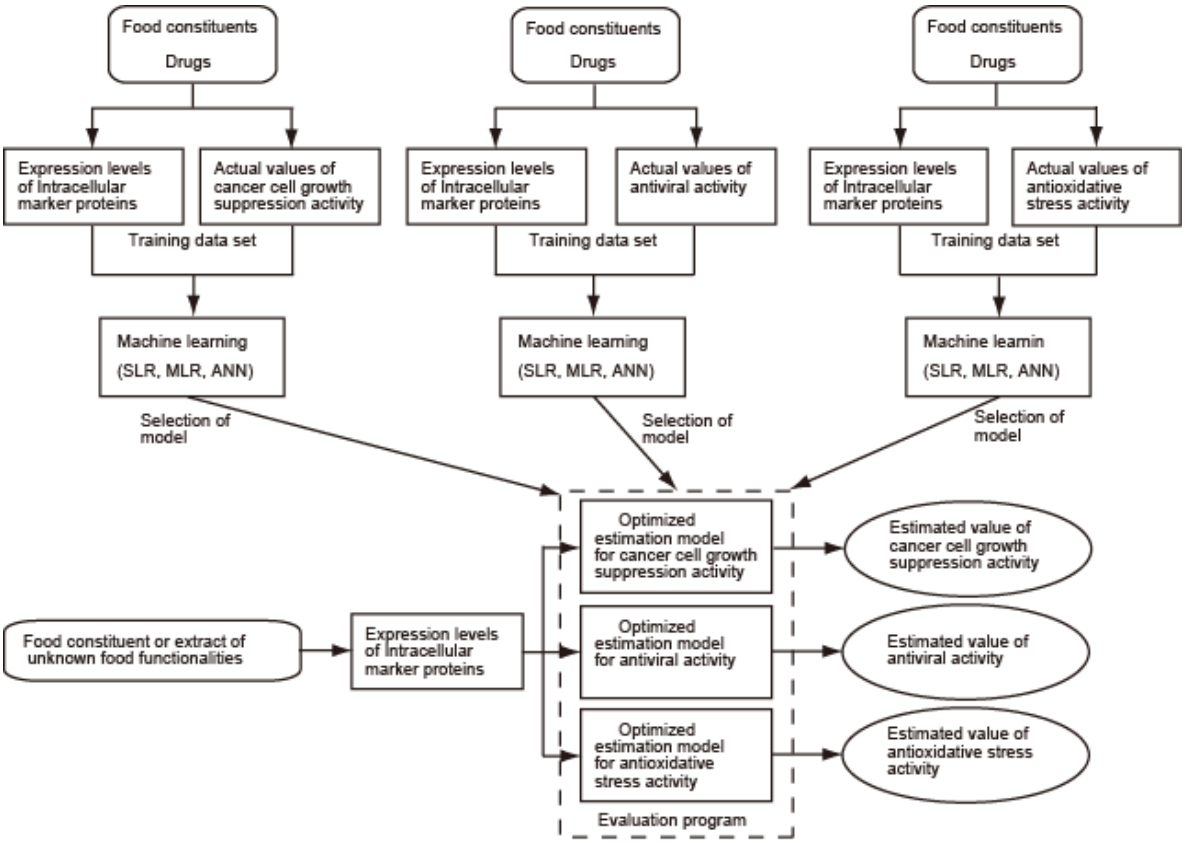

Figure I-1. Conceptual diagram of the evaluation system to estimate plural food functionalities of food constituents from expression levels of intracellular marker proteins. Training data sets were collected on activity values of food functionality and expression level of intracellular proteins by using the same food constituents. Then estimation models were constructed using food functionality as the dependent variable or output value, and relative expression of thirteen kinds of marker proteins as independent variables or input values. Subsequently, the optimized model was selected in all of the built models. Finally, activity values of plural food functionalities can be estimated simultaneously from the expression data of marker proteins by the evaluation system. This figure was modified from previously described figure.[77]

Table I-2. Training data set 1: Marker protein expression rate and experimental values of food functionalities used to build the models

Compounds	Conc	marker protein expression rate													food functionality				
	μmol/L	1[a]	2[b]	3[c]	4[d]	5[e]	6[f]	7[g]	8[h]	9[i]	10[j]	11[k]	12[l]	13[m]	A[n]	B[o]	C[p]	D[q]	E[r]
Lipoic acid	100	0.613	0.664	0.720	0.592	0.496	0.696	0.580	0.667	0.428	0.565	0.679	0.628	0.626	0.990	0.8957	0.834	1.112	NT[s]
	300	0.707	0.630	0.772	0.675	0.447	0.896	0.572	0.836	0.500	0.763	0.736	0.625	0.696	1.041	0.4827	1.251	1.291	NT
	1000	0.966	0.627	0.773	0.999	0.594	1.164	0.699	1.300	1.310	1.460	0.850	0.691	1.009	0.998	0.1178	2.711	1.048	NT
EGCG	7	0.878	0.881	0.723	0.768	0.872	0.781	0.714	0.771	0.569	0.967	0.925	0.743	0.762	0.944	1.3515	0.630	1.048	0.385
	9	0.932	1.061	0.897	0.855	0.784	0.921	0.831	0.835	0.846	0.975	0.896	0.872	0.864	NT	NT	NT	1.083	0.287
	20	0.882	0.734	0.589	0.656	0.671	0.694	0.399	0.622	0.446	0.902	0.868	0.609	0.625	0.905	0.9307	0.740	0.959	NT
	50	1.605	1.119	0.731	1.207	1.008	0.968	0.614	1.070	1.047	1.475	1.300	0.974	0.990	0.870	0.0354	0.672	1.068	NT
Daidzein	25	0.632	0.627	0.712	0.654	1.121	0.973	0.481	0.672	0.519	0.689	0.735	0.674	0.665	0.958	1.1245	2.891	1.056	1.905
	50	0.528	0.552	0.627	0.577	0.879	1.217	0.514	0.707	0.594	0.848	0.803	0.755	0.702	0.906	1.0149	2.519	0.951	0.939
	150	0.737	0.531	0.717	0.830	0.968	1.153	0.571	0.748	0.717	0.945	0.858	0.942	0.868	0.832	0.5375	1.806	0.429	NT
Glycitein	10	0.882	0.932	0.821	0.871	1.016	0.935	0.788	0.856	0.555	1.004	0.968	0.820	0.962	1.086	0.8283	0.995	1.135	1.160
	30	0.888	0.739	0.684	0.935	1.256	0.834	0.796	0.788	0.433	0.929	0.954	0.720	0.939	1.044	1.1602	1.476	1.176	0.729
	50	1.027	1.132	0.907	1.007	0.873	0.994	0.877	0.949	1.048	1.103	0.954	0.987	0.979	NT	NT	NT	1.033	NT
	100	1.652	0.604	0.802	1.343	1.850	0.773	0.679	1.082	0.759	1.129	1.242	1.029	1.379	0.966	0.9859	1.801	0.931	1.196
Quercetin	5	0.844	0.956	0.834	0.780	1.136	0.908	1.109	0.824	0.686	0.922	0.884	0.853	0.838	1.109	0.9532	0.860	0.925	1.125
	15	0.917	0.871	0.741	0.725	0.870	0.810	1.127	0.783	0.757	0.920	0.878	0.843	0.823	1.063	NT	0.733	0.616	1.354
	60	1.417	1.158	0.674	0.808	0.989	0.604	0.629	0.761	0.873	1.019	0.935	0.980	0.686	0.904	0.4172	2.871	0.228	NT
Cyanidin	40	0.633	0.749	0.847	0.726	1.134	0.891	0.600	0.742	0.640	0.744	0.798	0.833	0.784	0.983	1.2056	0.538	0.791	0.045
	150	0.536	0.738	0.673	0.658	0.903	0.683	0.459	0.678	0.632	0.854	0.879	0.856	0.739	0.822	0.0391	0.450	0.606	NT
	400	0.598	0.776	0.784	0.669	0.884	0.797	0.633	0.820	0.631	0.720	0.836	1.094	0.854	0.451	NT	0.538	0.372	NT
Pelargonidin	100	0.784	0.853	0.983	0.848	1.085	0.916	0.909	0.820	0.529	1.069	0.984	0.756	0.913	1.000	0.7858	0.402	0.898	0.679
	250	1.112	0.907	1.249	0.849	1.150	1.080	1.027	0.879	0.633	1.440	1.310	1.022	1.016	1.025	0.4207	NT	0.752	NT
	800	1.367	0.617	1.508	0.862	1.071	0.875	0.892	0.571	0.861	1.845	1.411	1.149	1.067	0.902	NT	2.330	0.526	NT
Delphinidin	15	1.032	0.956	0.995	1.050	1.083	1.020	0.816	1.017	0.521	1.066	1.125	0.924	0.953	0.966	1.0568	0.827	0.913	0.492
	70	1.216	0.871	0.902	1.169	1.256	0.931	0.882	0.842	0.487	0.970	1.163	0.976	0.847	0.847	0.5343	0.717	0.720	NT
	200	1.251	0.847	0.865	1.238	1.078	0.863	0.753	0.519	0.513	1.132	1.445	1.206	0.614	0.528	NT	1.930	0.467	NT

[a] 1: thioredoxin. [b] 2: survivin. [c] 3: FADD. [d] 4: TXNRD1. [e] 5: Hsp90. [f] 6: MxA. [g] 7: tNOX. [h] 8: NQO1. [i] 9: Hsp70. [j] 10: XIAP. [k] 11: ERK2. [l] 12: p53. [m] 13: Bcl-2. [n] A: Cancer cell growth suppression activity. [o] B: Antiviral activity. [p] C: Antioxidative stress activity. [q] D: HTLV-1-infected cell growth suppression activity. [r] E: Natural killer cell activation activity. [s] NT: Not tested. This table was modified from previously described figure.[77]

26

Table I-2. (Continued-1)

Compounds	Conc	marker protein expression rate													food functionality				
	μmol/L	1[a]	2[b]	3[c]	4[d]	5[e]	6[f]	7[g]	8[h]	9[i]	10[j]	11[k]	12[l]	13[m]	A[n]	B[o]	C[p]	D[q]	E[r]
Curcumin	0.027	0.734	0.878	0.882	0.877	0.878	0.945	0.684	0.742	0.682	0.919	0.928	0.865	0.831	NT[s]	NT	NT	NT	1.874
	4	0.952	0.952	1.003	0.824	1.554	1.400	0.672	0.989	0.776	0.950	0.944	0.977	0.894	1.009	1.1212	1.741	NT	1.637
	15	1.017	0.685	0.981	0.908	1.288	1.091	0.768	0.894	0.871	1.072	0.999	0.864	0.819	0.994	NT	NT	NT	NT
	40	2.934	0.692	2.250	1.122	1.963	1.373	0.800	0.898	0.900	1.377	1.155	1.015	0.839	1.021	NT	2.094	NT	NT
GABA[t]	100	0.995	1.255	0.911	1.021	1.390	1.190	1.209	1.064	0.743	0.951	1.177	0.964	1.035	1.002	1.0369	1.247	0.919	NT
	300	1.143	1.222	0.967	1.085	1.337	1.107	1.058	1.143	0.697	0.778	1.322	1.011	1.177	1.006	1.1237	0.941	0.863	NT
	1000	1.214	1.185	0.981	1.038	1.326	1.009	1.223	1.391	0.978	0.803	1.305	1.059	1.305	1.032	1.0846	0.788	0.888	NT
Resveratrol	10	0.724	0.79	0.797	0.851	0.785	0.979	0.622	0.731	0.406	1.049	1.017	0.893	0.914	0.960	NT	2.778	1.140	2.493
	30	0.598	0.778	0.913	0.841	0.705	0.931	0.460	0.647	0.305	1.010	1.009	1.041	0.880	0.858	NT	2.310	0.232	NT
	80	0.694	0.559	0.946	1.093	0.784	0.727	0.573	0.605	0.673	1.067	1.104	2.406	0.982	0.563	NT	1.172	0.064	NT
Arachidonic	15	1.016	1.041	0.982	0.874	1.139	0.940	1.086	0.891	0.572	0.903	1.128	1.013	0.912	1.030	0.7954	1.277	1.113	NT
acid	45	1.294	1.077	1.06	1.007	0.777	1.255	1.022	0.86	0.596	0.940	1.412	1.151	1.019	0.932	0.4984	1.073	1.233	NT
	100	1.718	0.895	1.032	1.121	1.091	1.111	0.981	0.699	0.823	1.015	1.566	1.199	1.005	0.806	0.0378	0.727	1.078	NT
*t*10, *c*12-CLA[u]	1	0.900	1.016	1.076	0.887	1.153	0.935	1.058	0.823	0.629	0.855	0.891	0.761	0.865	0.959	NT	1.203	1.019	NT
	3	0.929	1.09	1.132	0.949	1.799	1.009	1.012	0.854	0.987	0.875	0.961	0.931	0.951	0.962	0.7944	1.111	1.117	1.152
	10	0.953	1.002	1.021	0.951	1.318	0.986	0.923	1.061	1.048	0.899	0.949	0.926	1.011	0.965	0.1139	1.015	1.111	1.162
*c*9, *t*11-CLA[v]	10	1.032	0.887	0.995	1.054	1.183	0.871	1.198	0.883	0.727	0.909	0.974	0.955	0.837	0.898	0.5918	0.552	1.071	NT
	30	1.054	0.94	0.945	1.026	1.462	0.879	1.151	0.822	0.888	0.860	1.003	0.866	0.917	0.891	0.146	0.638	1.002	NT
	100	0.965	0.886	0.842	1.008	0.878	0.865	1.033	0.900	1.058	0.919	0.986	0.826	0.867	0.827	0.0358	0.935	0.982	NT
Kaempferol	6	0.967	0.987	0.827	0.939	1.349	1.162	0.900	1.003	0.943	1.328	1.376	0.977	0.917	0.981	NT	0.954	0.939	1.220
	20	1.047	0.998	0.838	0.949	1.466	1.294	0.710	0.983	1.040	1.312	1.468	1.024	0.963	0.928	NT	2.411	0.348	NT
	60	1.161	0.920	0.744	1.018	1.439	1.187	0.722	1.026	1.110	0.980	1.420	1.203	1.004	0.686	NT	2.924	0.269	NT
IFN[w]	100 IU/mL	0.921	0.870	0.843	0.996	1.424	1.240	0.863	2.603	0.665	1.158	1.145	0.898	1.006	1.014	0.0032	0.990	0.916	NT
	300 IU/mL	1.141	1.176	0.921	1.128	2.165	1.564	1.049	5.268	0.736	1.216	1.269	1.062	1.106	1.005	0.0003	1.433	0.844	NT
	1000 IU/mL	1.184	1.104	0.946	1.220	1.660	1.504	0.914	6.962	0.973	1.543	1.136	1.054	1.256	1.000	0.0001	1.030	0.766	NT

[a] 1: thioredoxin. [b] 2: survivin. [c] 3: FADD. [d] 4: TXNRD1. [e] 5: Hsp90. [f] 6: MxA. [g] 7: tNOX. [h] 8: NQO1. [i] 9: Hsp70. [j] 10: XIAP. [k] 11: ERK2. [l] 12: p53. [m] 13: Bcl-2. [n] A: Cancer cell growth suppression activity. [o] B: Antiviral activity. [p] C: Antioxidative stress activity. [q] D: HTLV-1-infected cell growth suppression activity. [r] E: Natural killer cell activation activity. [s] NT: Not tested. [t] GABA: gamma-aminobutyric acid. [u] *t*10, *c*12-CLA: *trans*-10, *cis*-12 conjugated linoleic acid. [v] *c*9, *t*11-CLA: *cis*-9, *trans*-11 conjugated linoleic acid. [w] IFN: interferon-alpha 2b. This table was modified from previously described figure.[77]

Table I-2. (Continued-2)

Compounds	Conc	marker protein expression rate													food functionality				
	μmol/L	1[a]	2[b]	3[c]	4[d]	5[e]	6[f]	7[g]	8[h]	9[i]	10[j]	11[k]	12[l]	13[m]	A[n]	B[o]	C[p]	D[q]	E[r]
Ribavirin	2 μg/mL	1.066	0.903	0.597	0.896	0.966	0.727	0.891	0.73	0.874	1.061	1.025	0.944	1.066	1.043	NT[s]	1.583	NT	NT
	10 μg/mL	1.096	0.626	0.549	0.776	1.045	0.655	0.759	0.627	1.009	1.173	1.137	1.475	0.935	0.971	0.4728	2.217	NT	NT
	30 μg/mL	1.186	0.479	0.523	0.759	1.180	0.602	0.536	0.800	1.109	1.037	0.939	1.259	0.884	0.926	0.0999	2.282	NT	NT
Fluvastatin	7.5	1.006	0.796	0.878	1.019	1.220	0.823	0.709	0.820	0.407	0.969	0.844	0.929	0.868	0.933	0.1470	0.973	0.789	2.046
	15	1.014	0.731	0.741	0.914	1.352	0.679	0.497	0.706	0.274	0.876	0.713	0.735	0.725	0.921	0.0641	0.845	0.654	2.209
	25	0.821	0.572	0.893	1.054	0.777	0.971	0.709	0.889	0.753	1.003	0.991	0.964	0.933	NT	NT	NT	0.321	2.314
	50	1.250	0.715	0.825	1.030	1.262	0.683	0.556	0.844	0.512	0.916	0.809	0.895	0.902	0.788	NT	0.728	0.078	NT
Atorvastatin	3.5	0.775	0.612	0.859	0.811	0.970	0.834	0.720	0.802	0.511	0.982	1.004	0.733	0.742	1.075	0.5317	1.675	1.073	1.913
	10	0.910	0.707	0.947	1.061	0.926	0.894	0.655	0.861	0.636	1.229	1.240	0.855	0.812	1.027	0.0386	1.396	0.587	2.049
	35	0.942	0.641	0.982	1.095	0.559	0.892	0.715	0.987	0.86	1.192	1.247	1.063	0.943	0.762	NT	1.076	0.037	NT
Simvastatin	3.5	1.087	0.916	0.869	0.839	1.334	0.853	0.912	0.799	0.885	1.169	1.014	0.765	0.799	1.028	0.8126	1.144	1.133	1.641
	10	1.099	0.886	0.848	0.833	0.969	0.682	0.695	0.826	0.635	1.235	1.096	0.907	0.835	0.949	0.0516	1.003	1.151	2.788
	35	1.590	0.902	1.214	0.938	1.830	1.076	0.673	1.180	1.059	1.236	1.279	1.029	1.019	0.586	NT	0.822	1.283	NT
Pravastatin	100	1.122	0.820	0.957	0.935	1.126	0.876	0.883	0.915	0.688	1.260	1.208	0.900	0.822	0.926	NT	1.586	0.899	1.634
	300	1.132	0.719	0.903	0.875	0.848	0.781	0.721	0.822	0.62	1.240	1.249	0.856	0.786	0.963	0.8990	1.117	0.866	NT
	1000	1.212	0.609	0.852	0.981	0.586	0.757	0.666	0.807	0.841	1.230	1.263	0.954	0.787	0.938	0.0402	0.856	0.764	NT
Chlorogenic	20	0.786	0.924	0.716	0.808	1.244	0.969	1.191	0.851	0.472	0.855	0.961	0.810	0.806	0.971	1.0075	0.950	1.078	NT
acid	70	0.889	0.981	0.670	0.826	1.513	1.066	1.326	0.985	0.497	0.877	1.076	0.871	0.888	1.001	NT	0.810	1.120	1.153
	200	1.053	1.025	0.794	0.917	1.840	0.998	1.378	1.176	0.785	0.937	1.107	1.054	1.049	0.924	0.5526	0.733	1.202	NT
Rosmarinic	5	0.638	0.673	0.688	0.759	0.604	0.827	0.864	0.822	0.554	0.739	0.881	0.673	0.859	0.949	1.2471	0.771	1.009	1.123
acid	15	0.55	0.672	0.653	0.885	0.659	0.900	0.795	0.877	0.489	0.757	0.958	0.705	0.855	0.982	1.0712	0.604	1.065	0.669
	50	0.509	0.733	0.587	0.699	0.684	0.780	0.817	0.819	0.729	0.771	0.886	0.774	0.830	0.993	1.3326	0.55	0.973	NT
Galangin	8	0.856	0.911	0.956	0.998	1.010	1.143	0.626	1.126	0.624	1.023	1.237	0.932	1.105	0.967	1.6717	1.885	0.825	1.883
	15	0.670	0.932	0.840	0.961	1.075	1.084	0.629	1.077	0.662	1.052	1.344	0.954	1.096	0.958	1.6554	1.686	0.868	NT
	50	0.823	0.703	0.743	1.006	0.818	0.876	0.550	1.065	1.067	1.555	1.374	0.940	1.174	0.665	NT	1.252	0.651	NT
Capsaicin	10	0.833	1.229	1.009	0.909	3.029	1.147	1.023	1.109	0.793	1.461	1.180	0.937	1.081	0.933	0.6250	0.922	NT	1.792
	60	1.113	1.246	1.066	0.957	2.759	1.144	1.181	1.131	0.847	1.530	1.272	1.018	1.131	0.860	0.6405	0.947	NT	2.944
	150	1.518	0.837	0.987	0.952	2.602	1.133	1.252	1.024	1.157	1.665	1.266	1.177	1.357	0.633	NT	0.567	NT	NT

[a] 1: thioredoxin. [b] 2: survivin. [c] 3: FADD. [d] 4: TXNRD1. [e] 5: Hsp90. [f] 6: MxA. [g] 7: tNOX. [h] 8: NQO1. [i] 9: Hsp70. [j] 10: XIAP. [k] 11: ERK2. [l] 12: p53. [m] 13: Bcl-2. [n] A: Cancer cell growth suppression activity. [o] B: Antiviral activity. [p] C: Antioxidative stress activity. [q] D: HTLV-1-infected cell growth suppression activity. [r] E: Natural killer cell activation activity. [s] NT: Not tested. This table was modified from previously described figure.[77]

28

Table I-2. (Continued-3)

Compounds	Conc	marker protein expression rate													food functionality				
	μmol/L	1[a]	2[b]	3[c]	4[d]	5[e]	6[f]	7[g]	8[h]	9[i]	10[j]	11[k]	12[l]	13[m]	A[n]	B[o]	C[p]	D[q]	E[r]
BITC[t]	1.5	1.104	1.089	1.204	0.836	4.098	1.31	1.352	1.113	0.646	1.683	1.346	1.054	1.127	0.925	0.9488	1.271	0.929	NT[s]
	5	1.459	1.265	2.104	0.915	6.846	1.702	1.639	1.442	0.786	2.615	1.747	1.404	1.484	0.912	0.3782	2.713	0.822	NT
	15	2.194	1.175	5.002	0.757	4.421	1.44	1.730	0.961	1.051	2.208	1.473	1.427	1.351	0.742	NT	NT	0.754	NT
Linoleic	20	0.942	1.028	1.102	1.036	1.249	0.941	1.458	0.863	0.682	0.824	0.928	0.714	0.805	0.935	NT	1.199	1.224	0.862
acid	50	0.970	0.920	1.010	0.987	1.441	1.027	1.476	0.851	0.834	0.912	1.019	0.664	1.051	0.945	0.7219	1.281	1.301	NT
	150	1.080	0.943	0.942	1.011	1.403	0.995	1.524	0.958	1.004	1.013	1.028	0.586	1.198	0.829	NT	2.901	1.180	NT
Genistein	10	0.766	0.759	0.726	0.730	0.624	0.842	0.672	0.870	0.559	0.760	0.919	0.915	0.817	NT	NT	NT	1.010	NT
	20	0.832	0.702	0.711	0.859	0.655	1.009	0.824	1.041	0.655	1.096	1.006	1.131	1.033	NT	NT	NT	0.915	NT
	30	0.920	1.068	0.941	0.894	0.880	0.953	0.798	0.869	0.900	1.030	0.966	0.900	0.935	NT	NT	NT	0.869	1.222
	60	1.412	1.533	0.853	1.357	0.774	1.364	0.912	1.520	1.919	1.866	1.354	3.824	1.767	NT	NT	NT	0.543	NT
Lovastatin	5	1.018	0.836	1.056	0.917	0.593	0.960	0.835	0.908	0.701	1.192	1.135	0.897	0.877	NT	NT	NT	1.231	1.360
	25	1.046	0.642	1.069	0.933	0.754	0.847	0.734	0.850	0.675	1.332	1.287	1.000	0.876	NT	NT	NT	1.348	1.652
	50	1.182	0.686	1.164	1.096	0.328	0.991	0.646	0.988	1.002	1.508	1.429	1.215	1.065	NT	NT	NT	1.340	NT
β-carotene	0.1	1.177	1.106	1.048	1.082	1.052	1.098	0.931	0.865	1.014	1.015	1.016	1.045	0.986	NT	NT	NT	NT	2.077
	10	1.110	1.212	1.136	1.043	1.227	1.166	0.966	0.871	0.950	1.135	1.123	1.057	1.015	NT	NT	NT	NT	1.486
DHA[u]	60	0.967	0.963	1.037	1.028	1.041	1.130	0.939	0.946	0.917	0.871	1.149	1.083	0.968	NT	NT	NT	NT	4.626
Caffeine	10	1.045	0.986	1.113	1.126	1.133	1.167	0.935	0.860	0.896	0.977	1.025	0.958	1.013	NT	NT	NT	NT	1.199
Astaxanthin	1600	1.126	1.220	1.216	1.022	1.082	1.097	1.029	0.888	0.931	1.174	1.196	1.102	1.048	NT	NT	NT	NT	1.348
tocopherol	350	1.087	1.054	0.974	1.062	0.932	1.047	0.832	1.036	0.935	1.083	0.990	1.037	1.062	NT	NT	NT	NT	1.063
EGC[v]	10	0.774	0.848	0.708	0.911	1.338	0.966	0.953	0.844	0.609	0.991	1.265	0.871	0.831	NT	NT	NT	1.078	NT
	30	1.066	1.012	0.798	1.086	1.207	1.068	1.026	1.053	0.695	1.154	1.649	1.106	1.045	NT	NT	NT	1.059	NT
	60	0.878	1.016	0.752	1.183	0.881	0.929	0.810	1.147	1.107	0.906	1.282	1.232	1.104	NT	NT	NT	1.108	NT

[a] 1: thioredoxin. [b] 2: survivin. [c] 3: FADD. [d] 4: TXNRD1. [e] 5: Hsp90. [f] 6: MxA. [g] 7: tNOX. [h] 8: NQO1. [i] 9: Hsp70. [j] 10: XIAP. [k] 11: ERK2. [l] 12: p53. [m] 13: Bcl-2. [n] A: Cancer cell growth suppression activity. [o] B: Antiviral activity. [p] C: Antioxidative stress activity. [q] D: HTLV-1-infected cell growth suppression activity. [r] E: Natural killer cell activation activity. [s] NT: Not tested. [t] BITC: benzyl isothiocyanate. [u] DHA: docosahexaenoic acid. [v] EGC: epigallocatechin. This table was modified from previously described figure.[77]

Table I-3. Test data sets for cancer cell growth suppression activity, antiviral activity, and antioxidative stress activity: Marker protein expression rate and experimental values of food functionalities used to verify the models and estimated values calculated from the optimized ANN2 models.

Food Extracts	Conc.[a]	marker protein expression rate													food functionalities					
															actual value			estimated value from ANN2		
	(μg/mL)	1[b]	2[c]	3[d]	4[e]	5[f]	6[g]	7[h]	8[i]	9[j]	10[k]	11[l]	12[m]	13[n]	A[o]	B[p]	C[q]	A[o]	B[p]	C[q]
blueberry leaves (HW[r])	5	0.913	1.128	0.966	0.811	0.967	0.997	0.898	0.809	0.784	1.133	0.919	0.979	0.934	0.948 ± 0.032	0.155 ± 0.031	0.662 ± 0.090	1.048	0.164	0.937
blueberry leaves (EtOH[s])	5	0.722	1.004	0.820	0.790	1.007	0.993	0.990	0.924	0.878	1.245	0.857	0.913	0.931	0.926 ± 0.058	0.023 ± 0.025	0.766 ± 0.219	1.046	0.179	1.148
Japanese radish roots	1000	0.827	0.949	0.896	0.875	1.113	1.034	0.846	0.738	0.722	0.929	0.929	0.917	0.888	0.905 ± 0.018	0.459 ± 0.148	1.173 ± 0.077	1.045	0.329	0.950
Japanese radish leaves	1000	1.718	1.149	1.171	1.061	1.209	0.966	1.084	1.116	1.039	1.266	1.323	1.096	0.847	0.559 ± 0.007	0.336 ± 0.184	2.233 ± 0.236	0.639	0.072	1.605
carrot leaves	400	3.240	1.288	1.604	0.977	1.363	1.182	1.276	0.620	0.666	1.703	2.373	1.653	0.665	0.873 ± 0.041	0.746 ± 0.295	1.401 ± 0.189	0.890	0.702	2.221
green tea leaves	40	0.932	1.091	1.132	0.952	1.740	1.125	1.133	0.918	0.750	1.186	1.307	1.186	0.944	0.902 ± 0.009	0.019 ± 0.012	0.914 ± 0.247	0.953	0.392	0.936
	120	1.282	1.198	1.237	1.098	1.627	1.211	0.952	1.036	1.085	1.457	1.566	1.412	1.082	0.738 ± 0.005	0.058 ± 0.067	0.921 ± 0.562	0.853	0.112	0.955
burdock roots	300	0.867	0.940	0.868	0.890	0.832	1.126	1.052	0.834	0.828	1.109	0.835	0.902	0.911	0.990 ± 0.004	0.054 ± 0.023	0.882 ± 0.152	1.047	0.207	0.962
	1000	1.006	0.967	0.844	0.873	0.874	1.126	1.245	0.812	0.837	1.252	0.784	0.920	0.838	0.941 ± 0.014	0.010 ± 0.011	1.877 ± 0.173	1.042	0.084	2.201
spearmint leaves	100	1.016	1.237	1.077	0.884	1.185	0.999	1.092	0.827	0.865	1.085	1.032	1.261	0.896	0.961 ± 0.016	0.318 ± 0.094	0.617 ± 0.178	1.009	0.159	0.935
rosemary leaves	50	1.567	0.598	1.653	1.363	1.352	1.345	1.303	0.869	1.267	1.206	1.150	0.905	1.115	0.768 ± 0.034	0.668 ± 0.481	2.666 ± 0.547	0.698	0.527	2.457
Lemon balm leaves	300	1.166	1.392	1.055	1.162	1.480	1.118	1.623	0.789	0.927	1.181	1.412	1.491	0.953	0.867 ± 0.058	0.374 ± 0.170	1.144 ± 0.100	0.886	0.073	0.936
stevia leaves	60	0.939	0.978	0.928	0.969	1.015	1.075	1.013	1.120	0.974	0.917	1.061	1.026	1.063	1.001 ± 0.026	0.477 ± 0.143	0.631 ± 0.084	0.947	0.457	0.933
	200	1.119	1.185	1.067	1.126	1.101	1.205	1.032	1.045	1.076	1.054	1.232	1.256	0.850	0.951 ± 0.012	0.158 ± 0.055	0.743 ± 0.053	0.877	0.081	0.938
sweet basil leaves	120	0.953	1.164	0.952	1.060	1.351	1.026	1.159	0.876	0.893	0.909	1.087	1.038	0.907	0.963 ± 0.020	0.068 ± 0.035	0.935 ± 0.084	0.920	0.128	0.933
	400	1.514	2.120	1.561	1.124	2.338	1.395	1.948	0.952	1.150	1.469	1.632	1.821	1.189	0.703 ± 0.032	0.086 ± 0.084	2.281 ± 0.202	0.857	0.072	1.340

	Conc	marker protein expression rate													food functionalities					
															actual value			estimated value from ANN2		
Compounds	(μmol/L)	1[b]	2[c]	3[d]	4[e]	5[f]	6[g]	7[h]	8[i]	9[j]	10[k]	11[l]	12[m]	13[n]	A[o]	B[p]	C[q]	A[o]	B[p]	C[q]
lovastatin	5	1.018	0.836	1.056	0.917	0.593	0.960	0.835	0.908	0.701	1.192	1.135	0.897	0.877	1.022 ± 0.044	0.799 ± 0.228	0.964 ± 0.234	1.038	0.616	1.133
	25	1.046	0.642	1.069	0.933	0.754	0.847	0.734	0.850	0.675	1.332	1.287	1.000	0.876	0.964 ± 0.032	0.032 ± 0.011	0.899 ± 0.051	0.977	0.113	1.146
genistein	20	0.832	0.702	0.711	0.859	0.655	1.009	0.824	1.041	0.655	1.096	1.006	1.131	1.033	0.832 ± 0.023	1.527 ± 0.095	1.772 ± 0.401	0.955	1.478	1.152
	60	1.412	1.533	0.853	1.357	0.774	1.364	0.912	1.520	1.919	1.866	1.354	3.824	1.767	0.582 ± 0.015	1.021 ± 0.187	2.392 ± 0.517	0.531	1.137	2.261
EGC[t]	30	1.066	1.012	0.798	1.086	1.207	1.068	1.026	1.053	0.695	1.154	1.649	1.106	1.045	0.972 ± 0.020	1.001 ± 0.153	0.575 ± 0.085	0.884	0.657	0.865
	60	0.878	1.016	0.752	1.183	0.881	0.929	0.810	1.147	1.107	0.906	1.282	1.232	1.104	1.007 ± 0.027	0.489 ± 0.098	0.674 ± 0.308	0.996	1.088	0.803

[a] Conc.: concentration. [b] 1: thioredoxin. [c] 2: survivin. [d] 3: Hsp70. [e] 4: XIAP. [f] 5: FADD. [g] 6: TXNRD1. [h] 7: Hsp90. [i] 8: MxA. [j] 9:. tNOX. [k] 10: NQO1. [l] 11: ERK2. [m] 12: p53. [n] 13: Bcl-2. [o] A: Cancer cell growth suppression activity. [p] B: Antiviral activity. [q] C: antioxidative stress activity. [r] HW: hot water extract. [s] EtOH: 80% ethanol extract. [t] EGC: epigallocatechin. This table was cited from previously described study.[77]

Table I-4. Test data sets for HTLV-1-infected cell growth suppression activity: Marker protein expression rate and experimental values of food functionalities used to verify the models and estimated values calculated from the optimized ANN2 models.

Food Extracts	Conc.[a]	marker protein expression rate													food functionalities	
															actual value	estimated value from ANN2
	(μg/mL)	1[b]	2[c]	3[d]	4[e]	5[f]	6[g]	7[h]	8[i]	9[j]	10[k]	11[l]	12[m]	13[n]	A[o]	
blueberry leaves (EtOH[p])	5	0.722	1.004	0.820	0.790	1.007	0.993	0.990	0.924	0.878	1.245	0.857	0.913	0.931	1.063 ± 0.159	1.091
	50	1.008	1.028	0.615	0.737	0.996	0.955	0.759	0.904	0.801	0.716	0.754	0.757	0.769	0.240 ± 0.126	0.563
Onion leaves	100	0.992	0.998	1.091	0.995	1.086	1.038	1.196	0.903	0.905	1.032	1.113	1.078	1.042	1.128 ± 0.086	1.091
	300	1.066	1.024	1.086	1.009	1.511	1.091	1.216	1.185	0.945	1.083	1.332	1.238	1.055	1.218 ± 0.161	1.092
Japanese radish roots	1000	0.827	0.949	0.896	0.875	1.113	1.034	0.846	0.738	0.722	0.929	0.929	0.917	0.888	0.849 ± 0.020	1.091
Bitter gourd placenta	300	1.001	1.013	0.919	1.085	0.750	0.853	0.951	1.146	1.123	1.321	0.837	1.077	1.047	0.896 ± 0.095	1.065
carrot leaves	400	3.240	1.288	1.604	0.977	1.363	1.182	1.276	0.620	0.666	1.703	2.373	1.653	0.665	0.284 ± 0.037	0.325
green tea leaves	20	0.897	0.933	1.001	0.916	1.033	0.952	1.139	0.811	0.765	1.029	1.076	1.024	0.910	1.017 ± 0.023	1.091
	40	0.932	1.091	1.132	0.952	1.74	1.125	1.133	0.918	0.75	1.186	1.307	1.186	0.944	1.048 ± 0.027	1.080
	120	1.282	1.198	1.237	1.098	1.627	1.211	0.952	1.036	1.085	1.457	1.566	1.412	1.082	0.714 ± 0.062	0.956
burdock roots	300	0.867	0.94	0.868	0.89	0.832	1.126	1.052	0.834	0.828	1.109	0.835	0.902	0.911	1.032 ± 0.125	1.090
soybean whole beans	1000	0.989	1.123	0.902	1.083	0.919	0.677	0.754	0.847	0.881	0.988	1.057	0.975	0.999	0.907 ± 0.090	1.083
komatsuna leaves	100	0.988	1.118	0.979	0.965	1.127	1.102	1.143	0.783	0.897	1.063	1.028	1.123	0.913	1.179 ± 0.166	1.091
suioh leaves	300	1.872	0.563	1.369	1.175	1.363	1.126	1.652	0.650	1.590	1.627	1.237	0.892	0.654	0.504 ± 0.029	0.500
chamomile flower	200	1.030	0.863	1.018	0.864	0.719	0.941	0.999	0.856	0.757	1.042	0.908	0.954	0.893	0.572 ± 0.097	0.857
spearmint leaves	100	1.016	1.237	1.077	0.884	1.185	0.999	1.092	0.827	0.865	1.085	1.032	1.261	0.896	0.928 ± 0.109	1.088
rosemary leaves	15	1.322	1.099	1.212	1.136	1.418	1.172	1.210	1.439	1.422	1.183	1.073	1.307	1.214	1.000 ± 0.214	1.089
	50	1.567	0.598	1.653	1.363	1.352	1.345	1.303	0.869	1.267	1.206	1.15	0.905	1.115	0.684 ± 0.122	0.650
lemon balm leaves	300	1.166	1.392	1.055	1.162	1.48	1.118	1.623	0.789	0.927	1.181	1.412	1.491	0.953	0.525 ± 0.035	1.049
stevia leaves	60	0.939	0.978	0.928	0.969	1.015	1.075	1.013	1.12	0.974	0.917	1.061	1.026	1.063	0.875 ± 0.053	1.089
	200	1.119	1.185	1.067	1.126	1.101	1.205	1.032	1.045	1.076	1.054	1.232	1.256	0.85	0.754 ± 0.055	0.825
sweet basil leaves	120	0.953	1.164	0.952	1.06	1.351	1.026	1.159	0.876	0.893	0.909	1.087	1.038	0.907	0.895 ± 0.126	1.082
	400	1.514	2.12	1.561	1.124	2.338	1.395	1.948	0.952	1.15	1.469	1.632	1.821	1.189	0.559 ± 0.086	0.818

[a] Conc.: concentration. [b] 1: thioredoxin. [c] 2: survivin. [d] 3: Hsp70. [e] 4: XIAP. [f] 5: FADD. [g] 6: TXNRD1. [h] 7: Hsp90. [i] 8: MxA. [j] 9:. tNOX. [k] 10: NQO1. [l] 11: ERK2. [m] 12: p53. [n] 13: Bcl-2. [o] A: HTLV-1-infected cell growth suppression activity. [p] EtOH: 80% ethanol extract. [f] EGC: epigallocatechin.

31

Table I-5. T[es]t data sets for NK cell activation activity: Marker protein expression rate and experimental values of food functionalities used to verify the models and estimated values calculated from the optimized ANN2 models.

	Conc.[a]	marker protein expression rate													food functionalities	
															actual value	estimated value from ANN2
Compounds	(μmol/L)	1[b]	2[c]	3[d]	4[e]	5[f]	6[g]	7[h]	8[i]	9[j]	10[k]	11[l]	12[m]	13[n]	A[o]	
delphinidin	70	1.216	0.871	0.902	1.169	1.256	0.931	0.882	0.842	0.487	0.970	1.163	0.976	0.847	0.428 ± 0.105	0.657
*t*10, *c*12-CLA[p]	1	0.900	1.016	1.076	0.887	1.153	0.935	1.058	0.823	0.629	0.855	0.891	0.761	0.865	0.857 ± 0.094	0.769
genistein	10	0.766	0.759	0.726	0.730	0.624	0.842	0.672	0.870	0.559	0.760	0.919	0.915	0.817	1.174 ± 0.147	1.337
chlorogenic acid	20	0.786	0.924	0.716	0.808	1.244	0.969	1.191	0.851	0.472	0.855	0.961	0.810	0.806	1.689 ± 0.347	1.392
EGC[q]	10	0.774	0.848	0.708	0.911	1.338	0.966	0.953	0.844	0.609	0.991	1.265	0.871	0.831	2.090 ± 0.719	1.915
fluvastatin	50	1.250	0.715	0.825	1.030	1.262	0.683	0.556	0.844	0.512	0.916	0.809	0.895	0.902	2.614 ± 0.393	2.513

[a] Conc.: concentration. [b] 1: thioredoxin. [c] 2: survivin. [d] 3: Hsp70. [e] 4: XIAP. [f] 5: FADD. [g] 6: TXNRD1. [h] 7: Hsp90. [i] 8: MxA. [j] 9:. tNOX. [k] 10: NQO1. [l] 11: ERK2. [m] 12: p53. [n] 13: Bcl-2. [o] A: NK cell activation activity. [p] *t*10, *c*12-CLA: *trans*-10, *cis*-12 conjugated linoleic acid. [p] EGC: epigallocatechin.

32

Data sets. The data sets used in this study consisted of 28 food constituents, 7 drugs and 18 food extracts **(Table I-2, I-3, I-4 and I-5)**. These data were divided into two groups, viz., training and test data sets. To construct the mathematical models, the training and test data sets were used to build the model and to verify the performance of the models, respectively. In addition, two kinds of training data sets were prepared.

Training data set 1. The training data set 1 for cancer cell growth suppression activity, antiviral activity, and antioxidative stress activity, consisted of 21 food constituents and 6 drugs **(Table I-2)**. The SLR and MLR were constructed by the training data set 1, and ANN1 was learned by the same data set.

Training data set 2. ANN2 were constructed to improve the prediction performance of ANN1 and learned by the data generated from training data set 1 in **Table I-2**. ANN2s for HTLV-1-infected cell growth suppression activity and NK cell activation activity were also learned by training data set 1 in **Table I-2**. To avoid overfitting to the training data set 1, the pseudo-random numbers were generated by the random function of the GNU Compiler Collection, and then were added to the training data set 1. A different size of noise was randomly and individually added to the relative expression of marker proteins and actual value of the health-promoting effect. Therefore, the additive noise was assumed to mimic the experimental error. Briefly, when the cells were treated with a certain concentration of food constituent, i, let m_j^i be the relative expression of marker protein j and let a_k^i be the actual value of the food functionality k. Then, an matrix illustrated by Equation (1) was created. Here, N is the number of all combinations of food constituents and concentration.

$$\begin{bmatrix} m_1^1 & \cdots & m_j^1 & \cdots & m_{13}^1 & a_k^1 \\ \vdots & \ddots & \vdots & \ddots & \vdots & \vdots \\ m_1^j & \cdots & m_j^i & \cdots & m_{13}^i & a_k^i \\ \vdots & \ddots & \vdots & \ddots & \vdots & \vdots \\ m_1^N & \cdots & m_j^N & \cdots & m_{13}^N & a_k^N \end{bmatrix} \quad (1)$$

Next, average of each column of Equation (1) were calculated using Equation (2) and (3), and an matrix illustrated by Equation (4) was created.

$$\bar{m_j} = \frac{1}{N}\sum_{i=1}^{N} m_j^i \quad (2)$$

$$\bar{a_j} = \frac{1}{N}\sum_{i=1}^{N} a_k \quad (3)$$

$$\begin{bmatrix} \bar{m_1} & \cdots & \bar{m_j} & \cdots & \bar{m_{13}} & \bar{a_k} \end{bmatrix} \quad (4)$$

Then, a noise to be added to $\bar{m_j}$ and $\bar{a_k}$ was generated. The noise, which generated against relative expression of marker proteins, ε_j, is uniform distribution random numbers which satisfy $-\alpha m_j \leq \varepsilon_j \leq +\alpha m_j$. Similarly, the noise for the actual value of the food functionality, ε_k', is uniform distribution random numbers which satisfy $-\alpha a_k \leq \varepsilon_k' \leq +\alpha a_k$. Here, α which satisfies $0 \leq \alpha \leq 0.1$ as cancer cell growth suppression, antioxidative stress activity and HTLV-1-infected cell growth suppression activity or $0 \leq \alpha \leq 0.05$ as antiviral activity or $0 \leq \alpha \leq 0.075$ as NK cell activation activity are constants. After some preliminary test run, α was determined to optimize performance. When the data of P piece for each certain concentration of food constituent were synthesized, let ε_j^p or ε'^p_k be the p-th noise. The training data sets including the noise

illustrated by Equation (5) were created by repetition processing by the addition of the random numbers to m_j^i or a_k^i.

$$\begin{bmatrix} m_1^1+\varepsilon_1^1 & \cdots & m_j^1+\varepsilon_j^1 & \cdots & m_{13}^1+\varepsilon_{13}^1 & a_k^1+\varepsilon'^1_k \\ \vdots & \ddots & \vdots & \ddots & \vdots & \vdots \\ m_1^1+\varepsilon_1^p & \cdots & m_j^1+\varepsilon_j^p & \cdots & m_{13}^1+\varepsilon_{13}^p & a_k^1+\varepsilon'^p_k \\ \vdots & \ddots & \vdots & \ddots & \vdots & \vdots \\ m_1^1+\varepsilon_1^P & \cdots & m_j^1+\varepsilon_j^P & \cdots & m_{13}^1+\varepsilon_{13}^P & a_k^1+\varepsilon'^P_k \\ m_1^2+\varepsilon_1^1 & \cdots & m_j^2+\varepsilon_j^1 & \cdots & m_{13}^2+\varepsilon_{13}^1 & a_k^2+\varepsilon'^1_k \\ \vdots & \ddots & \vdots & \ddots & \vdots & \vdots \\ m_1^2+\varepsilon_1^P & \cdots & m_j^2+\varepsilon_j^P & \cdots & m_{13}^2+\varepsilon_{13}^P & a_k^2+\varepsilon'^P_k \\ \vdots & \ddots & \vdots & \ddots & \vdots & \vdots \\ m_1^N+\varepsilon_1^1 & \cdots & m_j^N+\varepsilon_j^1 & \cdots & m_{13}^N+\varepsilon_{13}^1 & a_k^N+\varepsilon'^1_k \\ \vdots & \ddots & \vdots & \ddots & \vdots & \vdots \\ m_1^N+\varepsilon_1^P & \cdots & m_j^N+\varepsilon_j^P & \cdots & m_{13}^N+\varepsilon_{13}^P & a_k^N+\varepsilon'^P_k \end{bmatrix} \quad (5)$$

Test data sets. The unused data sets for training, i.e. two food constituents, a drug and twelve food extracts, were used for testing the performance of the SLR, MLR, ANN1, and ANN2 for cancer cell growth suppression activity, antiviral activity, and antioxidative stress activity **(Table I-3)**. Unlike the generated training data set 2, the test data sets did not add noise. To test whether a wide range of activities in compounds can be estimated by the mathematical model, two food constituents, i.e. genistein and EGC, and a drug, i.e. lovastatin, were used. Genistein has a cancer cell growth suppression activity[14, 61, 79-82], and a defense effect against oxidative stress[83-91]. Lovastatin[92-95] have a suppression activity against HCV replication. EGC was chosen as compound, which exhibited weak activity against the three food functionalities. Food extracts were used to test for crude samples. Test data sets **(Table I-4 and I-5)** were used for testing the performance of the ANN2 for HTLV-1-infected cell growth suppression activity and NK cell activation activity, respectively.

Linear regression model. Linear regression models were used to build models to estimate the three food functionalities (cancer cell growth suppression activity, antiviral activity, and antioxidative stress activity) from intracellular protein expression in response to stimulation with food constituents. Simple and multiple linear regressions are the most widely known modeling methods. The linear regressions relate one dependent variable y to one (SLR) or several (MLR) independent variables x_i by Equation (6):

$$y = \alpha + \sum_{i=1}^{n} \beta_i \cdot x_i \quad (6)$$

where y, α, β_i, and x_i represent the dependent variable, intercept, regression coefficient and independent variable, respectively. The models were constructed using food functionality as the dependent variable, and relative expression of marker protein as independent variables **(Table I-2)**. The goodness-of-fit was evaluated by coefficient of determination (R^2) and root mean square error (RMSE). The RMSE was calculated as follows:

$$RMSE = \sqrt{\frac{\sum_{i=1}^{n} (y_{pred} - y_{obs})^2}{n}} \quad (7)$$

where y_{pred}, y_{obs}, and n represent estimated value, actual value, and number of samples, respectively. *F*-test was used to test the significance of the established regression equations and $p<0.05$ was accepted as significant. SLR and MLR analysis were performed by the regression analysis tool of Microsoft Excel 2003.

ANN model. ANN is a computerized mathematical model designed to emulate the architecture of the brain and it is a powerful non-linear modeling technique offering solutions to problems that have not been clearly formulated. A multilayer feedforward network with a backpropagation learning algorithm, was used.[96] Every neuron in each layer is connected to every neuron of the adjacent layer by weighted links. To estimate with the least possible error, these weights must be adjusted. The activation function, Equation (8), means that the input, y_j, into a neuron are multiplied by their corresponding connection weights, w_{jk}, and summed. Then, the sum, x_k, is transformed using the sigmoid function, Equation (9). The sigmoid function is one of the most commonly used transfer functions. The calculated value, y_k, is the output of the considered neuron. All neurons in hidden and output layers are calculated similarly. Finally, the result was sent to the output neuron, and then the estimated value, y_k, was calculated. In Equations (8) and (9), j and k represent hidden and output layers, respectively.

$$x_k = \sum_{j=1} w_{jk} \cdot y_j \qquad (8)$$

$$y_k = f(x_k) = \left(\frac{1}{1+e^{-x_k}}\right) \qquad (9)$$

Structure of ANN. ANNs used in this paper were three-layer networks with 13 neurons in the input layer, 5 or 6 neurons in the hidden layer and 1 neuron in the output layer. After some preliminary test run, the number of neurons in the hidden layer was determined to optimize performance. ANN1 consisted of 5 neurons in the hidden layer, whereas ANN2 consisted of 6 neurons in the hidden layer. ANNs were constructed using the food

functionality as the output value, and relative expression of thirteen kinds of marker proteins as input data, namely TXN, survivin, Hsp70, XIAP, FADD, TXNRD1, Hsp90, MxA, tNOX, NQO1, ERK2, p53, and Bcl-2 **(Table I-2)**. The output variable data (also called teacher signal) should be normalized into the range from 0 to 1 for the transfer function using the sigmoid function. Therefore, the values were normalized by scaling linearly between 0.1 and 0.9 using minimums and maximums.

*Verification and selection of the optimized ANN. T*o select the optimized ANN, the main parameters of the ANNs were optimized. The range of initial weight was varied from -2 to 2. The learning rate of ANN1 was varied from 0.2 to 0.6 in steps of 0.1 and the momentum factor was varied from 0.2 to 0.8 in steps of 0.05. The learning rate of ANN2 was varied from 0.6 to 0.7 in steps of 0.05 and the momentum factor was 0.4 or 0.45. An ANN was trained repeatedly until the allowable error became less than 0.1 or until the learning epoch reached 40,000. Then, the trained ANN was retested by the training data sets. Additionally, the ANN was tested against the test data sets that had not been included in the ANN learning **(Table I-3, I-4, or I-5)**. The optimized ANN which gave the low RMSE and the high R^2 was selected in all of the built ANN.

Comparison of the prediction performance of the models. To verify the performance of each estimation model, SLR, MLR, ANN1, and ANN2 were examined using test data **(Table I-3, I-4 or I-5)**. The goodness-of-fit was evaluated by R^2 and RMSE. The similarity of the actual and estimated values was evaluated by analyzing their medians by the Mann-Whitney test. The variances of the actual and estimated values were also compared by

Levene's test. If the *p*-value is greater than 0.05, it indicated that there is no significant evidence to conclude that the actual data and the data from the models differ. All statistical analysis was performed with Systat 13 (Systat Software, Inc., Point Richmond, CA).

First screening of citruses by the optimized models. Citruses were collected in Miyazaki, Japan. The pericarp of bitter orange, hyuganatsu, and kumquat were extracted by described above method. After treatment of HepG2 cells with the citrus extracts, the expression levels of marker proteins were measured. And then, the optimized ANN models simultaneously estimated five food functionalities from the same expression data of marker proteins.

Results

Estimation of food functionality by SLR.

In this study, we have first attempted to build models to estimate three food functionalities, namely cancer cell growth suppression activity, antiviral activity, and antioxidative stress activity, from intracellular protein expression in response to stimulation with food constituents. A SLR model was first used to examine whether three food functionalities can be estimated by relative expression of a single marker protein compared with the control. The models were constructed using the food functionality as the dependent variable, and relative expression of a marker protein as the independent variable **(Table I-2)**. The regression coefficients, intercepts, and statistics of fits obtained from the SLR models are shown in **Table I-6**. An *F*-test was used to test the significance of the established regression equations. The models that had significant explanatory power were the regression equations using ERK2 or p53 for cancer cell growth suppression activity; TXN, XIAP, MxA, tNOX, NQO1 or p53 for antiviral activity; TXNRD1 or NQO1 for antioxidative stress activity **(Table I-6)**. Although the model estimated for cancer cell growth suppression activity by p53 had the highest coefficient of determination, R^2, in all SLR models, the model could explain only 22.4% of the total variance. Any SLR models by a single marker protein had low R^2. Therefore, a SLR model would not be adequate to estimate food functionality by marker protein expression.

Table I-6. Regression coefficients and statistics of the fits obtained from SLR models

Variables	Cancer cell growth suppression activity				Antiviral activity				Antioxidative stress activity			
	Intercept	Regression coefficient	R^2 [a]	RMSE[b]	Intercept	Regression coefficient	R^2	RMSE	Intercept	Regression coefficient	R^2	RMSE
TXN	0.965	-0.045	0.016	0.125	1.353	-0.710	0.171**	0.419	1.032	0.273	0.019	0.684
survivin	0.856	0.073	0.012	0.126	0.667	-0.015	0.000	0.460	1.761	-0.520	0.021	0.684
Hsp70	0.951	-0.033	0.019	0.125	0.834	-0.205	0.010	0.458	0.985	0.362	0.019	0.684
XIAP	1.043	-0.135	0.026	0.125	1.411	-0.833	0.083*	0.441	1.378	-0.074	0.000	0.691
FADD	0.936	-0.012	0.008	0.126	0.699	-0.034	0.005	0.459	1.164	0.112	0.019	0.684
TXNRD1	0.885	0.035	0.004	0.126	0.674	-0.020	0.000	0.460	0.617	0.714	0.052*	0.673
Hsp90	0.882	0.043	0.010	0.126	0.674	-0.023	0.000	0.460	1.588	-0.322	0.017	0.685
MxA	0.899	0.019	0.017	0.125	0.797	-0.129	0.080*	0.442	1.341	-0.029	0.001	0.690
tNOX	1.005	-0.118	0.041	0.124	1.219	-0.800	0.126**	0.430	0.858	0.621	0.038	0.677
NQO1	0.988	-0.064	0.027	0.125	1.146	-0.468	0.101*	0.436	0.666	0.601	0.071*	0.666
ERK2	1.068	-0.136	0.055*	0.123	0.901	-0.232	0.012	0.458	0.772	0.496	0.024	0.682
p53	1.152	-0.246	0.224***	0.111	1.289	-0.699	0.073*	0.443	0.971	0.360	0.016	0.685
Bcl2	0.987	-0.073	0.010	0.126	0.658	-0.004	0.000	0.460	0.964	0.371	0.009	0.688

[a] R^2: coefficient of determination. [b] RMSE: root mean square error. * P<0.05. ** P<0.01. *** P<0.001. This table was cited from previously described study.[77]

Table I-7. Correlation matrix between marker protein expressions as variables.

	TXN	survivin	Hsp70	XIAP	FADD	TXNRD1	Hsp90	MxA	tNOX	NQO1	ERK2	p53	Bcl-2
TXN	1												
survivin	0.244	1											
Hsp70	0.598	0.299	1										
XIAP	0.468	0.264	0.053	1									
FADD	0.428	0.523	0.609	0.099	1								
TXNRD1	0.323	0.511	0.464	0.252	0.617	1							
Hsp90	0.294	0.642	0.475	0.176	0.596	0.442	1						
MxA	0.097	0.316	0.031	0.341	0.194	0.508	0.136	1					
tNOX	0.425	0.193	0.215	0.266	0.224	0.269	0.252	0.180	1				
NQO1	0.529	0.272	0.596	0.224	0.720	0.505	0.331	0.228	0.417	1			
ERK2	0.520	0.430	0.397	0.515	0.487	0.506	0.350	0.164	0.369	0.681	1		
p53	0.321	0.085	0.312	0.295	0.316	0.172	0.083	0.071	0.269	0.412	0.519	1	
Bcl-2	0.383	0.466	0.407	0.446	0.614	0.550	0.529	0.363	0.482	0.599	0.622	0.399	1

This table was cited from previously described study.[77]

42

Estimation of food functionality by MLR.

SLR models that estimate food functionality by single marker protein expression did not have sufficient explanatory power, thus we attempted to build a MLR model using 13 marker protein expressions. **Table I-7** summarizes the correlation coefficient between any two descriptors, namely marker protein expressions. The mean was 0.372, and the highest correlation coefficient was 0.720. Thus, significant multicollinearity did not exist among marker proteins expressions. Then MLR models were constructed using food functionality as the dependent variable, and relative expression of thirteen kinds of marker proteins as independent variables, namely TXN, survivin, Hsp70, XIAP, FADD, TXNRD1, Hsp90, MxA, tNOX, NQO1, ERK2, p53, and Bcl-2 **(Table I-2)**. The regression coefficients, intercepts, and statistics of fits obtained from the MLR models are shown in **Table I-8**. The results of *F* testing showed that the MLR models for cancer cell growth suppression activity and antiviral activity estimation had significant explanatory power, whereas the MLR model for antioxidative stress activity was not useful to estimate activity. The R^2 of the MLR models that had significant explanatory power were higher than that of the SLR models. In addition, the model for antioxidative stress activity had also high R^2 in comparison with the SLR models. Furthermore, the RMSE from the MLR models were smaller than that of the SLR models, so that prediction error from any MLR models improved relative to the SLR models. These results suggest that the use of multimarker proteins may be appropriate for estimation of food functionality in comparison with that of a single marker protein.

Table I-8. Regression coefficients and statistics of the fits obtained from MLR models.

Variables	Cancer cell growth suppression activity		Antiviral activity		Antioxidative stress activity	
	Intercept	Regression coefficient	Intercept	Regression coefficient	Intercept	Regression coefficient
	1.060		1.291		0.753	
TXN		0.098		-0.310		0.200
survivin		0.086		0.476		-0.789
Hsp70		-0.065		-0.595		-0.388
XIAP		-0.205		-1.214		-0.253
FADD		-0.049		0.019		0.024
TXNRD1		0.110		0.288		1.552
Hsp90		0.095		-0.235		-0.414
MxA		0.013		-0.159		-0.199
tNOX		-0.161		-0.551		0.414
NQO1		0.083		-0.525		0.465
ERK2		-0.112		0.617		-0.189
p53		-0.181		-0.755		0.120
Bcl-2		0.124		2.065		-0.071
R^2	0.345**		0.567***		0.248	
Adjusted R^2	0.218		0.437		0.095	
RMSE	0.102		0.303		0.599	
N	81		57		78	

** $P< 0.01$. *** $P< 0.001$. This table was cited from previously described study.[77]

Estimation of food functionality by ANN.

Since the R^2 of the MLR models, types of linear models, were low, the models were not able to adequately explain the total variance. Therefore, we attempted to build ANN as a nonlinear model. The ANN models were trained with an error back propagation algorithm by using food functionality as the dependent variable, and relative expressions of 1 kinds of marker proteins as independent variables **(Table I-2)**. Optimized parameters and statistics of fits obtained from the ANN1 models are shown in **Table I-9**. Compared with the SLR and the MLR models, the R^2 of the optimized ANN1 models for three food functionality were improved. The ANN1 models were also improved in RSME compared with the SLR and the MLR models. These results suggest that the ANN1 models, types of nonlinear models, will be adequate to calculate food functionality from intracellular protein expressions.

Table I-9. Parameters of the optimized ANN1 models

	Cancer cell growth suppression activity	Antiviral activity	Antioxidative stress activity
Number of input neurons	13	13	13
Number of hidden neurons	5	5	5
Number of output neurons	1	1	1
Learning rate	0.80	0.70	0.75
Momentum factor	0.3	0.5	0.3
Final prediction error (Training data)			
R^2	0.799	0.954	0.828
RMSE	0.057	0.099	0.294

This table was cited from previously described study.[77]

Comparison of prediction performance of the models by the external test data.

Two food constituents, a drug, and 12 food extracts, which had not been used as the training data, were used as the test data for further external validation of the models **(Table I-3)**. Predictive abilities of the models were confirmed by the RMSE and the R^2 between actual and estimated values. Statistical differences between actual and estimated values were evaluated by Mann-Whitney and Levene's test. As can be seen in **Table I-10**, the most adequate values of the RMSE and R^2 of actual and estimated values are reached using the ANN1 models in each of three food functionalities. All the *p*-values from **Table I-10** indicate that there is no significant evidence to conclude that the actual data and the data

from the ANN1 models differ. Taken together, these results indicate that the most adequate models to estimate for three food functionalities are ANN1 models.

Table I-10. Comparison of the statistical parameters in the test data using every applied model

Test type		Cancer cell growth suppression activity					Antiviral activity					Antioxidative stress activity				
					Hypothesis testing					Hypothesis testing					Hypothesis testing	
		R	R^2	RMSE	Mann-Whitney	Levene's test	R	R^2	RMSE	Mann-Whitne	Levene's test	R	R^2	RMSE	Mann-Whitney	Levene's test
SLR	Variables															
	TXN	0.412	0.169	0.126	0.489	0.001	-0.188	0.035	0.604	0.062	0.226	0.408	0.166	0.612	0.027	0.001
	survivin	-0.434	0.188	0.151	0.734	0.001	0.194	0.038	0.475	0.010	0.000	-0.208	0.044	0.697	0.130	0.003
	Hsp70	0.382	0.146	0.131	0.534	0.000	0.148	0.022	0.456	0.008	0.000	0.440	0.194	0.621	0.030	0.001
	XIAP	0.516	0.266	0.122	0.319	0.002	-0.225	0.051	0.481	0.025	0.001	-0.487	0.237	0.652	0.040	0.000
	FADD	0.350	0.122	0.134	0.681	0.000	0.362	0.131	0.477	0.006	0.000	0.195	0.038	0.639	0.038	0.000
	TXNRD1	-0.533	0.284	0.139	0.716	0.000	-0.061	0.004	0.476	0.010	0.000	0.586	0.343	0.612	0.022	0.001
	Hsp90	-0.296	0.088	0.141	0.935	0.000	0.235	0.055	0.474	0.010	0.000	-0.410	0.168	0.684	0.056	0.001
	MxA	-0.450	0.203	0.136	0.630	0.000	-0.341	0.116	0.495	0.004	0.000	-0.224	0.050	0.649	0.040	0.000
	tNOX	0.635	0.403	0.112	0.265	0.003	-0.091	0.008	0.485	0.130	0.020	0.522	0.272	0.607	0.018	0.004
	NQO1	0.635	0.403	0.124	0.519	0.001	-0.147	0.022	0.470	0.021	0.000	0.515	0.266	0.604	0.024	0.002
	ERK2	0.307	0.094	0.125	0.392	0.001	-0.220	0.048	0.479	0.010	0.000	0.134	0.018	0.661	0.021	0.005
	p53	0.598	0.357	0.133	0.076	0.631	-0.305	0.093	0.672	0.275	0.335	0.417	0.174	0.618	0.020	0.004
	Bcl-2	0.509	0.259	0.127	0.550	0.001	-0.341	0.116	0.478	0.010	0.000	0.404	0.163	0.624	0.036	0.001
MLR		0.520	0.271	0.121	0.474	0.489	-0.104	0.011	0.725	0.647	0.192	0.401	0.161	0.605	0.065	0.061
ANN1		0.750	0.562	0.094	0.519	0.753	0.807	0.651	0.246	0.897	0.470	0.687	0.472	0.552	0.769	0.999

This table was cited from previously described study.[77]

48

Improvement in prediction performance of ANN models.

ANN models based on nonlinear systems were most adequate to estimate for three food functionalities from intracellular protein expressions. However, prediction performances of the ANN1 models were not enough to estimate because the training data might only include a relatively small number of data points against the number of variables. To improve the prediction performance of the ANN models, ANN2 models were built using the synthesized training data. Optimized parameters of the ANN2 models are shown in **Table I-11**. Prediction performances of the models were verified by the test data and the estimated values are shown in **Table I-3**. These results indicated that the ANN2 models gave basically correct estimated values, although a few exceptional errors between the actual and the estimated values were observed in the models for antiviral and antioxidative stress activities. Statistics of fits obtained from the optimized ANN2 models are shown in **Table I-11** and **Figure I-2**. The RMSE and R^2 from the ANN2 models were better than the ANN1 models **(Table I-10)** in each of the three food functionalities, so that prediction performances of the ANN2 models were more improved than those of the ANN1 models. In addition, all of the *p*-values in **Table I-11** were greater than 0.05 demonstrating that there were no statistically significant differences between the actual data and estimated values calculated by the ANN2 models. Therefore, the ANN2 models have a statistically satisfactory goodness of fit from the modeling point of view. These results showed that the most adequate models to estimate for three food functionalities were the ANN2 models that were built by the synthesized training data. Taken together, the ANN2 models could estimate three food functionalities simultaneously with reasonable accuracy.

Table I-11. Parameters and statistics of the fits obtained from the optimized ANN2 models for cancer cell growth suppression activity, antiviral activity, and antioxidative stress activity.

	Cancer cell growth suppression activity	Antiviral activity	Antioxidative stress activity
Number of input	13	13	13
Number of hidden	6	6	6
Number of output	1	1	1
Learning rate	0.70	0.65	0.70
Momentum factor	0.4	0.4	0.4
Final prediction error (training data)			
R^2	0.938	0.959	0.871
RMSE	0.054	0.109	0.284
Final prediction error (test data)			
R^2	0.714	0.741	0.646
RMSE	0.082	0.209	0.384
Hypothesis testing (*p*-value)			
Mann-Whitney	0.286	0.614	0.236
Levene's test	0.878	0.783	0.382

This table was cited from previously described study.[77]

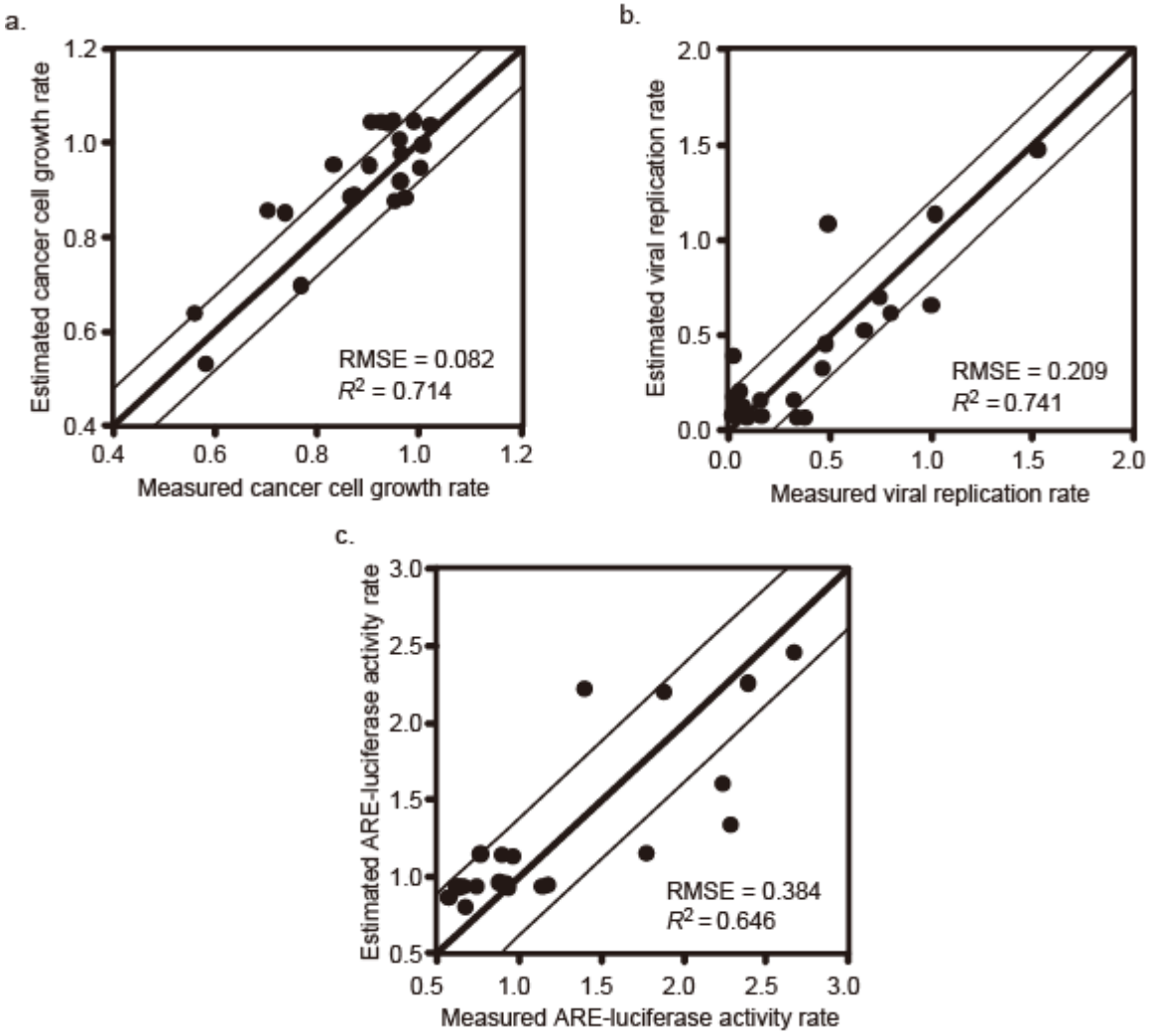

Figure I-2. Correlation of actual versus estimated values with test data using the optimized ANN2 models for cancer cell growth suppression activity, antiviral activity, and antioxidative stress activity.

a, Cancer cell growth suppression activity.

b, Antiviral activity.

c, Antioxidant stress activity.

The area between narrow lines expresses the range of the RMSE between actual and estimated values. The RMSE and the R^2 between actual and estimated values are given in each graph. This figure was modified from previously described figure.[77]

Addition of ANN models for two food functionalities.

To build the ANN models for HTLV-1-infected cell growth suppression activity and NK cell activation activity, ANN2 models were built using the synthesized training data set 2 from training data set 1 **(Table I-2)**. Optimized parameters of the ANN2 models are shown in **Table I-12**. Prediction performances of the models were verified by the test data and the estimated values are shown in **Table I-4 or I-5**. These results indicated that the ANN2 models gave basically correct estimated values, although a few exceptional errors between the actual and the estimated values were observed in the models for HTLV-1-infected cell growth suppression activity and NK cell activation activity. Statistics of fits obtained from the optimized ANN2 models are shown in **Table I-12** and **Figure I-3**. All the *p*-values from **Table I-12** indicate that there is no significant evidence to conclude that the actual data and the data from the ANN2 models differ. Therefore, the ANN2 models for two food functionalities have a statistically satisfactory goodness of fit from the modeling point of view. These results showed that the ANN2 models could also estimate HTLV-1-infected cell growth suppression activity and NK cell activation activity with reasonable accuracy.

Table I-12. Parameters and statistics of the fits obtained from the optimized ANN2 models for HTLV-1-infected cell growth suppression activity and NK cell activation activity.

	HTLV-1-infected cell growth suppression activity	NK cell activation activity
Number of input neurons	13	13
Number of hidden	6	6
Number of output	1	1
Learning rate	0.65	0.65
Momentum factor	0.45	0.40
Final prediction error (training data)		
R^2	0.830	0.954
RMSE	0.174	0.255
Final prediction error (test data)		
R^2	0.774	0.951
RMSE	0.162	0.190
Hypothesis testing (*p*-value)		
Mann-Whitney	0.059	0.937
Levene's test	0.477	0.755

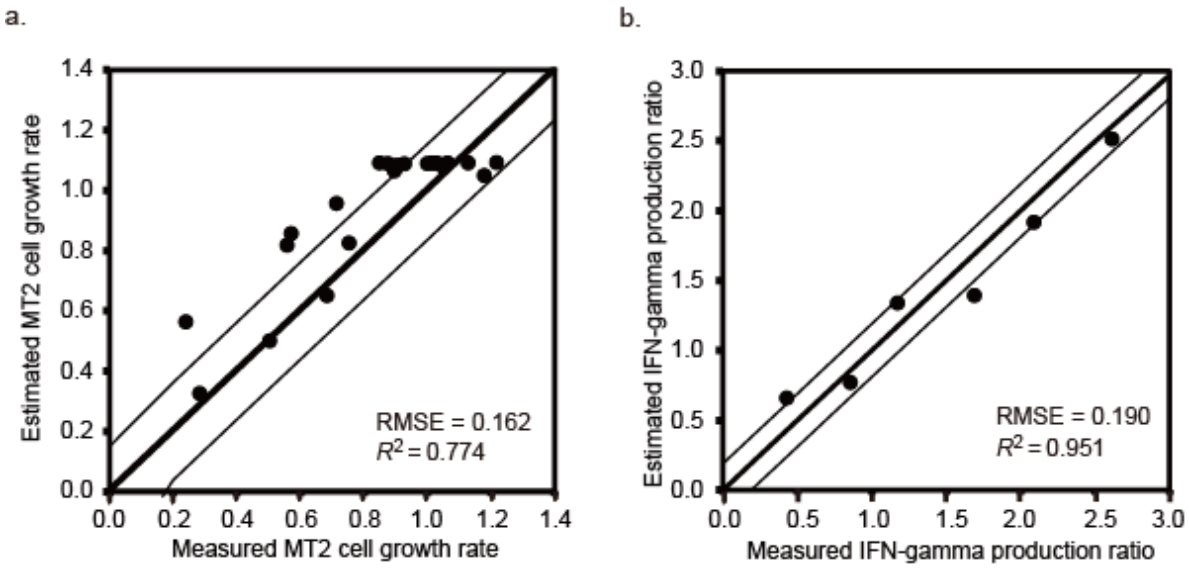

Figure I-3. Correlation of actual versus estimated values with test data using the optimized ANN2 models for HTLV-1-infected cell growth suppression activity and NK cell activation activity.

a, HTLV-1-infected cell growth suppression activity.

b, NK cell activation activity.

The area between narrow lines expresses the range of the RMSE between actual and estimated values. The RMSE and the R^2 between actual and estimated values are given in each graph.

First screening of citruses by the optimized models.

We screened pericarp extracts of four citruses, such as bitter orange, hyuganatsu, and kumquat, for five food functionalities using the optimized ANN2 models. The relative expression of thirteen kinds of marker proteins were input to each ANN2 models **(Table I-13)**. And then, their estimated values for five food functionalities were calculated by their ANN2 models. Results of estimation are shown in **Figure I-4**. All citruses were estimated to have NK cell activation activity. Among them, kumquat pericarp extract was found to have the strongest activity.

Table I-13. Marker protein expression rate of pericarp extracts of bitter orange, hyuganatsu, and kumquat.

Food Extracts	Conc.[a]	marker protein expression rate												
	(μg/mL)	1[b]	2[c]	3[d]	4[e]	5[f]	6[g]	7[h]	8[i]	9[j]	10[k]	11[l]	12[m]	13[n]
bitter orange pericarp	200	0.623	0.601	0.653	0.573	0.688	0.667	0.412	0.512	0.379	0.615	0.586	0.556	0.572
kumquat pericarp	200	0.923	0.968	0.962	1.008	1.191	1.111	0.989	1.022	1.083	0.878	0.990	0.926	0.974
hyuganatsu pericarp	200	0.872	0.914	0.874	0.873	1.055	0.952	0.986	0.826	0.623	0.941	1.002	0.973	0.880

[a] Conc.: concentration. [b] 1: thioredoxin. [c] 2: survivin. [d] 3: Hsp70. [e] 4: XIAP. [f] 5: FADD. [g] 6: TXNRD1. [h] 7: Hsp90. [i] 8: MxA. [j] 9:. tNOX. [k] 10: NQO1. [l] 11: ERK2. [m] 12: p53. [n] 13: Bcl-2

55

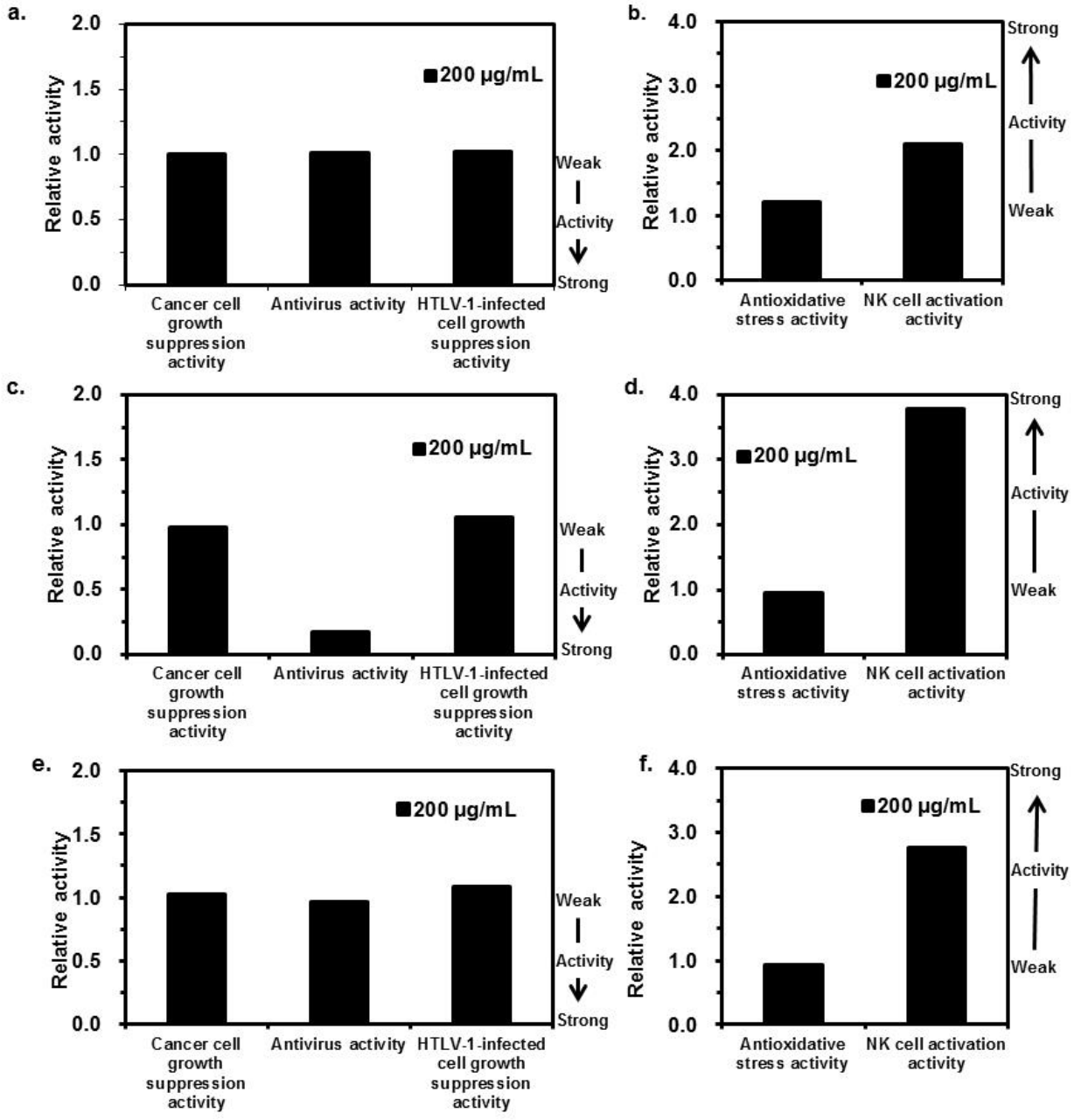

Figure I-4. Estimated values of four citruses pericarp extracts.

a and b, bitter orange pericarp extract.

c and d, kumquat pericarp extract.

e and f, hyuganatsu pericarp extract.

Discussion

A mathematical model with descriptors of compound structure and/or physical and chemical characteristics, a QSAR, is well known as a means of estimating the physiological and chemical activity of a compound in the field of pharmacy.[97-100] QSAR is an effective prediction method for a single compound whose structure is already known, however it is not suitable for a functional prediction of food constituents. Often a test sample is not an isolated or purified compound, and instead, a crude extract of food is evaluated. In this case, the molecular structure information of a test compound cannot be used as a descriptor. Hence, the expression data of marker proteins in the cell that replied to stimulation by a compound were utilized as the descriptors in this study. A change in expression level of an intracellular protein reflects the various phenomena that occur in a cell. It is known that some marker proteins are related to pathophysiological functions, for example, caspase family enzymes[101] and p53[102] contribute to apoptosis, and tumor necrosis factor-alpha[103, 104] and interleukin-6[103, 105] contribute to inflammation. In this study, an empirical modeling method was adopted because intracellular proteins including ones that have an unknown relationship to food functionalities were assumed marker proteins. An empirical modeling method is adaptable using experimental results. The model based on biochemical descriptors was able to estimate food functionality of a test sample within an allowable error even if the sample was an extract including a complex mixture of components. Furthermore, if the expression data of marker proteins are used as common data, it is expected that activities of plural food functionalities can be estimated at the same time. We evaluated three food functionalities, cancer cell growth suppression activity, antiviral activity and antioxidative stress activity, to check whether plural food functionalities could

be estimated at the same time. The model was able to estimate three food functionalities from the data common to plural effects, viz. expression data of marker proteins that was not used for learning of the model **(Table I-3)**. The estimated values obtained from the model were similar to the actual values for a wide range of activities. Physiological activities of the previously reported compounds and extracts were confirmed by the model. For example, genistein and the rosemary extract have a cancer cell growth suppression activity,[14, 61, 79-82] and a defense effect against oxidative stress.[83-91] Lovastatin[92-95] and blueberry leaves extract[49] have a suppression activity against HCV replication. Our results suggest that plural food functionalities of a compound or extract can be estimated from the expression data of marker proteins efficiently. Using only a single wet experiment, namely measurement of the expression level of a cellular protein in response to stimulation by a test compound, made it possible to estimate for multiple food functionalities using a calculation with a high accuracy.

Generally a clinical test involves a single tumor marker but there are many cases where a combination of several plural markers allows a more precise diagnosis. Prostate-specific antigen (PSA) is the most widely used serum biomarker for early detection of prostate cancer.[106] However, the utility of PSA has been limited by a lack of specificity within the 4 to 10 ng/mL range, such that a second biochemical marker, namely free PSA, must be measured and the free-to-total serum PSA ratio can be used to increase specificity.[107] Furthermore, according to a recent report, a mass spectral serum profiling method that is based on a multimarker was higher in accuracy, sensitivity, specificity, a positive predictive value, and a negative predictive value than diagnosis only by PSA.[108] Our results indicated that the MLR analysis model using the multimarker had higher prediction accuracy than the SLR analysis models using the single marker **(Table I-6 and 7)**. If a relationship between a marker protein and a food functionality does not depend on a protein

expression level, it may be difficult to predict a food functionality only using a single marker. In addition, it will be difficult to predict a food functionality only by a single marker when plural mechanisms are present for one food functionality. For example, the antiproliferative effect accompanying apoptosis and/or cell cycle arrest in cancer cells is regulated by a complex signal transduction pathway. p53, one of the tumor suppressor genes, participates in regulation of cell cycle progression at G_1/S and G_2/M phases and induction of apoptosis.[102] Genistein enhances p53 expression in HepG2 cells, and an antiproliferative effect is shown.[81] In this study, genistein enhanced expression of p53 and had an effect on the antiproliferation of HepG2 cells **(Table I-3)**. However, it is not always true that an antiproliferative effect in cancer cells is regulated via the p53-dependent pathway. Carnosic acid, a component of rosemary, shows an antiproliferative effect through G_2 cell cycle arrest in p53-deficient human prostatic cancer PC3 cells.[109] Additionally, to our knowledge there have been no previous reports of an antiproliferative effect through a p53-dependent pathway by rosemary extracts and/or components such as carnosic acid, carnosol and so on. As shown in **Table I-3**, an antiproliferative effect was shown by the rosemary and the Japanese radish leaves, and the expression level of p53 remained unchanged. In this way it would be difficult to evaluate a food functionality only by a single marker, when there was a large difference in the expression level of the intracellular protein that was influenced by the different constituents with a similar food functionality.

ANN was the best among the tested models. Therefore, it seems that a relationship between food functionality and expression patterns of marker proteins were non-linear. Because expression patterns of intracellular proteins are very complicated, linear separation may have been difficult. An ANN trained by error back propagation[96] can resolve a problem that could not be divided into a linear solution. Therefore, for solution of various complicated problems, ANN is applied in many

fields e.g. toxicology,[110] pharmacy,[111] food safety, and quality analysis.[112] ANN, which can solve a complicated problem, would be suitable for our model that has 13 descriptors of plural marker protein expression levels.

Though the plural food functionalities can be estimated from the expression data of marker protein, there are still some points that should be improved. Food constituents used for training data were biased towards polyphenols. Besides polyphenols of plant origin, food products contain many constituents e.g. proteins and peptides of animal and marine products origin, polysaccharides of mushrooms, fatty acids of animal, marine and plant origin. There is a possibility that an estimation method based on an empirical modeling approach cannot be estimated precisely in a constituent of the kind that is not learned. Therefore, the model must be trained using data of various kinds of food constituents. From the point of view of modeling, if the number of marker proteins, or descriptors, is increased, accuracy to estimate will rise. However, the number of necessary data points increases if the number of descriptors increases, because over-fitting occurs when the number of data is insufficient compared with the number of descriptors. Since it is difficult to collect enormous data to prevent over-fitting, adequate marker proteins should be chosen, and unnecessary markers should be excluded from the model. Therefore, in our laboratory we are currently studying ways to choose better marker proteins.

In conclusion, plural food functionalities can be estimated simultaneously from the expression data of marker proteins. This system will be effective as a prediction model that can estimate plural food functionalities simultaneously. Being able to presume plural food functionalities only by measuring the expression data of the marker proteins means they are more promptly and handily assessable because they need not be measured by using plural methods. Furthermore, if more food functionalities can be presumed from the expression data of the marker

proteins at the same time, it will be useful as a first screening method of food constituents for various beneficial purposes. In fact, blueberry leaves were found to have two food functionalities such as antiviral activity and HTLV-1-infected cell growth suppression activity by our system at same time. In addition, the pericarp extracts of four citruses, such as bitter orange, hyuganatsu, and kumquat, were estimated to have NK cell activation activity. The food factor that is common to citrus pericarp may participate in the activity. Further studies are needed to evaluate their activities *in vivo* and the molecular mechanism responsible for their activities *in vitro*.

Chapter II

Antiproliferative effect of oligomeric proanthocyanidin fraction from the leaves of *Vaccinium virgatum* Aiton on human T-cell lymphotropic virus type 1-associated cell lines

In Chapter I, we showed that *Vaccinium virgatum* Aiton (rabbiteye blueberry) leaf extracts have a strong growth inhibitory effect on HTLV-1-infected cell line MT2. However, the growth inhibitory potential of blueberry leaves (BBL) and their constituents on HTLV-1-associated cell lines are not well characterized.

The fruits and leaves of blueberry, a member of the Ericaceae family, contain high levels of polyphenols and have high antioxidant capacity. The content of polyphenols and the antioxidant activity of BBL are relatively high compared with fruits.[113] Despite the fact that BBL have high polyphenols content and antioxidant activity, the leaves have only been used in a tea as a folk medicine treatment for diabetics in Europe. Analysis of the chemical constituents by Matsuo *et al.* has revealed that the most abundant polyphenols in rabbiteye BBL are oligomeric proanthocyanidins.[114] Since they can suppress hepatitis C virus replication,[49, 77] BBL have recently come to be used as a tea also in both North America and Japan. Recent studies show that the proanthocyanidins from rabbiteye BBL exert not only suppressive effect on hepatitis C virus replication but also some health-promoting effects *in vitro* or *in vivo.*[49, 77, 115, 116] Noteworthy, orally administered proanthocyanidins fraction from rabbiteye BBL, which is separated by a similar method as our study, enhances lipolysis in the liver, resulting in the fraction exerts hypolipidemic

effect on obese Otsuka Long-Evans Tokushima Fatty rats.[116] Proanthocyanidins, compounds highly concentrated in dietary plants such as grapes and cacaos, is known to inhibit the proliferation of various cancer cells including breast cancer, lung cancer, and colorectal carcinoma.[117-120] However, to our knowledge, the growth inhibitory potential of BBL constituents has not been evaluated against HTLV-1-associated cell lines. Therefore, we evaluated the inhibition of cell growth by BBL fractions on HTLV-1-associated cell lines and the effects of those fractions on the cell cycle and induction of apoptosis. Moreover, we analyzed the molecular mechanisms responsible for the apoptotic effects and cell cycle arrest induced by the BBL fractions in HTLV-1-associated cell lines.

Experimental Procedures

Materials. Folin-Denis reagent, cyanidin chloride, chlorogenic acid, and rutin were purchased from Sigma Chemical Co. (St. Louis, MO, USA). Gallic acid monohydrate, (-)-epicatechin, and quinic acid were obtained from Wako Pure Chemical Industries, Ltd. (Osaka, Japan). (+)-catechin was purchased from Kurita Kogyo (Tokyo, Japan).

BBL fractions. The BBL fractions were separated by a previously described method with some modifications **(Figure II-1)**.[116] A lyophilized powder of fresh rabbiteye BBL was kindly supplied by Unkai Shuzo Co., Ltd. (Miyazaki, Japan). The lyophilized BBL powder (300 g) was extracted for 30 min with boiling water (15 L) and then cooled in an ice bath. After centrifugation (10 min at 1,700 × *g*), the supernatant was lyophilized and stored at -20°C until use. The lyophilized powder (57.7 g) of BBL hot water extracts (BBL-HWE) was suspended in distilled water (3 L), followed by sonication at 50°C for 30 min. Insoluble material was removed by filtration. The filtrate was directly subjected to Sephadex LH-20 column chromatography (5 cm i.d. × 100 cm), and eluted with water containing increasing proportions of methanol (100% water and then 20%, 40%, 60%, 80% and 100% methanol), and finally eluted with 60% acetone. The eluate was collected in test tubes (900 mL in each) to yield seven fractions (F1-F7), concentrated with a vacuum evaporator, and completely freeze dried.

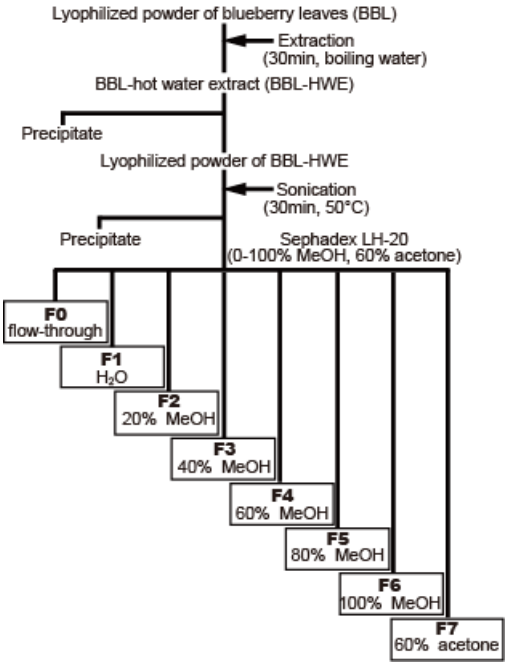

Figure II-1. Separation of the polyphenols from BBL-HWE using a Sephadex LH-20 column chromatography. This figure was cited from previously described figure.[121]

Chemical assays. The total phenols content was determined by modified Folin-Denis method.[122] Folin-Denis reagent (1 mL) was added to either appropriate dilution of the fractions (1 mL) or standard solution (1 mL). After 5 min, 1 mL of 10% (w/v) Na_2CO_3 was mixed. After 60 min of incubation at room temperature, the test solution was centrifuged at 10,000 × *g* for 5 min. The absorption value was determined at 700 nm, with gallic acid monohydrate used as a standard. The total phenols were expressed as mg gallic acid equivalent/g dry weight.

For quantification of proanthocyanidins, the fractions were measured using the HCl/butanol method.[49] Each fraction was quantitated from 0.5 mg/mL (for F0-F4) or 0.2 mg/mL (for F5-F7) in methanol. Briefly, 400 µL of the solution was mixed with 3.5 mL of *n*-butanol/HCl (95:5, v/v) and 100 µL of 2% (w/v) $NH_4Fe(SO_4)_2 \cdot 12H_2O$ in 2 mol/L HCl, heated in an oil bath at 105°C for 30 min. After heating, the reaction mixture was cooled in water for 15 min, and its absorbance at 550

nm was measured. The proanthocyanidins content was expressed in mg of cyanidin chloride equivalent/g dry weight.

The degree of polymerization of proanthocyanidins is estimated by thiolysis,[49] then reverse-phase high-performance liquid chromatography (HPLC). A solution of 10 mg/mL of a fraction in methanol (500 µL) was mixed with 1,000 µL of 5% (v/v) benzyl mercaptan in methanol and 500 µL of 3.3% (v/v) HCl in methanol, heated at 50°C for 30 min, and then kept at room temperature for 3 h. The resulting thiolytic products were filtered and then the filtrate (1,000 µL) was injected into the HPLC system. The HPLC was carried out on a Shimadzu HPLC system (Kyoto, Japan) equipped with a SPD-20A photodiode array detector and an Atlantis T3 column (4.6 mm × 150 mm, 3 µm, Waters, Millford, MA, USA). The separation conditions were as follows: flow rate, 1 mL/min; elution solvent, A (water) and B (methanol); and the gradient program, 15% to 25% B from 0 to 10 min, 25% to 100% B from 10 to 50 min, 100% B from 50 to 65 min. UV detection was performed at 280 nm. The mean degree of polymerization was calculated as follows: mean degree of polymerization = [sum of (benzylthio adducts × n) + sum of (free flavan-3-ol × n)]/[total free flavan-3-ol] where n represents degree of polymerization of detected flavan-3-ol by thiolysis.

Cell culture. We used five HTLV-1-associated cell lines: two HTLV-1-infected T-cell lines and three ATLL-derived cell lines. HTLV-1-infected T-cell lines MT2 and HUT-102 (obtained from the Fujisaki Cell Center, Hayashibara Biochemical Laboratories, Okayama, Japan) were established from HTLV-1-transformed umbilical cord blood T-cell lines [76] and a patient with cutaneous T-cell lymphoma,[123] respectively. ATLL-derived cell lines Su9T01 and S1T [124] (kindly provided by Dr. N. Arima, Kagoshima University, Japan) and ED-40515 [125] (kindly provided by Dr. M. Maeda, Kyoto University, Japan) were originally established from peripheral blood lymphocytes of a patient with ATLL. HTLV-1-infected T-cell lines, ATLL-derived cell lines, and the human T-cell acute

lymphoblastic leukemia cell line MOLT-4 (obtained from the Fujisaki Cell Center) were cultured in RPMI 1640 medium (Sigma-Aldrich Co., St. Louis, MO, USA) supplemented with 10% fetal calf serum and penicillin-streptomycin (100 U/mL penicillin and 100 μg/mL streptomycin) (Sigma-Aldrich Co.). All cells were maintained in a humidified atmosphere containing 5% CO_2 at 37°C.

Cell growth assay. The effect of the extract of BBL on cell growth was examined by the WST-8 [2-(2-methoxy-4-nitrophenyl)-3-(4-nitrophenyl)-5-(2,4-disulfophenyl)-2*H*-tetrazolium, monosodium salt] cell-counting kit (Dojindo, Kumamoto, Japan), based on the fact that the water soluble formazan reaction occurs only in viable cells. Briefly, cells were inoculated into a 96-well microtiter plate at 9×10^3 cells/well, and cultured for 24 h. The cells were treated with various concentrations of BBL extracts or fractions or compounds (quinic acid, chlorogenic acid, rutin, (+)-catechin, and (-)-epicatechin) or vehicle control (dimethyl sulfoxide). After 72 h of incubation, WST-8 (10 μL) was added for 4 h of incubation, and the absorbance was measured at 450 nm with a reference wavelength of 650 nm using a multichannel microtiter plate reader (Emax; Molecular Devices, Redwood City, CA, USA). The effect of BBL extract on cell growth was calculated as the percent of control (vehicle-treated cells), which was arbitrarily assigned a value of 100% growth.

Cell cycle and apoptosis analysis. MT2 and Su9T01 cells (1×10^5 cells/mL) were treated with or without F7 for 24 h. Retrieved cells were then washed with cold phosphate buffered saline (PBS) and fixed in ice-cold methanol at -20°C for at least 30 min. Cells were then treated with 10 μg/mL propidium iodide and 10 μg/mL Ribonuclease A (Sigma-Aldrich Co.), and incubated in the dark at room temperature. Analysis of the cell cycle and detection of the sub-G_1 population were performed using an Epics XL flow cytometer (Beckman Coulter, Fullerton, CA, USA) equipped with MultiCycle software (San Diego, CA, USA). Cells were excited with a 488 nm argon laser

line and the fluorescence of propidium iodide was analyzed on FL3 (610 nm), counting 10,000 events per sample.

Western blot analysis. MT2 and Su9T01 cells (1×10^5 cells/mL) were treated with or without F7 for 24 h. The cells were harvested and collected by centrifugation at 180 × *g* for 5 min. The cell pellet was washed with ice-cold PBS, and then lysed in lysis buffer [50 mmol/L Tris–HCl (pH 7.5), 0.5% Nonidet-P40, 5 mmol/L EDTA and 150 mmol/L NaCl], supplemented with Complete EDTA-free protease inhibitor cocktail (Roche, Basel, Switzerland). After vortexing, the cell lysates were centrifuged at 8,000 × *g* for 20 min at 4°C, and the supernatant was stored at -80°C until required. Stepwise extraction of the cytosolic fraction and organelle/membrane fractionation was performed with a subcellular proteome extraction kit (Merck, Darmstadt, Germany) according to the manufacturer's instructions. The total protein content was determined by the DC protein assay (Bio-Rad Laboratories, Hercules, CA, USA). Aliquots of the protein samples were separated by electrophoresis on sodium dodecyl sulfate-polyacrylamide gels, and then transferred onto polyvinylidene difluoride membranes (Millipore, Bedford, MA, USA). For blocking, 5% skim milk in PBS containing 0.1% TritonX-100 was used. The following primary antibodies were applied: cleaved caspase-3, cleaved caspase-8, cleaved caspase-9 (Asp 315 and 330), cleaved poly (ADP-ribose) polymerase (PARP), p53, $p21^{Waf1/Cip1}$, cyclin B1, and cdc2 (Cell Signaling, Danvers, MA, USA), Bax (Biolegend, San Diego, CA, USA), Bcl-2, survivin, X-linked inhibitor of apoptosis protein (XIAP) (R&D Systems, Minneapolis, MN, USA), and death receptor (DR) 4 and DR5 (ProScience Inc., Poway, CA, USA). β-Actin (Sigma-Aldrich Co.) was used as a loading control. The antibodies were incubated overnight at 4°C. Secondary horseradish peroxidase-conjugated anti-mouse, and rabbit antibodies (Cell Signaling), and anti-goat antibody (Pierce, Rockford, IL, USA) were applied for 1 h at room temperature. Primary and secondary antibodies were diluted in

Canget signal solution (TOYOBO, Tokyo, Japan). The immunoblots were visualized using Immunostar Zeta (Wako Pure Chemical Industries, Ltd., Osaka, Japan), and a Chemi Doc XRS-J digital densitometer (Bio-Rad Laboratories). Band intensities were quantified with Quantity One Software (Bio-Rad Laboratories).

Statistical analysis. All results are expressed as the means ± standard error (SE) of at least three independent experiments. A one-way analysis of variance (ANOVA) and Dunnett's post test were used to evaluate the differences between the means of the results for non-HTLV-1-infected leukemic Molt-4 T cells and HTLV-1-related cells or the control and treated samples. A *p*-value of <0.05 was considered significant. Statistical analysis was performed using GraphPad Prism version 5.0 (GraphPad Software, San Diego, CA, USA).

Results

Inhibition of the proliferation of HTLV-1-associated cell lines by BBL-HWE and fraction

We have recently shown that an 80% ethanol extract of BBL inhibits the proliferation of HTLV-1-associated cell lines. As BBL have been used in Europe as a tea, we first examined whether BBL-HWE also inhibited the proliferation of several HTLV-1-associated cell lines. The BBL-HWE suppressed the cell growth of two HTLV-1-infected T-cell lines (MT2 and HUT-102) and three ATLL-derived cell lines (S1T, ED-40515, and Su9T01) in a dose-dependent manner **(Figure II-2)**. Cell growth of a control HTLV-1-negative T-cell line, MOLT-4, was also inhibited, but MOLT-4 cells were less susceptible to BBL-HWE than HTLV-1-associated cell lines. Inhibition of cell growth was significantly greater in all HTLV-1-associated cell lines than in MOLT-4 cells at 100 μg/mL of BBL-HWE.

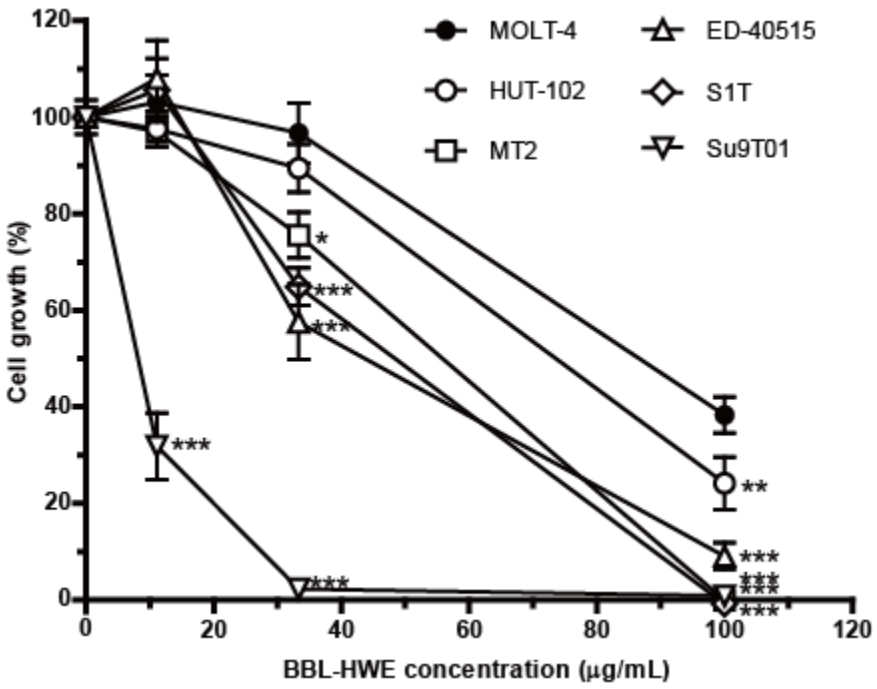

Figure II-2. Cell growth inhibitory effects of BBL-HWE in HTLV-1-associated cell lines. Cells were treated in the presence or absence of BBL-HWE and cell growth was measured by the WST-8 assay at 72 h. The relative growth of the cultured cell is presented as the mean ± SE (n=3). The data obtained were statistically analyzed using one way ANOVA followed by Dunnett's test for individual comparison of groups with HTLV-1-negative leukemic Molt4 T cells. *p<0.05, **p<0.01, and ***p<0.001. This figure was cited from previously described figure.[121]

We next separated BBL-HWE by modifications of the method of Inoue *et al.* **(Figure I-1)**.[116] Then, the effect of the BBL-HWE fractions on MT2 cell proliferation was examined by the WST-8 assay. As shown in **Table II-1**, the F7 (60% acetone fraction) exhibited lower IC_{50} values than the other fractions (F0-F6), showing the strongest inhibitory effect. Previous studies reported that acetone (50-60%) fraction from BBL by Sephadex LH-20 contained more total phenols and condensed tannins (proanthocyanidins) than the other fractions.[116, 126] We then performed chemical analysis of the fractions including total phenols content, proanthocyanidins content, and the mean degree of polymerization. Total phenols and proanthocyanidins contents varied greatly among all

the fractions, the highest value being measured for F7 **(Table II-1)**. Although F6 and F7 showed very similar values of total phenols content, proanthocyanidins content of F7 was 2.1-fold higher than that of F6. The F7 may contain lower content of monomeric proanthocyanidins such as (−)-epicatechin and (+)-catechin than F6, because the HCl/butanol method is applied to detect the oligomeric forms in proanthocyanidins. The mean degree of polymerization for F6 and F7 was 2.4 and 3.1, respectively. F7 was found to be a complex mixture of proanthocyanidins, namely, oligomeric proanthocyanidins (OPA) with mean degree of polymerization of 3.1. Then, as proanthocyanidins from BBL were mainly composed of epicatechin and catechin units,[116] we examined the growth inhibitory effects of (−)-epicatechin and (+)-catechin in MT2 cells. However, these compounds did not have the effects in the cells **(Figure II-3)**. These results suggest that OPA (except for monomer) from BBL exhibit the growth inhibitory effects on HTLV-1-associated cells. Moreover, a recent study by Matsuo *et al.* has reported that freeze-dried BBL contain 11.34% OPA, 6.16% quinic acid, 2.28% chlorogenic acid, and 0.92% rutin.[114] Then, we also examined the growth inhibitory effects of quinic acid, chlorogenic acid and rutin in three ATLL-derived cell lines (S1T, ED-40515, and Su9T01). IC_{50} values of quinic acid, chlorogenic acid and rutin for three cell lines were >100 μg/mL, showing lack of inhibitory effects **(Table II-2)**.

Table II-1. Fractionation of growth inhibition potency of BBL-HWE toward MT2 Cells.

	Weight (g)	IC_{50}[a] (μg/mL)	Specific activity ($1/IC_{50}$)	Total phenols content[b] (mg/g)	Proanthocyanidins content[c] (mg/g)	Total activity per total phenols (mg/IC_{50})	Total activity per proanthocyanidins (mg/IC_{50})	Mean degree of polymerization
BBL-HWE[d]	57.74	39.5	2.53×10^{-2}	NT[e]	NT	NT	NT	NT
F0	21.40	>100.0	$<1.00\times10^{-2}$	22.8	0.1	<0.2	<0.0	NT
F1	6.46	>100.0	$<1.00\times10^{-2}$	74.1	1.9	<0.8	<0.0	NT
F2	1.56	67.2	1.49×10^{-2}	297.6	1.2	4.4	<0.0	NT
F3	1.17	>100.0	$<1.00\times10^{-2}$	417.9	0.8	<4.2	<0.0	NT
F4	2.69	>100.0	$<1.00\times10^{-2}$	445.5	2.6	<4.5	<0.0	NT
F5	3.89	>100.0	$<1.00\times10^{-2}$	415.1	17.0	<4.2	<0.2	NT
F6	4.71	51.2	1.95×10^{-2}	606.4	95.6	11.8	1.9	2.4
F7	8.69	13.8	7.25×10^{-2}	670.0	202.4	48.6	14.7	3.1

[a] IC_{50}: 50% inhibitory concentration. [b] expressed in mg gallic acid equivalents per gram of dry weight. [c] expressed in mg cyaniding chloride equivalents per gram of dry weight. [d] BBL-HWE: Blueberry leaf hot water extract. [e] NT: Not tested. This table was cited from previously described study.[121]

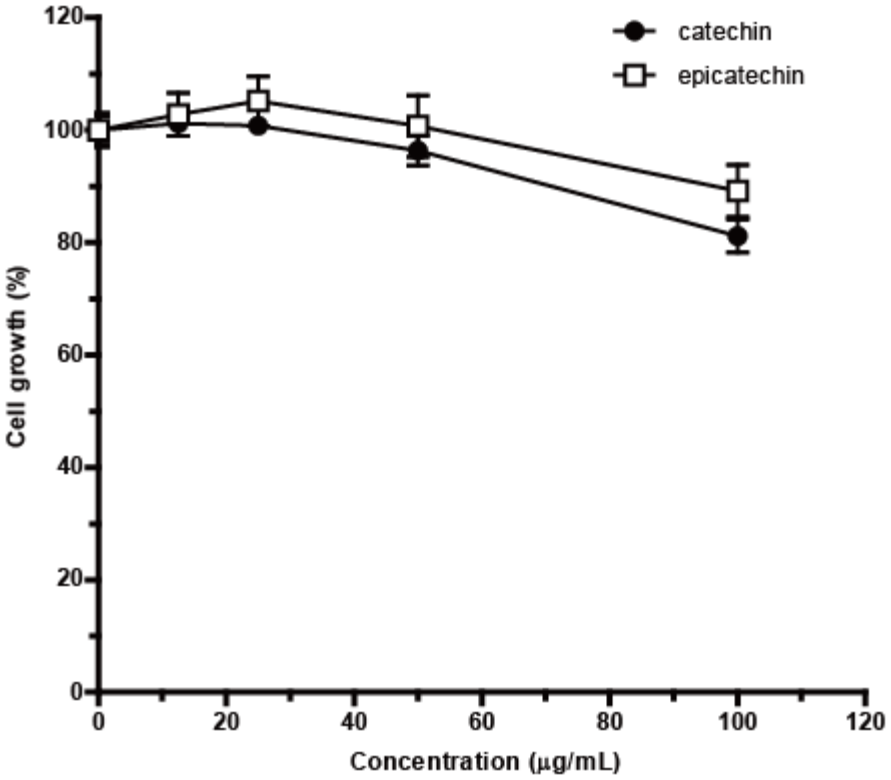

Figure II-3. Cell growth inhibitory effects of (−)-epicatechin and (+)-catechin in MT2 cells. Cells were treated in the presence or absence of (−)-epicatechin or (+)-catechin and cell growth was measured by the WST-8 assay at 72 h. The relative growth of the cultured cell is presented as the mean ± SE (n = 3). This figure was cited from previously described figure.[121]

Table II-2. Growth inhibition effects of quinic acid, chllorogenic acid and rutin on ATLL-derived cell lines.

Compounds	IC_{50}[a] (μg/mL)		
	S1T	ED-40515	Su9T01
Quinic acid	>100.0	>100.0	>100.0
Chlorogenic acid	>100.0	>100.0	>100.0
Rutin	>100.0	>100.0	>100.0

[a] IC_{50}, 50% inhibitory concentration. This table was cited from previously described study.[121]

The growth inhibitory effects of the OPA-F7 were also evaluated against five HTLV-1-associated cell lines and the HTLV-1-negative T-cell line MOLT-4 **(Figure II-4)**. Although the growth of all tested cell lines was inhibited by the fraction in a dose-dependent manner, MOLT-4 cells (IC_{50}, 32.4 μg/mL) had a lower sensitivity to the fraction than HTLV-1-associated cell lines (IC_{50}, 2.8-22.2 μg/mL). The ATLL-derived cell lines, ED-40515, S1T, and Su9T01, were more sensitive to the OPA fraction compared with the HTLV-1-infected T-cell lines, MT2 and HUT-102. In HTLV-1-infected T-cell lines, MT2 cell growth was more strongly inhibited by the OPA fraction than HUT-102 cell growth. Moreover, Su9T01 cells (IC_{50}, 2.8 μg/mL) had the highest sensitivity to the fractions among all of the tested cell lines. Therefore, we focused on the defining the mechanism of action of the OPA fraction against MT2 and Su9T01 cell growth.

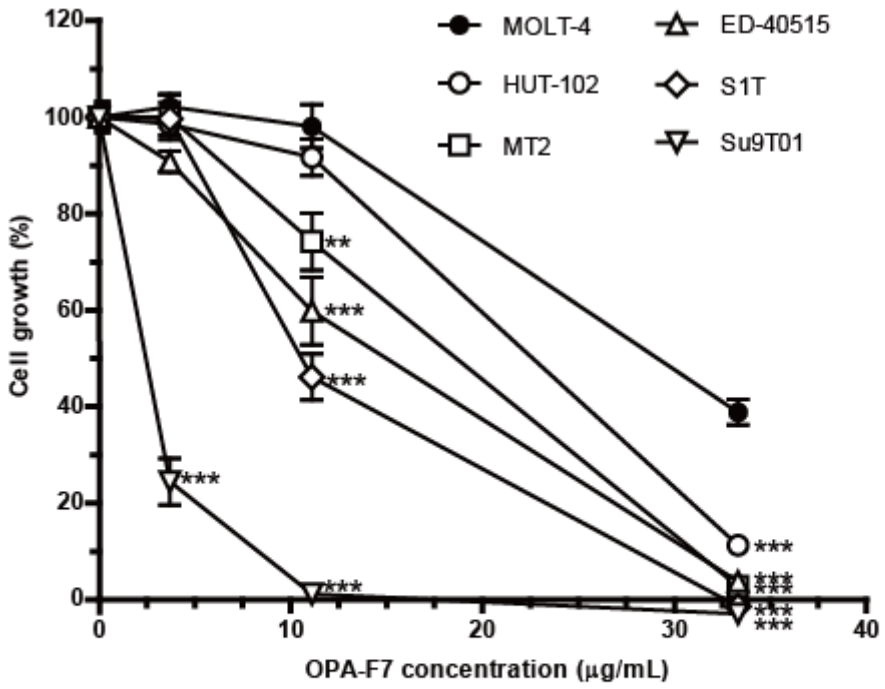

Cell Line	IC_{50} (μg/mL)	Cell Line	IC_{50} (μg/mL)
MOLT-4	32.4	ED-40515	12.7
HUT-102	22.2	S1T	10.7
MT2	13.8	Su9T01	2.8

Figure II-4. Cell growth inhibitory effects of OPA-F7 in HTLV-1-associated cell lines. Cells were treated in the presence or absence of OPA-F7 and cell growth was measured by the WST-8 assay at 72 h. The relative growth of the cultured cell is presented as the mean ± SE (n = 3). The data obtained were statistically analyzed using one way ANOVA followed by Dunnett's test for individual comparison of groups with HTLV-1-negative leukemic Molt4 T cells. $^{**}p<0.01$, and $^{***}p<0.001$. IC_{50} data are summarized in the corresponding table below graph. This figure was cited from previously described figure.[121]

Induction of apoptosis in MT2 and Su9T01 cells by OPA fraction 7

To investigate whether induction of apoptosis account for the cell growth inhibition observed in HTLV-1-associated cell lines (MT2 and Su9T01), cells were treated with OPA–F7 for 24 h. Then, the amount of dying and dead cells in the cell populations was determined by flow cytometric analysis and corresponded to the percentage of hypodiploid cells present in the sub-G_1

region. In MT2 cells, OPA-F7 induced a significant dose-dependent increase in the sub-G_1 population, regarded as apoptotic cells **(Figure II-5a)**. As shown in **Figure II-5b**, OPA-F7 also significantly induced cell death in Su9T01 cells at high concentration. Moreover, we examined the effect of OPA-F7 on the expression of several intracellular regulators of apoptosis by western blot analysis. We first investigated whether the observed apoptosis was due to caspase activation. Indeed, in both MT2 and Su9T01 cells, OPA-F7-induced apoptosis was associated with caspase activation, as shown by PARP cleavage into its death-associated fragment **(Figure II-5c)**. Moreover, OPA-F7 treatment resulted in increases of cleaved/activated caspase-3, -8, -9 in MT2 and Su9T01 cells **(Figure II-5c)**. These results show that OPA-F7 treatment induces apoptosis in HTLV-1-associated cell lines (MT2 and Su9T01).

We then examined the protein expression levels of the pro- and antiapoptotic proteins Bax, survivin, XIAP and Bcl-2. As shown in **Figure II-5c**, the protein expression levels of Bax and XIAP remained unchanged in MT2 cells. OPA-F7 treatment significantly decreased the expression of survivin, whereas it significantly increased the expression of Bcl-2 in MT2 cells. In contrast, OPA-F7 did not alter Bax, survivin, XIAP and Bcl-2 expression levels in Su9T01 cells **(Figure II-5c)**. Apoptosis is induced via two main routes, involving either the mitochondrial pathway (the intrinsic pathway) or the death receptor-dependent pathway (the extrinsic pathway). Each is initiated by an individual initiator caspase, caspase-9 in the mitochondrial pathway, and caspase-8 and -10 in the death receptor-dependent pathway.[127] OPA-F7 resulted in activation of caspase-8 and -9 in MT2 and Su9T01 cells **(Figure II-5c)**. Therefore, both the mitochondrial and death receptor-dependent pathways may be involved in OPA-F7-induced apoptosis. However, the expression of Bcl-2 in MT2 cells was elevated by OPA-F7 **(Figure II-5c)**. Overexpression of Bcl-2 blocks the mitochondrial pathway.[128] We then investigated whether the death receptor-dependent pathway was

involved in the observed apoptosis. After OPA-F7 treatment, cells were separated into cytosolic and membrane fractions. The expression level of DR4 and DR5 were analyzed by western blot analysis. As shown in **Figure II-5d**, the up-regulation of DR5 expression by OPA-F7 mainly occurred in the membrane fraction (right) and not in the cytosolic fraction (left) in MT2 and Su9T01 cells. The protein expression levels of DR4 remained mostly unchanged in both the cytosolic and membrane fractions. These results likely suggest that OPA-F7-induced apoptosis occurs through the death receptor-mediated caspase-dependent pathway of cell death.

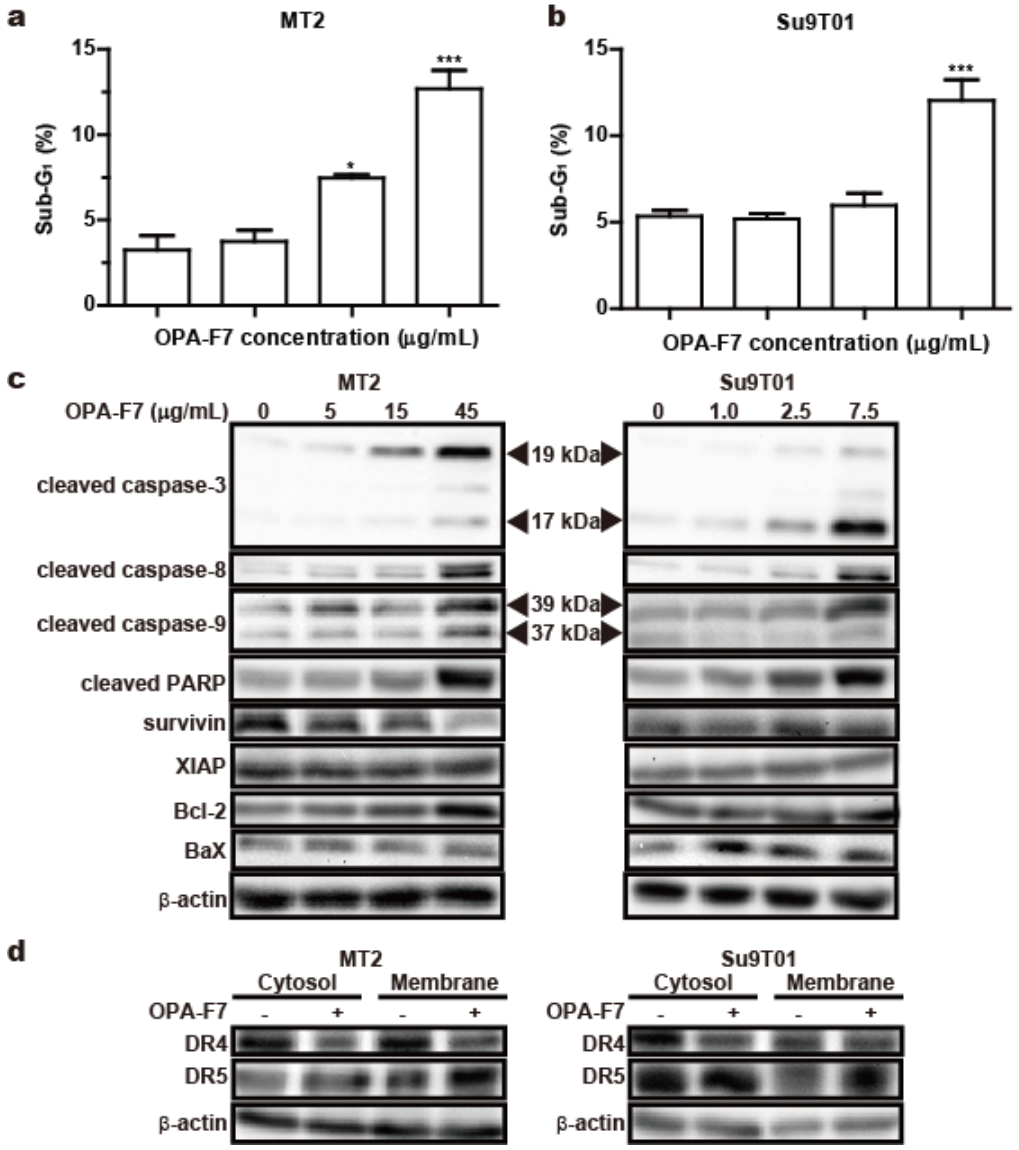

Figure II-5. OPA-F7 induces apoptosis in HTLV-1-associated cell lines. (a) Sub-G_1 analysis of MT2 treated with OPA-F7, (b) Sub-G_1 analysis of Su9T01 treated with OPA-F7. Cells were treated in the absence or presence of OPA-F7 for 24 h. Sub-G_1 percentage represents apoptotic cells. The results are representative of three independent experiments. The data obtained from the experiment were statistically analyzed using one way ANOVA followed by Dunnett's test for individual comparison of groups with non-treated cells. *p<0.05, and ***p<0.001. (c) Amounts of apoptotic proteins cleaved caspase-3, -8, -9 and PARP, survivin, XIAP, Bcl-2 and Bax. (d) The cytosolic fraction (left) and membrane fraction (right) were extracted. Western blot analysis was carried out with anti-DR4 and DR5 antibodies. To assure comparable loading, the same blot was probed with anti-β-actin antibody. This figure was cited from previously described figure.[121]

Induction of cell cycle arrest in MT2 and Su9T01 cells by OPA fraction 7

To investigate also whether induction of cell cycle arrest account for the cell growth inhibition observed in HTLV-1-associated cell lines (MT2 and Su9T01), cells were treated with OPA–F7 for 24 h. Then, the cellular DNA content was also measured by flow cytometric analysis. After OPA-F7 treatment at high concentrations (15 and 45 µg/mL), the G_2/M cell population in MT2 cells was significantly increased with a decrease in G_1 distribution **(Figure II-6a)**. Treatment with OPA-F7 (7.5 µg/mL) caused the accumulation of Su9T01 cells at G_2/M which was accompanied by a simultaneous decrease in the G_1 and S populations **(Figure II-6b)**. These results indicate that the OPA-F7 inhibits G_2/M progression. Moreover, we examined the effect of OPA-F7 on the expression of several intracellular regulators of cell cycle by western blot analysis. The cell cycle is regulated at different check points by the interaction of a variety of cyclins and cyclin-dependent kinases (CDKs). One of the checkpoints, the G_2/M, is regulated by cyclin B1 and the cdc2/CDK1 complex. Our results showed that OPA-F7 treatment down-regulated the protein level of cyclin B1 and cdc2 in MT2 and Su9T01 cells as shown in **Figure II-6c and 6d**. p53 plays a critical role in the regulation of the cell cycle and apoptosis. $p21^{Waf1/Cip1}$ is the principal mediator of cell cycle arrest and is also involved in many important cellular processes including cell cycle progression, apoptosis, and transcriptional regulation through both p53-dependent and p53-independent pathways.[129] Treatment of the HTLV-1-infected T-cells MT2 resulted in a significant increase in p53 and $p21^{Waf1/Cip1}$ protein levels **(Figure II-6c)**. In contrast, p53 and $p21^{Waf1/Cip1}$ were undetected in the ATLL-derived cells Su9T01. These results suggest that the p53-dependent pathway is involved in OPA-F7-induced growth inhibition of the HTLV-1-infected T-cells MT2, whereas the p53-independent pathway is involved in the inhibition of the ATLL-derived cells Su9T01.

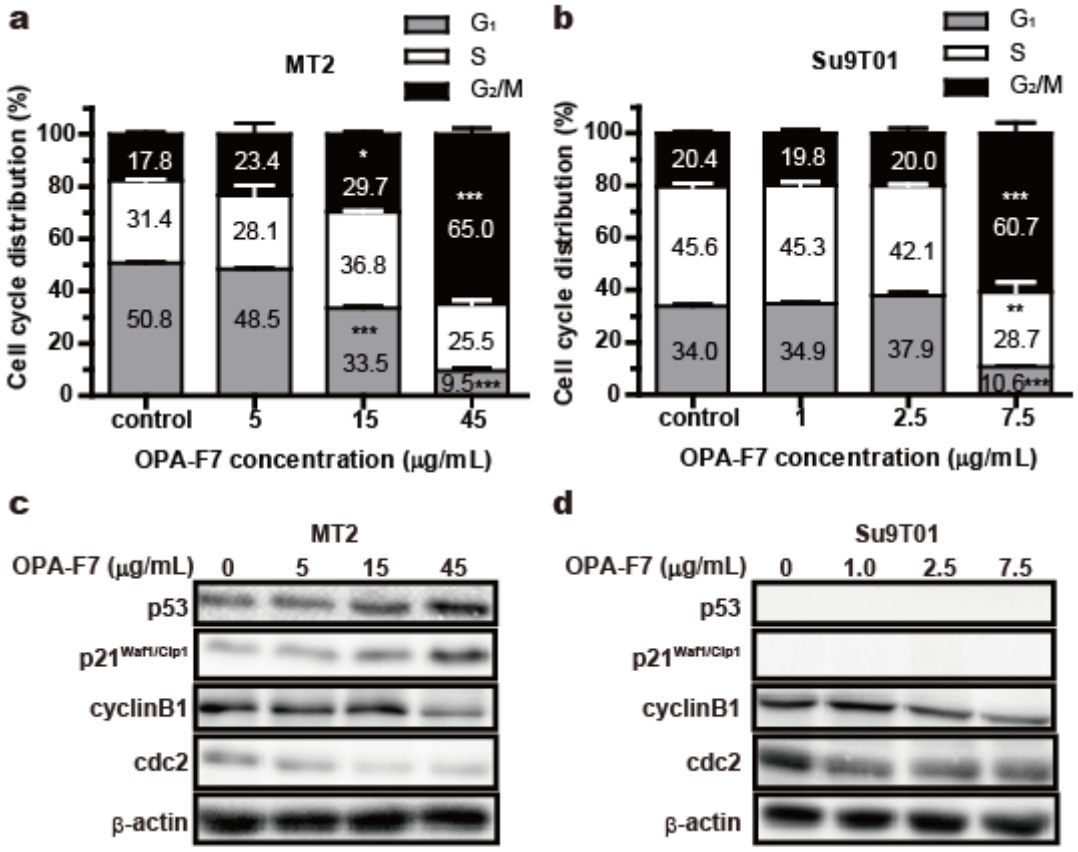

Figure II-6. OPA-F7 induces G2/M cell cycle arrest in HTLV-1-associated cell lines. (a) Cell cycle analysis of MT2 treated with OPA-F7, (b) Cell cycle analysis of Su9T01 treated with OPA-F7. Cells were treated in the absence or presence of OPA-F7 for 24 h. DNA content was analyzed to indicate the stage of the cell cycle. Data represent the mean percentages of the cells at each stage of the cell cycle from three independent experiments. The data obtained from the experiment were statistically analyzed using one way ANOVA followed by Dunnett's test for individual comparison of groups with non-treated cells. *p<0.05, **p<0.01, and ***p<0.001. Amounts of cell cycle-associated proteins cyclin B1, cdc2, $p21^{Waf1/Cip1}$, and p53 in (c) MT2 and (d) Su9T01 cells. To assure comparable loading, the same blot was probed with anti-β-actin antibody. This figure was cited from previously described figure.[121]

Discussion

Proanthocyanidins, naturally occurring phytochemicals, induce cell cycle arrest at the G_0/G_1 and/or G_2/M checkpoint and/or apoptosis, resulting in inhibition of cell growth in various cancer cells.[130] In the present study, our data revealed that an OPA fraction from BBL apparently inhibited the growth of HTLV-1-associated cell lines **(Figure II-4)**. Chemical characteristics of proanthocyanidins, such as the galloylation of catechins and the degree of polymerization, are related to their bioactive capacity. For example, the antiproliferative capacity of a proanthocyanidins fraction toward human colorectal adenocarcinoma HT29 cells is enhanced by both polymerization and galloylation.[131] As shown in **Table II-1**, the most effective fraction (F7) contained OPA with the highest mean degree of polymerization and the highest total activity per proanthocyanidins. Thiol degradation products of an OPA fraction from BBL contained catechin, epicatechin, and epicatechin-4-hydroxyethylthio ether,[116] although it did not contain galloylated catechins such as epigallocatechin and epicatechin gallate. Therefore, proanthocyanidin polymerization should play a more important role than galloylation in the antiproliferative effect of the OPA fraction from BBL. We further showed that the cell growth inhibitory effect was due to an induction in G_2/M cell cycle arrest together with induction of apoptosis in MT2 and Su9T01 cells **(Figure II-5 and 6)**. A previous report shows that proanthocyanidins from various plants mainly cause G_1 cell cycle arrest.[130] For example, proanthocyanidins from grape seed, cranberry, apple, cocoa, and green tea leaves arrest the cell cycle at G_1 in breast carcinoma cells, esophageal adenocarcinoma cells, non-small cell lung cancer cells, epidermoid carcinoma cells, and head and neck squamous cell carcinoma cells.[117, 119, 120, 132-137] In contrast, proanthocyanidins originated from

cocoa, grape seed and pine bark cause G_2/M arrest of the cell cycle in colon carcinoma cells and pancreatic cancer cells.[118, 131, 138] Interestingly, studies of proanthocyanidins from grape seed by Katiyar *et al.* show that proanthocyanidins arrest the cell cycle at G_1 in non-small cell lung cancer cells, epidermoid carcinoma cells, and head and neck squamous cell carcinoma cells,[120, 136, 137] whereas it arrested it at G_2/M in pancreatic cancer cells.[138] It is evident from these results that whether a cell is arrested at G_1 or G_2/M by proanthocyanidins depends on the cell type. Although the OPA fraction from BBL induced G_2/M cell cycle arrest in HTLV-1-associated cell lines, the fraction might induce G_1 cell cycle arrest in other types of cancer cells. It also remains controversial what cellular environment influences proanthocyanidins-induced cell cycle arrest at G_1 or G_2/M.

Cellular responses in the HTLV-1-infected T-cells MT2 and ATLL-derived cells Su9T01 by OPA-F7 differed in the expression of some apoptosis- and cell cycle-related proteins. Moreover, OPA-F7 inhibited the cell growth of Su9T01 cells at low concentrations (7.5 μg/mL) compared with treatment of MT2 cells at 45 μg/mL. By western blot analysis, the protein expression of p53 and $p21^{Cip1/Waf1}$ were increased by OPA-F7 treatment of MT2 cells, whereas the proteins could not be detected in Su9T01 cells. Induction of the CDK inhibitor $p21^{Cip1/Waf1}$ is mediated by both p53-dependent and -independent mechanisms of cellular stress and causes cell cycle arrest at G_1 or G_2/M resulting in a damage response and cell senescence.[139] Besides cell cycle arrest, $p21^{Cip1/Waf1}$ plays essential roles in damage response by regulating fundamental processes like apoptosis and transcription.[140] A recent study reported that the expression of $p21^{Cip1/Waf1}$ is very low in ATLL-derived cell lines, although its expression is high in HTLV-1-infected cell lines.[141] ATLL-derived cell lines have a significantly decreased rate of growth after UV irradiation, although the rate of growth of HTLV-1-infected cell lines is not changed.[141] In the colon carcinoma cells HCT116,

ionizing radiation treatment clearly induces death of $p21^{Cip1/Waf1}$ deficient HCT116 cells, whereas the treatment only slightly induces the death of wild-type HCT116 cells.[142] These findings indicate that low expression of $p21^{Cip1/Waf1}$ may increase in response to cellular stress. Therefore, Su9T01 cells without $p21^{Cip1/Waf1}$ expression may be more strongly inhibited by treatment with OPA-F7 in comparison to MT2 cells which express higher levels of $p21^{Cip1/Waf1}$. As another factor, HTLV-1 Tax, the virus-encoded regulatory protein, may also be able to explain the strong growth inhibitory effect of OPA-F7 in Su9T01 cells. Tax has been shown to play a critical role in cellular transformation by interfering with genome instability, cell cycle and apoptosis.[143] Moreover, Tax enhances expression of various antiapoptotic proteins, including c-Flip, Bcl-xL, Bfl-1, and Hiap-1.[144] Although primary ATLL cells and ATLL-derived cell lines do not express significant levels of Tax, HTLV-1-infected cell lines highly express Tax.[141] Due to Tax-mediated antiapoptotic effects in HTLV-1-infected cell lines MT2, Su9T01 cells without Tax expression may be more strongly inhibited by treatment with OPA-F7 in comparison to MT2 cells which express higher levels of Tax.

In response to various cellular stress including DNA damage, ribonucleotide depletion, and abnormal proliferative signals, p53 activates transcription of target genes with functions in cell cycle control, DNA repair, and apoptosis.[145] Treatment of MT2 cells with OPA-F7 clearly increased p53, cleaved caspase-9, caspase-3, and PARP, and decreased survivin expression. Survivin directly blocks the processing and activation of effector caspases 3 and 7.[146] Moreover, DNA damage induces the p53-survivin signaling pathway and down-regulates survivin expression, resulting in cell cycle arrest and apoptosis.[147] Therefore, the antiapoptotic protein survivin was down-regulated by OPA-F7 treatment of MT2 cells, suggesting that survivin also plays a role in OPA-F7-induced apoptosis. In addition to apoptosis induction, treatment of OPA-F7 also induced

cell cycle arrest at G_2/M. The role of p53 in G_2/M cell cycle arrest in response to DNA damage is multiple targets that can generally be considered to influence either the cell cycle (i.e., cyclin-B, cdc2) or the mitotic machinery (i.e., topoisomerase II).[148] Interestingly, cocoa-derived proanthocyanidins significantly reduces topoisomerase II activity and proliferation in cancer cell lines.[149] Therefore, the growth inhibitory effect induced by OPA-F7 may cause by interference with topoisomerase II.

Caspase 8 is activated by DRs including tumor necrosis factor-related apoptosis-inducing ligand (TRAIL) receptors (DR4 and DR5) and CD95. The OPA fraction from BBL significantly increased cleaved/active caspase 8 in MT2 and Su9T01 cells **(Figure II-5c)**. The fraction also increased DR5 protein in the membrane fraction of these cells **(Figure II-5d)**, suggesting that the DRs will trigger signaling pathways in the treated cells. TRAIL interacts with the death domain-containing receptors DR4 and DR5, resulting in apoptosis induction.[150] TRAIL selectively induces apoptosis in tumor cells without damaging normal tissues.[150] Therefore, TRAIL is one of the most promising therapeutic agents against different types of cancer. However, some tumor cells remain resistant to TRAIL-induced apoptosis.[151] Recent studies have reported that DR can be up-regulated by some natural phytochemicals including quercetin,[152] flavonolignan silibinin,[153] and apple procyanidins,[154, 155] with a resulting decrease in TRAIL-induced resistance to apoptosis. ATLL is also highly resistant to TRAIL-mediated cell death. Rocaglamide, a naturally occurring herbal compound, reduces TRAIL resistance in HTLV-1-associated cells.[156] Wogonin and the structurally related natural flavones apigenin and chrisin also reduce TRAIL resistance in HTLV-1-associated cell lines by up-regulation of DR5.[157] Therefore, OPA-F7 from BBL may also limit TRAIL resistance in HTLV-1-associated cell lines.

Conclusions

This is the first study to show the cell growth inhibitory effect of an OPA fraction from BBL on HTLV-1-associated cell lines. The fraction inhibited the growth of these cell lines by inducing apoptosis and G_2/M cell cycle arrest. OPA fraction-induced apoptosis of HTLV-1-associated cell lines requires the death receptor-mediated caspase-dependent pathway of cell death and treatment of the fraction resulted in arrest at G_2/M by down-regulation of cyclin B1 and cdc2. The OPA fraction from BBL may have the potential to serve as a source of novel compounds for reducing the risk of developing ATLL. However, the growth inhibitory effect induced by the OPA fraction has not yet been verified *in vivo*. Although proanthocyanidins from BBL are high-molecular weight oligomers, orally administered proanthocyanidins must be absorbed from the digestive tract to provide beneficial effects. Recent studies provide evidence that orally administered apple proanthocyanidins (consisting of dimers to pentamers) can be rapidly absorbed and reach both the plasma and liver tissue.[158-160] Moreover, orally administered proanthocyanidins from grape seed inhibit the growth of tumor cells in mouse tumor models.[120, 138] Recent *in vivo* studies of ATLL have shown that food and plant constituents such as curcumin, soy-isoflavones, fucoidan, fucoxanthin, and Bidens pilosa inhibit the growth of tumor cells in immunodeficient mice transplanted with HTLV-1-associated cell lines.[59, 61-64] Further studies of the OPA fraction from BBL on HTLV-1-associated cell lines are needed to evaluate the growth inhibitory effect *in vivo* and the molecular mechanism responsible for the effect *in vitro*.

Chapter III

Effect of kumquat (*Fortunella crassifolia*) pericarp on natural killer cell activity *in vitro* and *in vivo*

In Chapter I, we showed that kumquat (*Fortunella crassifolia*) pericarp extracts have a strong NK cell activation activity. However, the NK cell activation potential of kumquat pericarp and their constituents are not well characterized and the effect has not yet been verified *in vivo*.

Psychological stress induces immune dysregulation, and negative effects are associated with the increased risk of developing diseases such as infectious diseases and cancer.[161-163] During stress, the hypothalamic-pituitary-adrenal axis regulates the systemic release of glucocorticoids and catecholamines which are known to suppress both innate and adaptive immune responses.[164, 165] Glucocorticoids induce apoptosis in lymphocytes[166] and suppress NK cell activity and cytokine production, including IFN-γ, IL-6, and tumor necrosis factor-alpha.[167]

Kumquats (*Fortunella* spp.), a member of the *Citrus* genus, have long been cultivated in China, Japan, Taiwan, and Southeast Asia. As the peel is sweet and the fruit is sour, kumquats are usually eaten raw and whole, or only the peel is consumed. They are also used in the production of candied kumquats, marmalade, kumquat compote, liqueurs, and sauces. In addition to use in the food industry, kumquats have been used in folk medicine for treating sore throats and coughing. Kumquat fruit and peel have previously been reported to contain various nutrients and constituents such as ascorbic acid,[168] carotenoids,[168-170] essential oils[171] and flavonoids.[168, 170, 172] Several studies on kumquats have provided evidence of their health-promoting effects and pharmacological

activities, including antioxidant activity,[172-174] anti-metabolic disorder effects,[175] and antimicrobial activity.[176] However, to our knowledge, NK cell activation potential of kumquat (*Fortunella crassifolia*) pericarp has not been evaluated. Therefore, we investigated the effect of kumquat pericarp acetone fraction (KP-AF) on human KHYG-1 NK cells *in vitro*, and *in vivo* using a restraint stress mouse model. We report here that eating kumquat can help maintain NK cell activity in a stressful environment.

"A part of this chapter is an Author's Original Manuscript of an article published by Taylor & Francis in *Bioscience, Biotechnology, and Biochemistry* available online at http://dx.doi.org/10.1080/09168451.2015.1025033."

Experimental Procedures

Materials. Acetone, *n*-hexane, ethanol, ethyl acetate (EtOAc), acetonitrile, tetrahydrofuran, methanol, RPMI 1640 medium with and without phenol red, penicillin-streptomycin solution, recombinant human interleukin-2, β-carotene, and concanavalin A were obtained from Wako Pure Chemical Industries, Ltd. (Osaka, Japan). Calcein-acetoxymethyl (calcein-AM) and HEPES were purchased from Dojindo (Kumamoto, Japan). Mineral oil light white was purchased from MP Biomedicals LLC (Illkirch, France). AssayMax Corticosterone enzyme-linked immunosorbent assay (ELISA) Kit was purchased from AssayPro (Charles, MO, USA). Lutein, zeaxanthin, and β-cryptoxanthin were obtained from Extrasynthese (ZI Lyon-Nord, Genay, France). *d*-Limonene was purchased from Accustandard Inc. (New Haven, CT, USA). Human and mouse IFN-γ ELISA Development Kit were purchased from PeproTech (Rocky Hill, NJ, USA).

Preparation of kumquat pericarp fraction (KPF). Kumquats (*Fortunella crassifolia*) larger than 33 mm in diameter and over 16 brix were harvested in Miyazaki, Japan, 210 days after flowering. A lyophilized powder of kumquat pericarp (KP) was kindly supplied by Miyazaki JA Food Research & Development Inc. (Miyazaki, Japan). The fractionation scheme for KP is shown in **Figure III-1**. The lyophilized KP powder (30.1 g) was mixed with Na_2CO_3 (0.6 g) and 90 mL of cold acetone. The mixture was stirred for 3 min in an ice bath, filtered through filter paper (No 2; ADVANTEC, Tokyo, Japan), and the filtrate saved. The extraction and filtration was repeated four times using the residue from the first extraction. The filtrate was extracted twice with *n*-hexane/water (1:1.7) and the organic layer was dried (Na_2SO_4) and concentrated with a vacuum evaporator to give KP-AF (273 mg).

The residue from the acetone extraction was extracted another three times with ethanol for 24 h at 40 °C. The ethanol extract was concentrated and the resultant solid (10.25 g) was redissolved in EtOAc to give the EtOAc-soluble solution and EtOAc-insoluble material KP-F8 (9.19 g). The EtOAc-soluble solution was acidified with 1 mol/L HCl to pH 3, then the aqueous layer (A1) was basified with 1 mol/L NaOH to pH 10 in the presence of EtOAc. The aqueous layer (A1-A) was lyophilized to give KP-F1 (6.8 g). The EtOAc layer (A1-E) was washed twice with water, dried with Na_2SO_4 and concentrated to give KP-F2 (3.3 mg). The EtOAc layer (E1) was basified with 1 mol/L NaOH to pH 10. The EtOAc extract (E1-E) was washed twice with water, dried with Na_2SO_4, and concentrated with a vacuum evaporator (KP-F4; 183 mg), while the aqueous layer (E1-A) was further acidified with 1 mol/L HCl to pH 3 in the presence of EtOAc. The aqueous layer (E1-AA) was lyophilized (KP-F3; 4.0 g), and the EtOAc layer (E1-AE) was shaken with 10% $NaHCO_3$ until the aqueous layer reached pH 9. The EtOAc layer (E1-AE-E) was washed twice with water, dried with Na_2SO_4, and concentrated with a vacuum evaporator (KP-F7; 39 mg). The aqueous layer (E1-AE-A) was again acidified with 1 mol/L HCl to pH 3 in the presence of EtOAc. The EtOAc layer (E1-AE-AE) was washed twice with water, dried with Na_2SO_4, and concentrated with a vacuum evaporator (KP-F6; 79 mg). The aqueous layer (E1-AE-AA) was lyophilized (KP-F5; 5.0 g). For *in vivo* experiments, KP-AF (1.04 g) was obtained from the lyophilized powder (54.5 g) of KP.

Chemical assays. Carotenoids used were β-carotene, β-cryptoxanthin, lutein, and zeaxanthin, in agreement with previous kumquat studies.[168, 170] The KP-AF used for the chemical assays was divided into two groups; an unheated group and a heated group (90 °C, 10 min). Each KP-AF sample was dissolved in acetone. The solutions were analyzed for β-carotene and β-cryptoxanthin after 100 times dilution with acetone, and for lutein and zeaxanthin after 10 times dilution with

acetone. High-performance liquid chromatography analysis was performed using Shimadzu LC-10AD vp pumps (Shimadzu, Tokyo, Japan), a SPD-M10 Avp photodiode array detector (Shimadzu), and a Mightysil RP-18 GP C 18 column (250 × 4.6 mm i.d., 5 μm; Kanto Chemical Co., Inc., Tokyo, Japan). The analysis was carried out under isocratic conditions with a flow rate of 1.0 mL/min, and injection volume 10 μL. The mobile phase consisted of acetonitrile (solvent A)/ethanol (solvent B) (8/2, v/v) for β-carotene and β-cryptoxanthin, and tetrahydrofuran/methanol/water (40/30/25, v/v/v) for lutein and zeaxanthin. The column temperature was 50 °C and the absorbance was read at 450 nm. The standard curves were obtained in the concentration range of 0.25–5 μg /mL (β-carotene and β-cryptoxanthin) and the concentration range of 0.2–5 μg /mL (lutein and zeaxanthin).

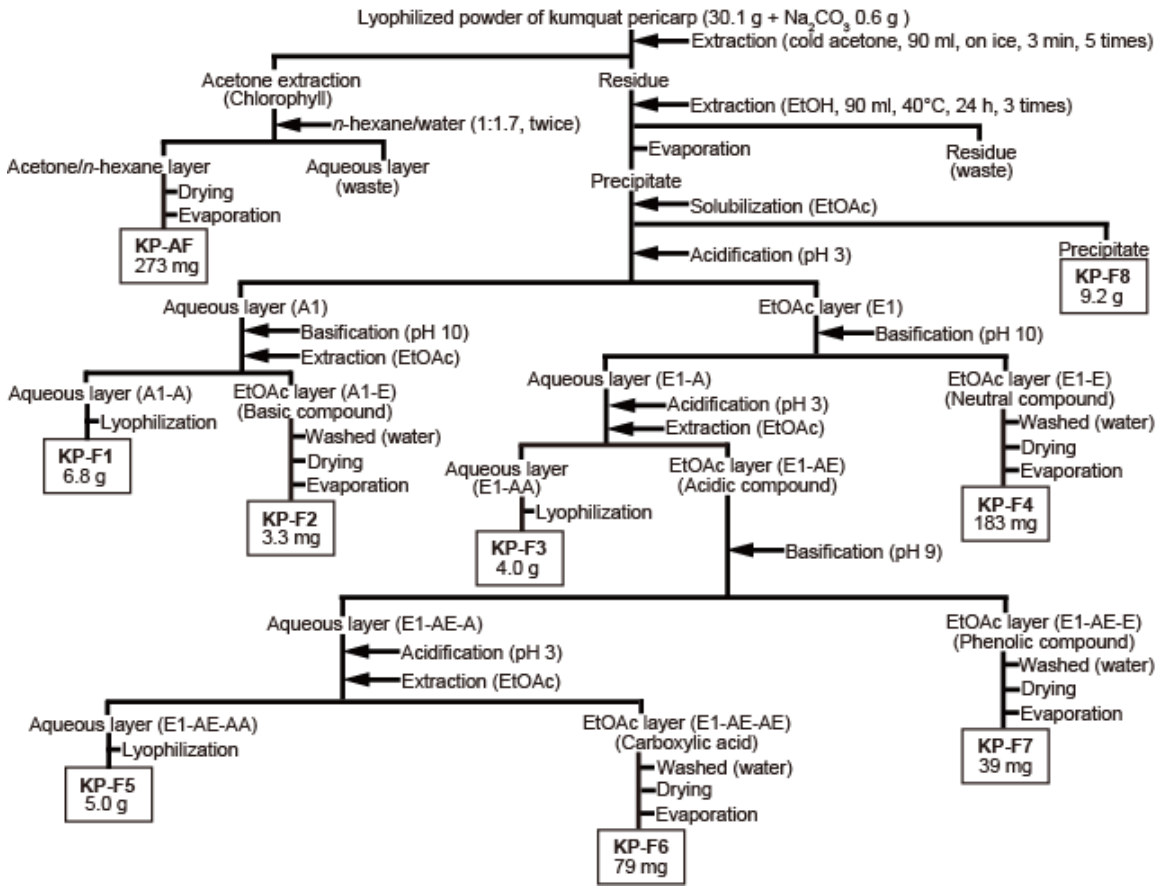

Figure III-1. Fractionation of kumquat pericarp (KP). This figure was cited from previously described figure.[177]

***Cells*.** Human natural killer cells KHYG-1 were obtained from the Japanese Collection of Research Bioresources (Osaka, Japan) and maintained in RPMI 1640 medium supplemented with 10% fetal calf serum, penicillin-streptomycin (100 U/mL penicillin and 100 µg/mL streptomycin), and 100 U/mL interleukin-2. The human chronic myeloid leukemia cells K562 and mouse lymphoma cells YAC-1 were cultured in RPMI 1640 medium supplemented with 10% fetal calf serum and penicillin-streptomycin (100 U/mL penicillin and 100 µg/mL streptomycin). All cells were maintained in a humidified atmosphere containing 5% CO_2 at 37 °C.

Animals and treatment. Male 7-week-old C57BL/6N mice were obtained from Japan SLC, Inc. (Shizuoka, Japan). The mice were acclimatized for a week prior to the experiment. All mice were housed under controlled conditions of temperature at 24 ± 1 °C and 12 h light/12 h dark cycle (lights on from 07:00 to 19:00), and fed with CRF-1 (Oriental Yeast Co. Ltd., Tokyo, Japan) and water *ad libitum*. Mice were treated according to the Animal Experiment Committee of Miyazaki University. The experimental protocol was approved by the ethics committee of Miyazaki University (permit number 2013-040).

The experimental mice were divided into three groups: normal, model control (restraint stress), and KP-AF (restraint stress + KP-AF administration). After acclimatization for 1 week, KP-AF was orally administered to the mice at a dose of 0.6 mg/kg body weight/day for 7 consecutive days. The normal and model control mice were orally administered with mineral oil light white as a vehicle control. On the 7th day of administration, the mice were subjected to restraint stress according to a previously described method with some modifications.[178] Briefly, the mice were first wetted with water and physically restrained for 15 h (19:00 to 10:00) in a restraint cage. The cage was a 50 mL polypropylene centrifuge tube with numerous air holes to increase ventilation, with half of the tube replaced by Mouse Net (BP98-NTM, Natsume Seisakusho, Tokyo, Japan). Normal mice were fed with food and water *ad libitum* for a whole day.

Measurement of plasma corticosterone levels. After restraint, the mice were weighed and small blood samples were collected from the tail vein into a heparin-coated capillary tube (Drummond Scientific, Broomall, PA, USA). Plasma was isolated by centrifugation at 1500 × *g* for 5 min at 4 °C and the samples were stored at −80 °C until measurement. Plasma corticosterone levels were determined using a quantitative competitive sandwich enzyme immunoassay technique using an AssayMax Corticosterone ELISA Kit according to the manufacturer's instructions.

Spleen lymphocytes preparation. The spleens were harvested, washed in RPMI 1640 medium with 10 mmol/L HEPES on ice, and mashed with a plunger on a 70 μm cell strainer (Greiner Bio-one, Frickenhausen, Germany). Collected splenocytes were centrifuged at 400 × *g* for 5 min and hemolyzed with a lysis buffer (0.75% NH_4Cl, 17 mmol/L Tris-HCl, pH 7.65). The lymphocytes were then washed twice with cold RPMI 1640 medium containing 10 mmol/L HEPES, resuspended in cold RPMI 1640 medium without phenol red, and supplemented with 10% fetal calf serum. The cells were then filtered through a 40 μm cell strainer (Greiner Bio-one) and the total number of spleen lymphocytes was determined using a hemocytometer.

NK Cell Cytotoxicity Assay. NK cytotoxic activity was measured using the calcein-AM-release assay, a fluorometric assay comparable to the traditional ^{51}Cr-release assay.[179] Target K562 or YAC-1 cells (1×10^6 cells/mL) were labeled with 10 μg/mL calcein-AM for 1 h at 37 °C with gentle rotation and washed.

NK cell cytotoxicity assay *in vitro* was determined by the cytotoxicity of effector NK cells KHYG-1 against target cells K562. KHYG-1 cells (2×10^5 cells/mL) were treated with KPF, β-cryptoxanthin or vehicle control (dimethyl sulfoxide). After 24 h, retrieved cells were then washed with cold phosphate buffered saline (PBS), resuspended in RPMI 1640 medium without phenol red, and supplemented with 1% bovine serum albumin. KHYG-1 cells (1×10^5 cells/well) and calcein AM-labeled K562 cells (1×10^4 cells/well) were co-cultured at an effector-to-target cell (E:T) ratio of 10:1 on 96-well U-bottomed plates, and incubated at 37 °C for 4 h. Maximum release was produced by incubation of only target cells in medium with 2% Triton X-100. Spontaneous release was produced by incubation of only target cells in medium. After incubation, the cultured mixtures in the 96-well plates were centrifuged at 260 × *g* for 10 min, and 100 μL of the supernatant was transferred to a new plate. The fluorescence was measured with a Spectramax Gemini XS

Fluorescence Microplate Reader (Molecular Devices, Sunnyvale, CA, USA) (excitation filter 485 nm, emission filter 538 nm). The percentage of specific lysis was calculated as follows: Specific lysis (%) = [(experimental release − spontaneous release) / (maximum release − spontaneous release)] × 100.

NK cell cytotoxicity assay *in vivo* was determined by the cytotoxicity of mouse splenocytes against YAC-1 cells. Mouse splenocytes (effector cells) and calcein AM-labeled YAC-1 (target) cells were co-cultured at various E:T ratios (100:1, 50:1, 25:1 and 12.5:1) on 96-well U-bottomed plates, and incubated at 37 °C for 4 h. The percentage of specific lysis was calculated in the same manner as described above. Specific lysis values obtained from the calcein-AM-release assay were converted to lytic units. Calculation of lytic units (LU) has been defined as previously report. [180] LU is defined as the number of cells required to cause 10% target cell lysis relative to 10^6 effector cells, were determined by the equation:

$$LU_{10}/10^6 = 10^6 \times \exp\{(\bar{Y}^* - Y_p^*)/C\}/(T \times \bar{X}_G)$$

Where $\bar{Y}^*$ is the mean of the logistically transformed specific lysis values, p is the reference lysis percentage used in defining the lytic unit (in this case, p = 10%), Y_p^* = ln(p/100 – p)), C is a constant set to 1, T is the number of target YAC-1 cells, and $\bar{X}_G$ is the geometric mean of the E:T ratio used in the assay. The NK activity per spleen (LU_{10}/spleen) was calculated as follows:

$$LU_{10}/\text{spleen} = \text{splenocyte numbers} \times \exp\{(\bar{Y}^* - Y_p^*)/C\}/(T \times \bar{X}_G)$$

***Measurement of Cytokine production*.** Human NK cell line KHYG-1 cells were inoculated into a 48-well microtiter plate at 6 × 10^4 cells/well and treated with KPF, experimental compounds (β-cryptoxanthin, β-carotene, zeaxanthin or Lutein) or vehicle control (dimethyl sulfoxide). After 24 h of incubation, the culture medium was centrifuged at 180 × *g* for 5 min to remove the cells. IFN-γ

levels in the supernatants were determined using a Human IFN-γ ELISA Development Kit according to the manufacturer's instructions.

The levels of IFN-γ in mouse plasma were also measured by commercially available ELISA kits according to the manufacturer's instructions.

Statistical analysis. The results are expressed as the means ± standard error (SE) or the means ± standard deviation (SD). A one-way analysis of variance (ANOVA) and Dunnett's post-hoc test were used to evaluate the differences between the means of the results for the control and treated samples. Multiple comparisons were performed using one-way ANOVA followed by Tukey–Kramer as a post-hoc test. Statistical differences between two groups were determined by Student's *t*-test. A *p*-value of <0.05 was considered significant. Statistical analysis was performed using GraphPad Prism version 5.0 (GraphPad Software, San Diego, CA, USA).

Results and Discussion

KP-AF activation of KHYG-1 NK cells

We screened pericarp extracts of three citruses, such as bitter orange (*Citrus aurantium*), hyuganatsu (*Citrus tamurana* hort. ex Tanaka), and kumquat, for five food functionalities using the optimized ANN2 models **(chapter I).** As a result of screening, all pericarp extracts were shown to activate NK cells, with kumquat pericarp extract having the strongest activity. Therefore, we separated various fractions from KP using pH-dependent extractions with various organic solvents (**Figure III-1**). The effect of the different KP fractions on NK cell activation was determined by IFN-γ production using human NK cell line, KHYG-1. As shown in **Figure III-2**, the KP-AF showed the strongest NK cell activation effect as it exhibited higher relative IFN- γ production values than the other fractions (KP-F1–F8).

We next examined the thermal stability of KP-AF on NK cell activation. The KP-AF was divided into two groups, an unheated and a heated group (90 °C, 10 min). The effect of the unheated and heated KP-AF on NK cell activation was determined by IFN-γ production and NK cytotoxic activity using KHYG-1 cells. As shown in **Figure III-3**, unheated KP-AF treatment significantly increased IFN-γ production and NK cytotoxic activity in KHYG-1 cells. Interestingly, this increase was not observed after heat-treatment at 90 °C for 10 min (**Figure III-3**). These results suggest that the reduction of activity in KP-AF may be due to the thermolability of active components.

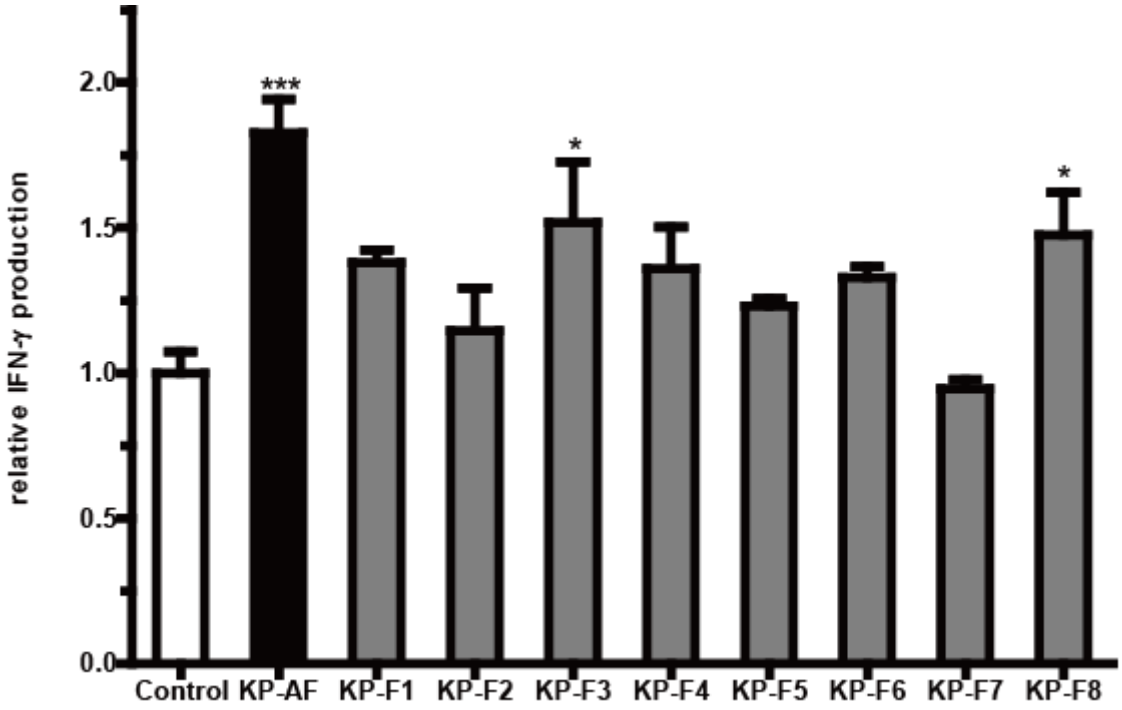

Figure III-2. NK cell activation effects of KP fractions in KHYG-1 cells. Cells were treated in the presence or absence of KP fractions (50 μg/mL) at 24 h and IFN-γ production in culture supernatant was measured by ELISA. The relative IFN-γ production is presented as the mean ± standard error (n = 6). The data obtained were statistically analyzed using one way ANOVA followed by Dunnett's test for individual comparison of groups with control. $^{*}p < 0.05$ and $^{***}p < 0.001$. This figure was cited from previously described figure.[177]

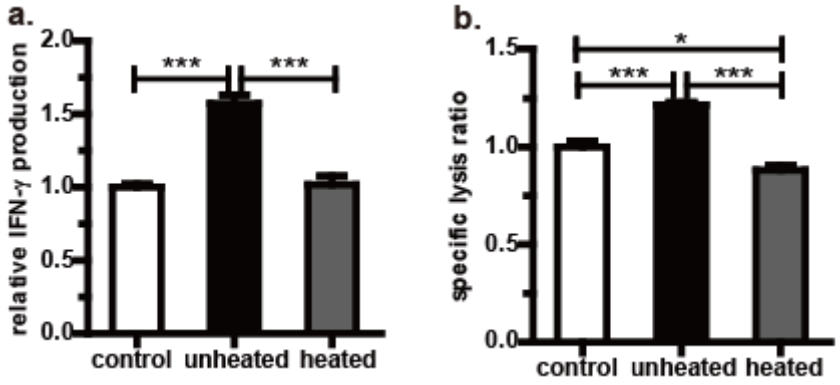

Figure III-3. NK cell activation effects of KP-AF in KHYG-1 cells. Cells were treated in the presence or absence of non-heat- and heat-treated KP-AF (50 μg/ml) at 24 h. (a.) relative IFN-γ production in culture supernates. (b.) NK cytotoxic activity. The relative IFN-γ production and specific lysis ratio are presented as the mean ± standard error (n=5 or 6). Multiple comparisons were performed using one-way ANOVA followed by Tukey–Kramer as a post-hoc test. *p<0.05 and ***p<0.001. This figure was cited from previously described figure.[177]

Carotenoids enhancement of IFN-γ production on KHYG-1 cells and determination of carotenoid levels

Kumquat has been reported to contain various constituents such as carotenoids,[168-170] essential oil[171] and polyphenols.[168, 170, 172] Among them, *d*-limonene,[181] which is one of the main components of essential oil, and the flavonoid chrysin[182] have been shown to possess NK cell activation effects *in vitro* or *in vivo*. The carotenoids β-cryptoxanthin[183] and citrus coumarin auraptene[184] have also been reported to have immunomodulation effects *in vitro* and *in vivo*. Therefore, we examined IFN-γ production against KHYG-1 cells treated with these four compounds. The concentrations of the tested compounds were determined from previous reports.[181-184] As shown in **Figure III-4**, IFN-γ production was increased with auraptene and β-cryptoxanthin treatment of KHYG-1 cells. A similar result has been reported for the effect of IFN-γ production enhancement by auraptene on

mouse splenocytes.[184] However, to our knowledge, IFN-γ production enhancement with β-cryptoxanthin has not yet been reported. Although chrysin and *d*-limonene were reported to activate NK activity,[181, 182] no increase in IFN-γ production was observed in KHYG-1 cells (**Figure III-4**). KP-AF is a dark red oil with a distinctive fragrant flavor, characteristic of kumquat.[171] We tested the effect of *d*-limonene on KHYG-1 cells, as it is the main essential oil constituent in kumquats, but found that it did not increase IFN-γ production. This demonstrates that KP-AF NK cell activation is not due to *d*-limonene. The dark red color of KP-AF is probably attributed to carotenoids, and IFN-γ production enhancement by the carotenoid β-cryptoxanthin was the highest amongst those tested (**Figure III-4**). Kumquat contains β-cryptoxanthin as well as various other carotenoids such as β-carotene, lutein and zeaxanthin, which have all been reported in previous kumquat studies.[168, 170] Therefore, we examined the effects of these carotenoids (**Figure III-5**) and determined the quantities of them in KP-AF.

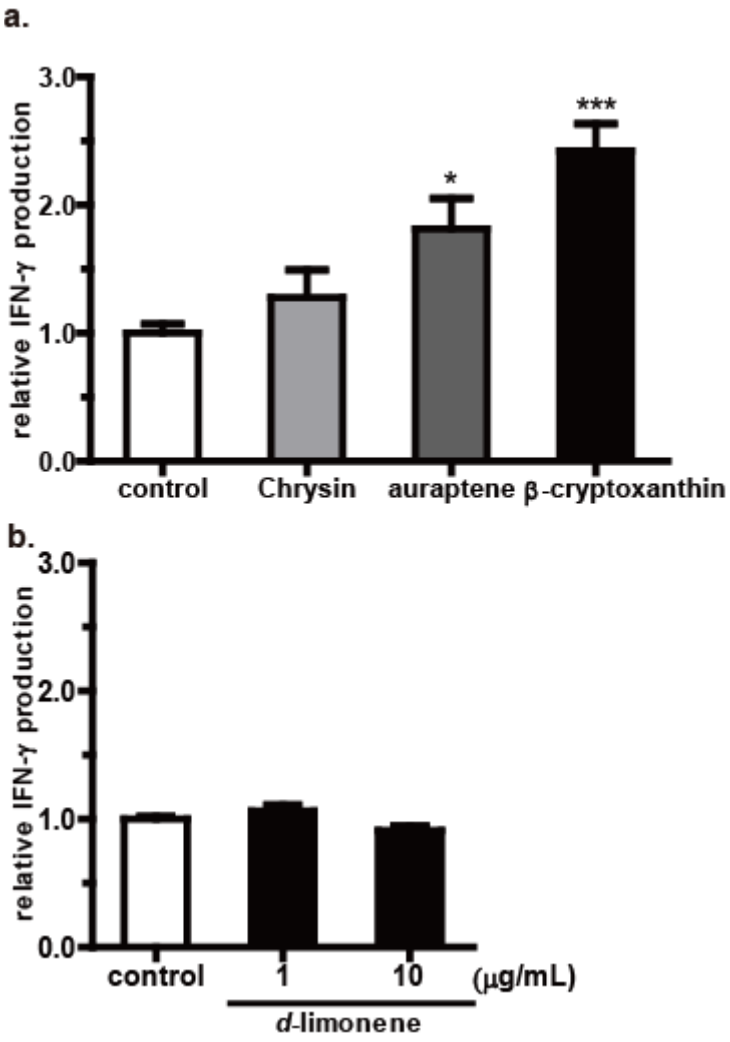

Figure III-4. Effect of IFN-γ production enhancement by carotenoids and other constituents on KHYG-1 cells. Cells were treated in the presence or absence of chrysin (50 μg/mL), auraptene (50 μg/mL), β-cryptoxanthin (25 μg/mL), and *d*-limonene (1 and 10 μg/mL) at 24 h. (a) Relative IFN-γ production in culture supernatant by chrysin, auraptene, β-cryptoxanthin, and (b) d-limonene. The relative IFN-γ productions are presented as the mean ± standard error (n = 6). The data obtained were statistically analyzed using one way ANOVA followed by Dunnett's test for individual comparison of groups with control. $^{*}p < 0.05$ and $^{***}p < 0.001$. This figure was cited from previously described figure.[177]

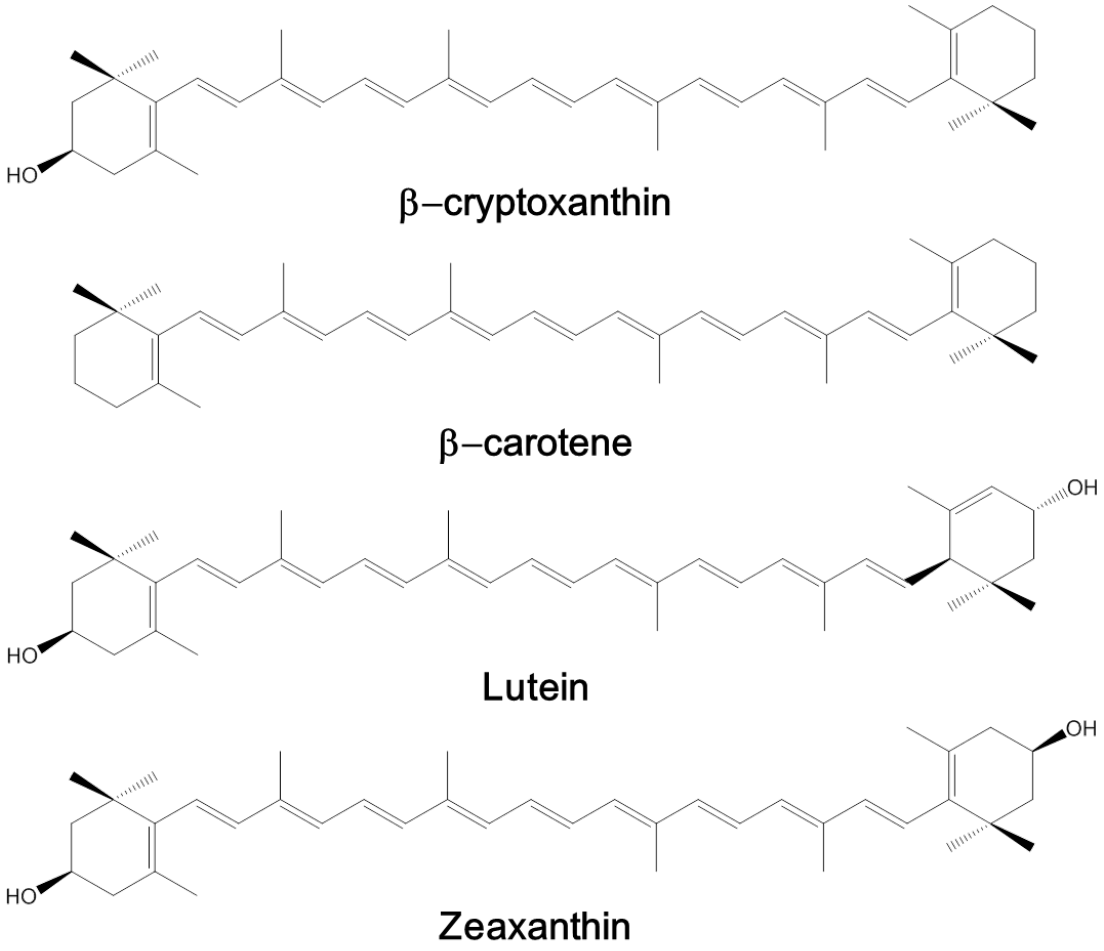

Figure III-5. Chemical structures of carotenoids used in this study

Of the four carotenoids, only β-cryptoxanthin (25 μg/mL) treatment significantly increased the IFN-γ production on KHYG-1 cells (**Figure III-6a**). Treatment with β-carotene (25 μg/mL) tended to increase the IFN-γ production, but not significantly. Lutein and zeaxanthin (oxygenated carotenoids and stereoisomers; **Figure III-5**) did not enhance IFN-γ production. Although oral administration of β-carotene has been reported to enhance NK cytotoxic activity in elderly men,[72] the enhancement of IFN-γ production on KHYG-1 cells was weak, and β-cryptoxanthin showed a stronger effect (**Figure III-6a**). We also evaluated the effect of β-cryptoxanthin on NK cytotoxic

activity. As shown in **Figure III-6b**, β-cryptoxanthin (25 μg/mL) treatment significantly increased NK cytotoxic activity in KHYG-1 cells. These results show that β-cryptoxanthin may be one candidate active constituent. To our knowledge, there have been no previously published studies examining a single oral administration of β-cryptoxanthin to human subjects. In a clinical trial of viral hepatitis patients with cirrhosis, cumulative incidence of hepatocellular carcinoma development in β-cryptoxanthin-enriched mandarin orange juice with carotenoids mixture capsules-oral administrated group was lower than that in the control group.[185] A cohort study also reported that a high serum β-cryptoxanthin concentration was significantly associated with reduced risk of lung cancer.[186] Although NK cytotoxic activity was not demonstrated in these studies, the reduced risk of these cancers may be related to NK cytotoxic activity. Therefore, oral administration of β-cryptoxanthin may be also expected to enhance NK cytotoxic activity in human.

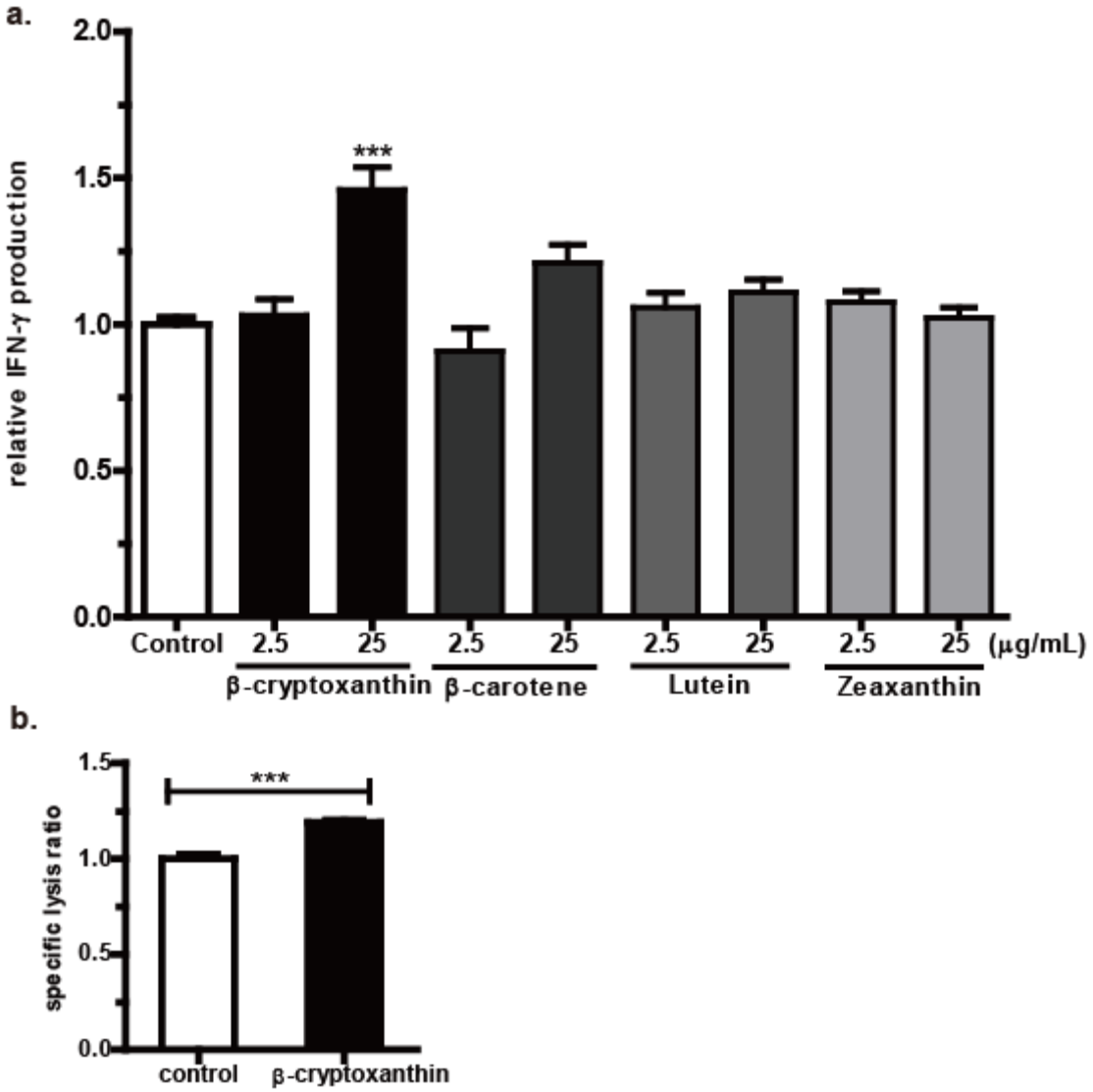

Figure III-6. NK cell activation effects of carotenoids in KHYG-1 cells. Cells were treated in the presence or absence of β-cryptoxanthin, β-carotene, lutein, and zeaxanthin at 24 h. (a) Relative IFN-γ production in culture supernatant. (b) NK cytotoxic activity by β-cryptoxanthin (25 μg/mL). The relative IFN-γ production and specific lysis ratio are presented as the mean ± standard error (n = 5 or 6). Statistically significant differences were determined by one way ANOVA followed by Dunnett's test for individual comparison of groups with control (a) or Student's *t*-test (b). $^{***}p < 0.001$. This figure was cited from previously described figure.[177]

Carotenoids are generally known to be thermally labile,[187] so we quantified the amount of carotenoids (including β-cryptoxanthin, β-carotene, lutein and zeaxanthin) in unheated and heated KP-AF. As shown in **Table III-1**, the level of β-cryptoxanthin in KP-AF (98.2 ± 7.1 μg/g) was highest, followed by β-carotene (56.5 ± 10.1 μg/g), lutein (19.8 ± 14.1 μg/g), and zeaxanthin (10.1 ± 7.2 μg/g). β-Cryptoxanthin and β-carotene were the major carotenoids, whereas lutein and zeaxanthin were the minor carotenoids in KP-AF. A similar tendency was reported for kumquat fruit cultivated in Taiwan,[170] but the carotenoid content of kumquats cultivated in Italy[168] was different from that of KP-AF. Such a difference will depend on various factors such as cultivar, harvesting area, and harvest timing. Carotenoid levels in heated KP-AF tended to be lower than that of unheated KP-AF. However, there were no statistically significant differences between the unheated and heated KP-AF in all four carotenoids tested. In addition, the percentage of each carotenoid per total carotenoids was maintained between unheated and heated KP-AF. These results show that the composition of carotenoids and the levels in KP-AF are unaffected by heat-treatment in at least these four carotenoids. A previous study has reported the influence of heating on carotenoids in vegetables and fruits. Heat-treatment (98 °C, 10 min) of some fruits and vegetables caused a decrease in the carotenoid levels, while levels in other fruits and vegetables were maintained.[188] The levels of carotenoids in KP-AF may not be easily influenced by heating. Unheated KP-AF significantly increased both IFN-γ production and NK cytotoxic activity in KHYG-1 cells, although this increase was not observed after heat-treatment at 90 °C for 10 min (**Figure III-3**). Carotenoids are degraded by oxidation by heat, light, oxygen, acid, transition metals, or interactions with radical species.[187] Therefore, reduction in NK activity in heated KP-AF may be caused by thermal oxidation of carotenoids, not by a quantitative change. It is also worth

considering that KP-AF may not only enhance NK cell activity by carotenoids such as β-cryptoxanthin, but also by the interaction of carotenoids with other constituents.

Table III-1. Carotenoids contents in unheated and heated KP-AF.

	carotenoids contents (μg/g[a])[b]	
	unheated KP-AF	heated KP-AF
β-carotene	56.5 ± 10.1	55.1 ± 34.8
β-cryptoxanthin	98.2 ± 7.1	91.5 ± 62.5
lutein	19.8 ± 14.1	12.1 ± 2.4
zeaxanthin	10.1 ± 7.2	6.1 ± 2.0
total carotenoids[c]	184.6 ± 24.7	164.8 ± 101.0
	percent of carotenoids per total carotenoids (%)	
	unheated KP-AF	heated KP-AF
β-carotene	30.7 ± 4.6	33.4 ± 1.2
β-cryptoxanthin	53.9 ± 5.6	50.1 ± 11.2
lutein	10.2 ± 6.1	11.3 ± 7.7
zeaxanthin	5.2 ± 3.1	5.2 ± 2.9

[a] expressed as microgram per gram of KP-AF. [b] Data are presented as means ± standard deviation (n=3). [c] a total of four carotenoids. This table was cited from previously described study.[177]

Effect of KP-AF on NK cell activation in restraint stress mice

We also investigated whether orally administered KP-AF enhances the NK cell activation of restraint stress mice. As shown in **Table III-2**, restraint stress significantly reduces spleen weight, spleen index, and spleen lymphocyte number by about 31% ($p < 0.001$), 17% ($p < 0.01$), and 61% ($p < 0.001$), respectively. However, oral administration of KP-AF did not recover spleen weight, spleen index or spleen lymphocyte number in stressed mice. We then evaluated plasma corticosterone levels, as acute stress increases levels of glucocorticoids such as corticosterone. The plasma corticosterone level in restraint stressed mice was approximately 4.7-fold higher than that in

normal mice (**Figure III-7a**). However, the increase in the plasma corticosterone levels caused by restraint stress was not reduced by the orally administered KP-AF (**Figure III-7a**). These results suggest that oral administration of KP-AF does not suppress the increment in the plasma corticosterone level by restraint stress, resulting in reduction of spleen weight, spleen index, and spleen lymphocyte number. A previous report suggests that restraint stress markedly reduces spleen lymphocyte number and causes spleen atrophy owing to spleen lymphocyte apoptosis by stress-induced glucocorticoid overflow.[189] KP-AF was not involved in the protective effect of the reduction of spleen lymphocytes caused by restraint stress.

Table III-2. Effect of KP-AF on spleen weight, spleen index, and spleen lymphocyte number in restraint-stressed mice.

Group	Spleen weight (mg)	Spleen index (%)	Spleen lymphocyte number (10^7)
Normal (n = 10)	73.67 ± 4.58^a	0.30 ± 0.02^a	8.4 ± 0.7^a
Model (Restraint) (n = 15)	50.73 ± 2.06^b	0.25 ± 0.01^b	3.3 ± 0.2^b
Restraint+KP-AF (0.6 mg/Kg) (n = 10)	46.91 ± 1.86^b	0.24 ± 0.01^b	3.6 ± 0.3^b

The results represent mean ± standard error. Different alphabet letters indicate the statistical significance at $p < 0.01$ (ANOVA followed by Tukey–Kramer's test). This table was cited from previously described study.[177]

Moreover, effect of KP-AF on cytokine production was also examined in the plasma as shown in **Figure III-7b**. The plasma IFN-γ levels in restraint-stressed mice were significantly reduced compared with those in normal mice. Oral administration of KP-AF significantly improved the suppressed plasma IFN-γ levels in stressed mice (**Figure III-7b**, $p < 0.01$). This KP-AF enhancement of IFN-γ production shown *in vivo* is similar to *in vitro* experimental results using KHYG-1 cells.

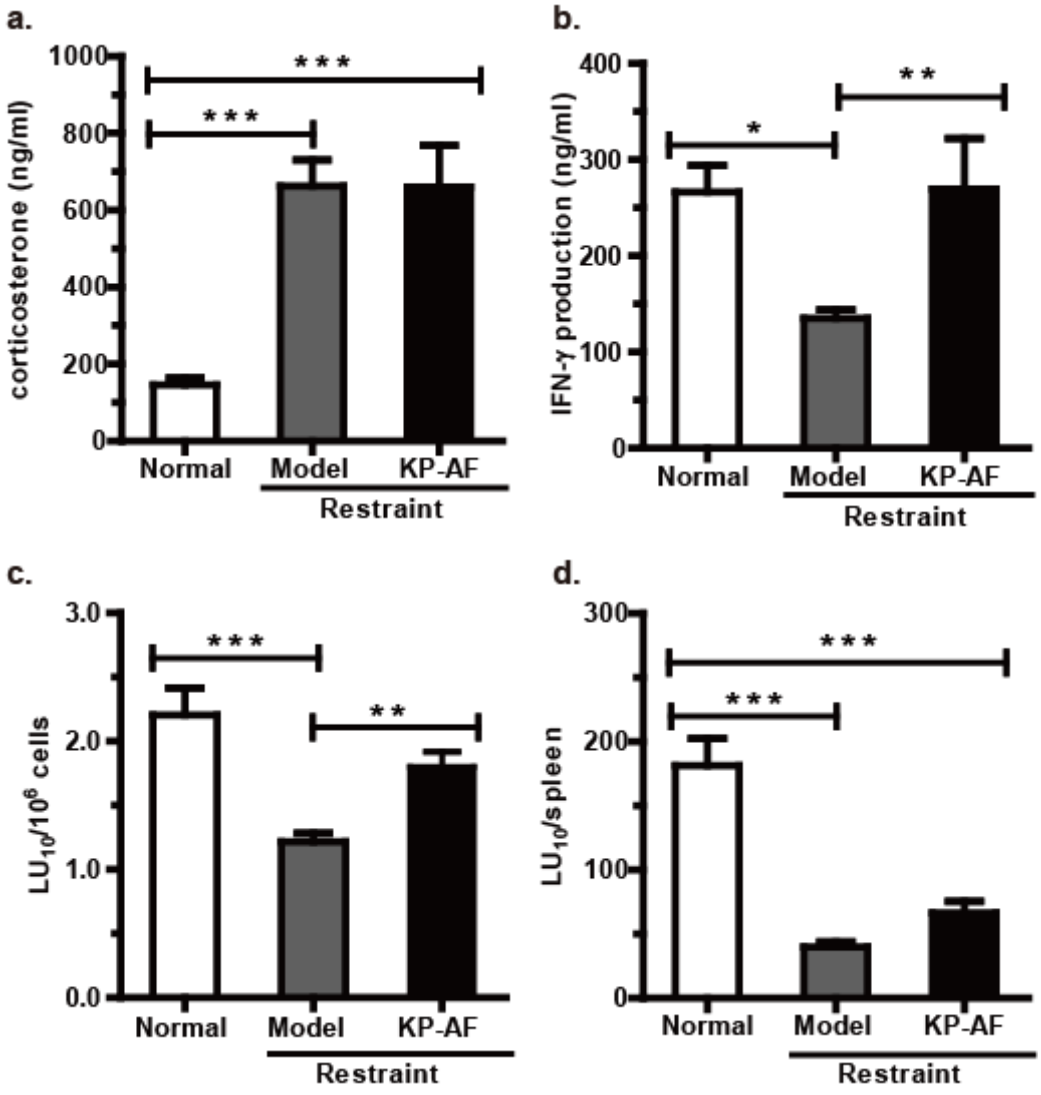

Figure III-7. Effect of KP-AF on plasma corticosterone levels, IFN-γ level and NK cell cytotoxicity of restraint-stressed mice. (a) Plasma corticosterone levels were determined by a quantitative competitive ELISA. (b) Plasma IFN-γ levels were determined using an ELISA. (c) and (d) In the determination of NK cell cytotoxic activity, calcein AM-labeled YAC-1 (target) cells were mixed with spleen lymphocytes and incubated for 4 h. After incubation, NK cell activity was determined using an calcein-AM-release assay. (c) NK cytotoxic activity per splenocyte ($LU_{10}/10^6$ cells). (d) NK cytotoxic activity per spleen (LU_{10}/spleen). The results data are presented as the mean ± standard error (n = 10 or 15). Multiple comparisons were performed using one-way ANOVA followed by Tukey–Kramer as a post-hoc test. $^{***}p < 0.001$. This figure was cited from previously described figure.[177]

We also evaluated the effects of KP-AF on NK cytotoxic activity in the spleen using a calcein-AM-release assay. As shown in **Figure III-7c** and d, restraint stress significantly reduces both NK cytotoxic activity per splenocyte ($LU_{10}/10^6$ cells) and NK cytotoxic activity per spleen (LU_{10}/spleen) compared with normal mice. Oral administration of KP-AF significantly improves the suppressed NK cytotoxic activity per splenocyte ($LU_{10}/10^6$ cells) in stressed mice (**Figure III-7c**; $p<0.01$), and so the NK cell activation effects of KP-AF *in vitro* were confirmed by these *in vivo* experiments. Although oral administration of KP-AF tends to improve the suppressed NK cytotoxic activity per spleen (LU_{10}/spleen), this is not significant (restraint vs KP-AF; **Figure III-7d**). This result means that KP-AF is not involved in the protective effect on the reduction of splenocytes by stress-induced corticosterone. In contrast to our study, recent *in vivo* studies in restraint stress mice have shown that carnosine (β-alanyl-L-histidine) can maintain spleen lymphocyte numbers to prevent immunocompromise caused by restraint stress, although carnosine administration had no obvious effect on NK cytotoxic activity per splenocyte.[189] The major food source of carnosine is foods containing muscle tissue, such as chicken and beef. Kumquat and carnosine eaten at the same time could prevent most immunocompromise caused by stress.

Among the tested compounds, only β-cryptoxanthin showed enhancement of IFN-γ production in KHYG-1 cells. β-cryptoxanthin was also enhanced KHYG-1 cytotoxic activity. These suggest that the NK cell activation effect of KP-AF may be caused by carotenoids such as β-cryptoxanthin. Reactive oxygen species contribute to NK cell dysfunction such as loss of numbers and activities.[190] Carotenoids from kumquats have been shown to possess antioxidant activity.[172] In restraint stress mice, apple polyphenols extract[191] and astaxanthin[192] elevated immune functions of stressed animals because of antioxidant activities directly or indirectly in immunocytes. Oral administration of KP-AF may also enhance NK cell activation of restraint stress mice because of

antioxidant activities of carotenoids including β-cryptoxanthin. However, the bioactivity of the antioxidant may not be solely due to the anti-oxidative capacity. For example, epigallocatechin-3-gallate (a polyphenol found in green tea) has been reported to exert various bioactivities such as anti-cancer activity,[193] anti-allergic activity,[194] and anti-inflammatory activity[195] through the 67-kDa laminin receptor. The active component in KP-AF may also enhance NK activity through another cell surface receptor.

In conclusion, this is the first study to show NK cell activation effects of KP-AF from kumquats *in vitro* and *in vivo*. KP-AF treatment significantly increased both IFN-γ production and NK cytotoxic activity in human KHYG-1 NK cells. Moreover, we examined whether orally administered KP-AF could also enhance the NK cell activation of restraint stress mice. Oral administration of KP-AF significantly improved both suppressed plasma IFN-γ levels and NK cytotoxic activity per splenocyte in stressed mice. However, the increased IFN-γ production in KHYG-1 cells was not observed after heat-treatment at 90 °C for 10 min (**Figure III-3**). The reduction in KP-AF activity may be caused by the thermolability of its active components. The heat-processed kumquat was not expected to have the same level of activation of NK activity as the unheated sample. However, the thermolability of the active components may not be important for kumquats because they are also eaten raw (whole fruit or pericarp). Recently, kumquat consumption by eating raw is increasing. Given the benefits of eating raw, we should draw additional attention to functionality of thermolabile compounds for utilizing advantage of raw diet. Further studies of KP-AF are needed to identify the active components and to evaluate the molecular mechanism responsible for the NK cell activation effect.

Concluding remarks

In chapter I, the authors have developed a new system that allows for the simultaneous estimation of multiple functionalities of food constituents using bioinformatics. The model utilizes expression data of intracellular marker proteins as descriptors that respond to stimulation by a constituent. Even if the information regarding the chemical structure of the compound is unclear, the expression data of marker proteins in the cells can be quantified using the information of a compound influencing the cells. Therefore, our model was able to estimate food functionality of a test sample without crossing the limit of allowable error even if the sample was an extract consisting of a complex mixture of components. However, two aspects require further improvement; the first being the method used to determine the expression of intracellular marker proteins. Although ELISA is a specific, sensitive, and convenient method to quantify intracellular marker proteins, the quality of the antibodies may not be stable, especially in the case of polyclonal antibodies. Therefore, it is necessary to measure the expression of intracellular marker proteins by a new method that does not depend on antibodies. Quantitative proteomics by liquid chromatography and tandem mass spectrometry[196] might be used as an alternative to ELISA for the measurement of marker protein expression. Second, the system was built using ANN. Food functionalities can be estimated from the expression data of marker proteins by using ANN. However, conversely, it is difficult to clarify the marker protein affecting the food functionality using ANN because the information in ANN is unable to confirm this directly. However, extended-weight-updating self-organizing map makes confirmation of the information possible.[197] Moreover, the self-organizing map can also estimate the values of food functionality. Thus, the food functionality evaluation

system has become a more powerful tool by using the extended-weight-updating self-organizing map.

In chapter II, based on the estimation by our systems (chapter I), the author observed that *Vaccinium virgatum* Aiton (rabbiteye blueberry) leaf extracts have a strong growth inhibitory effect on the HTLV-1-infected cell line MT2. OPA from blueberry leaf inhibited the growth of MT2 cells by inducing apoptosis and G_2/M cell cycle arrest. OPA-induced apoptosis of HTLV-1-infected cells was mediated by death receptor-mediated caspase-dependent pathways. Induction of G_2/M arrest by OPA resulted from the down-regulation of cyclin B1 and cdc2. OPA from blueberry leaf might be a source of novel compounds for reducing the risk of developing ATLL.

In chapter III, based on the estimation by our system (chapter I), the authors validated the NK cell activation activity of kumquat (*Fortunella crassifolia*) pericarp *in vitro* and *in vivo*. In *in vitro* experiments using human NK cells KHYG-1, the acetone fraction from kumquat pericarp (KP-AF) was found to have the strongest NK cell activity and thermolability. KP is known to contain carotenoids, essential oils, and flavonoids. Among the seven tested compounds, only β-cryptoxanthin enhanced IFN-γ production in KHYG-1. These results suggested that the NK cell activation effects of KP-AF from kumquat might be attributed to carotenoids such as β-cryptoxanthin. The authors examined whether orally administered KP-AF also enhanced the NK cell activity of restraint stressed mice. Oral administration of KP-AF significantly improved the suppressed NK cytotoxic activity per splenocyte in stressed mice. These results suggested that oral administration of KP-AF enhanced NK cytotoxic activity of splenocyte. NK cell activation effects of KP-AF were confirmed by both *in vivo* and *in vitro* studies.

In conclusion, the authors developed a new food functionality evaluation system. The system was helpful in clarifying the active components and the mechanism of action *in vitro*.

Additionally, the effects estimated by the system were confirmed by *in vivo* studies. Furthermore, if more food functionalities can be presumed simultaneously from the expression data of marker proteins, then the system can be used as the first screening method of food constituents being evaluated for various beneficial purposes.

References

1. Arai, S.; Osawa, T.; Ohigashi, H.; Yoshikawa, M.; Kaminogawa, S.; Watanabe, M.; Ogawa, T.; Okubo, K.; Watanabe, S.; Nishino, H.; Shinohara, K.; Esashi, T.; Hirahara, T., A mainstay of functional food science in Japan--history, present status, and future outlook. *Biosci. Biotechnol. Biochem.* **2001**, *65*, 1-13.

2. Arai, S., Functional food science. *J. Sci. Food Agric.* **2005**, *85*, 1603-1605.

3. Takachi, R.; Inoue, M.; Ishihara, J.; Kurahashi, N.; Iwasaki, M.; Sasazuki, S.; Iso, H.; Tsubono, Y.; Tsugane, S.; Group, J. S., Fruit and vegetable intake and risk of total cancer and cardiovascular disease: Japan Public Health Center-Based Prospective Study. *Am. J. Epidemiol.* **2008**, *167*, 59-70.

4. Yamaji, T.; Inoue, M.; Sasazuki, S.; Iwasaki, M.; Kurahashi, N.; Shimazu, T.; Tsugane, S.; Group, J. S., Fruit and vegetable consumption and squamous cell carcinoma of the esophagus in Japan: the JPHC study. *Int. J. Cancer* **2008**, *123*, 1935-1940.

5. Riboli, E.; Norat, T., Epidemiologic evidence of the protective effect of fruit and vegetables on cancer risk. *Am. J. Clin. Nutr.* **2003**, *78*, 559S-569S.

6. Scalbert, A.; Manach, C.; Morand, C.; Rémésy, C.; Jiménez, L., Dietary polyphenols and the prevention of diseases. *Crit. Rev. Food Sci. Nutr.* **2005**, *45*, 287-306.

7. Schlesier, K.; Harwat, M.; Böhm, V.; Bitsch, R., Assessment of antioxidant activity by using different *in vitro* methods. *Free Radic. Res.* **2002**, *36*, 177-187.

8. Cao, G.; Alessio, H.; Cutler, R., Oxygen-radical absorbance capacity assay for antioxidants. *Free Radic. Biol. Med.* **1993**, *14*, 303-311.

9. Shishu; Kaur, I. P., Antimutagenicity of curcumin and related compounds against genotoxic heterocyclic amines from cooked food: The structural requirement. *Food Chem.* **2008**, *111*, 573-579.

10. Spada, P.; de Souza, G.; Bortolini, G.; Henriques, J.; Salvador, M., Antioxidant, mutagenic, and antimutagenic activity of frozen fruits. *J. Med. Food* **2008**, *11*, 144-151.

11. King, A.; Shaughnessy, D.; Mure, K.; Leszczynska, J.; Ward, W.; Umbach, D.; Xu, Z.; Ducharme, D.; Taylor, J.; Demarini, D.; Klein, C., Antimutagenicity of cinnamaldehyde and vanillin in human cells: Global gene expression and possible role of DNA damage and repair. *Mutat. Res.* **2007**, *616*, 60-69.

12. Chu, Y.; Sun, J.; Wu, X.; Liu, R., Antioxidant and antiproliferative activities of common vegetables. *J. Agric. Food Chem.* **2002**, *50*, 6910-6916.

13. Sun, J.; Chu, Y.; Wu, X.; Liu, R., Antioxidant and antiproliferative activities of common fruits. *J. Agric. Food Chem.* **2002**, *50*, 7449-7454.

14. Cheung, S.; Tai, J., Anti-proliferative and antioxidant properties of rosemary *Rosmarinus officinalis*. *Oncol. Rep.* **2007**, *17*, 1525-1531.

15. Chen, D.; Milacic, V.; Chen, M. S.; Wan, S. B.; Lam, W. H.; Huo, C.; Landis-Piwowar, K. R.; Cui, Q. C.; Wali, A.; Chan, T. H.; Dou, Q. P., Tea polyphenols, their biological effects and potential molecular targets. *Histol. Histopathol.* **2008**, *23*, 487-496.

16. Hodgson, J. M.; Croft, K. D., Tea flavonoids and cardiovascular health. *Mol. Aspects Med.* **2010**, *31*, 495-502.

17. Lambert, J. D.; Elias, R. J., The antioxidant and pro-oxidant activities of green tea polyphenols: a role in cancer prevention. *Arch. Biochem. Biophys.* **2010**, *501*, 65-72.

18. Thielecke, F.; Boschmann, M., The potential role of green tea catechins in the prevention of the metabolic syndrome - a review. *Phytochemistry* **2009**, *70*, 11-24.

19. Singh, R.; Akhtar, N.; Haqqi, T. M., Green tea polyphenol epigallocatechin-3-gallate: inflammation and arthritis. *Life Sci.* **2010**, *86*, 907-918.

20. Michelini, E.; Cevenini, L.; Mezzanotte, L.; Coppa, A.; Roda, A., Cell-based assays: fuelling drug discovery. *Anal. Bioanal. Chem.* **2010**, *398*, 227-238.

21. Bajorath, J., Computational analysis of ligand relationships within target families. *Curr. Opin. Chem. Biol.* **2008**, *12*, 352-358.

22. Ekins, S.; Mestres, J.; Testa, B., *In silico* pharmacology for drug discovery: applications to targets and beyond. *Br. J. Pharmacol.* **2007**, *152*, 21-37.

23. Ekins, S.; Mestres, J.; Testa, B., *In silico* pharmacology for drug discovery: methods for virtual ligand screening and profiling. *Br. J. Pharmacol.* **2007**, *152*, 9-20.

24. Valerio, L. G., *In silico* toxicology for the pharmaceutical sciences. *Toxicol. Appl. Pharmacol.* **2009**, *241*, 356-370.

25. Martinez-Mayorga, K.; Medina-Franco, J. L., Chemoinformatics-applications in food chemistry. *Adv. Food Nutr. Res.* **2009**, *58*, 33-56.

26. Valerio, L. G.; Arvidson, K. B.; Chanderbhan, R. F.; Contrera, J. F., Prediction of rodent carcinogenic potential of naturally occurring chemicals in the human diet using high-throughput QSAR predictive modeling. *Toxicol Appl Pharmacol* **2007**, *222*, 1-16.

27. Cabrera, A. C.; Prieto, J. M., Application of artificial neural networks to the prediction of the antioxidant activity of essential oils in two experimental *in vitro* models. *Food Chem.* **2010**, *118*, 141-146.

28. Bucinski, A.; Zielinski, H.; Kozlowska, H., Artificial neural networks for prediction of antioxidant capacity of cruciferous sprouts. *Trends Food Sci. Technol.* **2004**, *15*, 161-169.

29. Nordenstedt, H.; White, D. L.; El-Serag, H. B., The changing pattern of epidemiology in hepatocellular carcinoma. *Dig. Liver Dis.* **2010**, *42 Suppl 3*, S206-S214.

30. Sawada, N.; Inoue, M.; Iwasaki, M.; Sasazuki, S.; Shimazu, T.; Yamaji, T.; Takachi, R.; Tanaka, Y.; Mizokami, M.; Tsugane, S.; Group, J. P. H. C.-B. P. S., Consumption of n-3 fatty acids and fish reduces risk of hepatocellular carcinoma. *Gastroenterology* **2012**, *142*, 1468-1475.

31. Inoue, M.; Kurahashi, N.; Iwasaki, M.; Shimazu, T.; Tanaka, Y.; Mizokami, M.; Tsugane, S.; Group, J. P. H. C.-B. P. S., Effect of coffee and green tea consumption on the risk of liver cancer: cohort analysis by hepatitis virus infection status. *Cancer Epidemiol. Biomarkers Prev.* **2009**, *18*, 1746-1753.

32. Kurahashi, N.; Inoue, M.; Iwasaki, M.; Tanaka, Y.; Mizokami, M.; Tsugane, S.; Group, J. S., Vegetable, fruit and antioxidant nutrient consumption and subsequent risk of hepatocellular carcinoma: a prospective cohort study in Japan. *Br. J. Cancer* **2009**, *100*, 181-184.

33. Wang, Y.; Wu, J.; Lin, B.; Li, X.; Zhang, H.; Ding, H.; Chen, X.; Lan, L.; Luo, H., Galangin suppresses HepG2 cell proliferation by activating the TGF-β receptor/Smad pathway. *Toxicology* **2014**, *326C*, 9-17.

34. Stagos, D.; Amoutzias, G. D.; Matakos, A.; Spyrou, A.; Tsatsakis, A. M.; Kouretas, D., Chemoprevention of liver cancer by plant polyphenols. *Food Chem. Toxicol.* **2012**, *50*, 2155-2170.

35. Nair, S. V.; Ziaullah; Rupasinghe, H. P., Fatty acid esters of phloridzin induce apoptosis of human liver cancer cells through altered gene expression. *PLoS One* **2014**, *9*, e107149.

36. Mann, C. D.; Neal, C. P.; Garcea, G.; Manson, M. M.; Dennison, A. R.; Berry, D. P., Phytochemicals as potential chemopreventive and chemotherapeutic agents in hepatocarcinogenesis. *Eur. J. Cancer Prev.* **2009**, *18*, 13-25.

37. Glauert, H. P.; Calfee-Mason, K.; Stemm, D. N.; Tharappel, J. C.; Spear, B. T., Dietary antioxidants in the prevention of hepatocarcinogenesis: a review. *Mol. Nutr. Food Res.* **2010**, *54*, 875-896.

38. Sakamoto, H.; Okamoto, K.; Aoki, M.; Kato, H.; Katsume, A.; Ohta, A.; Tsukuda, T.; Shimma, N.; Aoki, Y.; Arisawa, M.; Kohara, M.; Sudoh, M., Host sphingolipid biosynthesis as a target for hepatitis C virus therapy. *Nat. Chem. Biol.* **2005**, *1*, 333-337.

39. Lavanchy, D., The global burden of hepatitis C. *Liver Int.* **2009**, *29 Suppl 1*, 74-81.

40. Lohmann, V.; Körner, F.; Koch, J.; Herian, U.; Theilmann, L.; Bartenschlager, R., Replication of subgenomic hepatitis C virus RNAs in a hepatoma cell line. *Sci.* **1999**, *285*, 110-113.

41. Yano, M.; Ikeda, M.; Abe, K.; Dansako, H.; Ohkoshi, S.; Aoyagi, Y.; Kato, N., Comprehensive analysis of the effects of ordinary nutrients on hepatitis C virus RNA replication in cell culture. *Antimicrob. Agents Chemother.* **2007**, *51*, 2016-2027.

42. Chen, M. H.; Lee, M. Y.; Chuang, J. J.; Li, Y. Z.; Ning, S. T.; Chen, J. C.; Liu, Y. W., Curcumin inhibits HCV replication by induction of heme oxygenase-1 and suppression of AKT. *Int. J. Mol. Med.* **2012**, *30*, 1021-1028.

43. Ahmed-Belkacem, A.; Ahnou, N.; Barbotte, L.; Wychowski, C.; Pallier, C.; Brillet, R.; Pohl, R. T.; Pawlotsky, J. M., Silibinin and related compounds are direct inhibitors of hepatitis C virus RNA-dependent RNA polymerase. *Gastroenterology* **2010**, *138*, 1112-1122.

44. Bachmetov, L.; Gal-Tanamy, M.; Shapira, A.; Vorobeychik, M.; Giterman-Galam, T.; Sathiyamoorthy, P.; Golan-Goldhirsh, A.; Benhar, I.; Tur-Kaspa, R.; Zemel, R., Suppression of hepatitis C virus by the flavonoid quercetin is mediated by inhibition of NS3 protease activity. *J. Viral Hepat.* **2012**, *19*, e81-e88.

45. Lin, Y. T.; Wu, Y. H.; Tseng, C. K.; Lin, C. K.; Chen, W. C.; Hsu, Y. C.; Lee, J. C., Green tea phenolic epicatechins inhibit hepatitis C virus replication via cycloxygenase-2 and attenuate virus-induced inflammation. *PLoS One* **2013**, *8*, e54466.

46. Shen, H.; Yamashita, A.; Nakakoshi, M.; Yokoe, H.; Sudo, M.; Kasai, H.; Tanaka, T.; Fujimoto, Y.; Ikeda, M.; Kato, N.; Sakamoto, N.; Shindo, H.; Maekawa, S.; Enomoto, N.; Tsubuki,

M.; Moriishi, K., Inhibitory effects of caffeic acid phenethyl ester derivatives on replication of hepatitis C virus. *PLoS One* **2013**, *8*, e82299.

47. Leu, G.; Lin, T.; Hsu, J., Anti-HCV activities of selective polyunsaturated fatty acids. *Biochem. Biophys. Res. Commun.* **2004**, *318*, 275-280.

48. Li, S.; Kodama, E. N.; Inoue, Y.; Tani, H.; Matsuura, Y.; Zhang, J.; Tanaka, T.; Hattori, T., Procyanidin B1 purified from *Cinnamomi cortex* suppresses hepatitis C virus replication. *Antivir. Chem. Chemother.* **2010**, *20*, 239-248.

49. Takeshita, M.; Ishida, Y.; Akamatsu, E.; Ohmori, Y.; Sudoh, M.; Uto, H.; Tsubouchi, H.; Kataoka, H., Proanthocyanidin from blueberry leaves suppresses expression of subgenomic hepatitis C virus RNA. *J. Biol. Chem.* **2009**, *284*, 21165-21176.

50. Ratnoglik, S. L.; Aoki, C.; Sudarmono, P.; Komoto, M.; Deng, L.; Shoji, I.; Fuchino, H.; Kawahara, N.; Hotta, H., Antiviral activity of extracts from *Morinda citrifolia* leaves and chlorophyll catabolites, pheophorbide a and pyropheophorbide a, against hepatitis C virus. *Microbiol. Immunol.* **2014**, *58*, 188-194.

51. Chen, W. C.; Wang, S. Y.; Chiu, C. C.; Tseng, C. K.; Lin, C. K.; Wang, H. C.; Lee, J. C., Lucidone suppresses hepatitis C virus replication by Nrf2-mediated heme oxygenase-1 induction. *Antimicrob. Agents Chemother.* **2013**, *57*, 1180-1191.

52. Boerboom, A.; Vermeulen, M.; van der Woude, H.; Bremer, B.; Lee-Hilz, Y.; Kampman, E.; van Bladeren, P.; Rietjens, I.; Aarts, J., Newly constructed stable reporter cell lines for mechanistic studies on electrophile-responsive element-mediated gene expression reveal a role for flavonoid planarity. *Biochem. Pharmaco.l* **2006**, *72*, 217-226.

53. Kansanen, E.; Kuosmanen, S. M.; Leinonen, H.; Levonen, A. L., The Keap1-Nrf2 pathway: Mechanisms of activation and dysregulation in cancer. *Redox Biol.* **2013**, *1*, 45-49.

54. Gijsbers, L.; Van Eekelen, H. D. L. M.; Nguyen, T. H.; De Haan, L. H. J.; Van Der Burg, B.; Aarts, J. M. M. J. G.; Rietjens, I. M. C. M.; Bovy, A. G., Induction of electrophile-responsive element (EpRE)-mediated gene expression by tomato extracts *in vitro*. *Food Chem.* **2012**, *135*, 1166-1172.

55. Chen, C.; Yu, R.; Owuor, E. D.; Kong, A. N., Activation of antioxidant-response element (ARE), mitogen-activated protein kinases (MAPKs) and caspases by major green tea polyphenol components during cell survival and death. *Arch. Pharm. Res.* **2000**, *23*, 605-612.

56. van Cruchten, S. T. J.; de Haan, L. H. J.; Mulder, P. P. J.; Kunne, C.; Boekschoten, M. V.; Katan, M. B.; Aarts, J. M. M. J. G.; Witkamp, R. F., The role of epoxidation and electrophile-responsive element-regulated gene transcription in the potentially beneficial and harmful effects of the coffee components cafestol and kahweol. *J. Nutr. Biochem.* **2010**, *21*, 757-763.

57. Iwanaga, M.; Watanabe, T.; Yamaguchi, K., Adult T-cell leukemia: a review of epidemiological evidence. *Front. Microbiol.* **2012**, *3*, 322.

58. Langner, E.; Rzeski, W., Dietary derived compounds in cancer chemoprevention. *Wspolczesna Onkologia* **2012**, *16*, 394-400.

59. Tomita, M.; Kawakami, H.; Uchihara, J. N.; Okudaira, T.; Masuda, M.; Takasu, N.; Matsuda, T.; Ohta, T.; Tanaka, Y.; Ohshiro, K.; Mori, N., Curcumin (diferuloylmethane) inhibits constitutive active NF-kappaB, leading to suppression of cell growth of human T-cell leukemia

virus type I-infected T-cell lines and primary adult T-cell leukemia cells. *Int. J. Cancer* **2006**, *118*, 765-772.

60. Yamasaki, M.; Mukai, A.; Ohba, M.; Mine, Y.; Sakakibara, Y.; Suiko, M.; Morishita, K.; Nishiyama, K., Genistein induced apoptotic cell death in adult T-cell leukemia cells through estrogen receptors. *Biosci. Biotechnol. Biochem.* **2010**, *74*, 2113-2115.

61. Yamasaki, M.; Fujita, S.; Ishiyama, E.; Mukai, A.; Madhyastha, H.; Sakakibara, Y.; Suiko, M.; Hatakeyama, K.; Nemoto, T.; Morishita, K.; Kataoka, H.; Tsubouchi, H.; Nishiyama, K., Soy-derived isoflavones inhibit the growth of adult T-cell leukemia cells *in vitro* and *in vivo*. *Cancer Sci.* **2007**, *98*, 1740-1746.

62. Ishikawa, C.; Tafuku, S.; Kadekaru, T.; Sawada, S.; Tomita, M.; Okudaira, T.; Nakazato, T.; Toda, T.; Uchihara, J. N.; Taira, N.; Ohshiro, K.; Yasumoto, T.; Ohta, T.; Mori, N., Anti-adult T-cell leukemia effects of brown algae fucoxanthin and its deacetylated product, fucoxanthinol. *Int. J. Cancer* **2008**, *123*, 2702-2712.

63. Haneji, K.; Matsuda, T.; Tomita, M.; Kawakami, H.; Ohshiro, K.; Uchihara, J. N.; Masuda, M.; Takasu, N.; Tanaka, Y.; Ohta, T.; Mori, N., Fucoidan extracted from *Cladosiphon okamuranus* Tokida induces apoptosis of human T-cell leukemia virus type 1-infected T-cell lines and primary adult T-cell leukemia cells. *Nutr. Cancer* **2005**, *52*, 189-201.

64. Nakama, S.; Ishikawa, C.; Nakachi, S.; Mori, N., Anti-adult T-cell leukemia effects of Bidens pilosa. *Int. J. Oncol.* **2011**, *38*, 1163-1173.

65. Biron, C. A.; Brossay, L., NK cells and NKT cells in innate defense against viral infections. *Curr. Opin. Immunol.* **2001**, *13*, 458-464.

66. Levy, E. M.; Roberti, M. P.; Mordoh, J., Natural killer cells in human cancer: from biological functions to clinical applications. *J. Biomed. Biotechnol.* **2011**, *2011*, 676198.

67. Biron, C. A.; Nguyen, K. B.; Pien, G. C.; Cousens, L. P.; Salazar-Mather, T. P., Natural killer cells in antiviral defense: function and regulation by innate cytokines. *Annu. Rev. Immunol.* **1999**, *17*, 189-220.

68. Imai, K.; Matsuyama, S.; Miyake, S.; Suga, K.; Nakachi, K., Natural cytotoxic activity of peripheral-blood lymphocytes and cancer incidence: an 11-year follow-up study of a general population. *Lancet* **2000**, *356*, 1795-1799.

69. Evans, D. L.; Ten Have, T. R.; Douglas, S. D.; Gettes, D. R.; Morrison, M.; Chiappini, M. S.; Brinker-Spence, P.; Job, C.; Mercer, D. E.; Wang, Y. L.; Cruess, D.; Dube, B.; Dalen, E. A.; Brown, T.; Bauer, R.; Petitto, J. M., Association of depression with viral load, CD8 T lymphocytes, and natural killer cells in women with HIV infection. *Am. J. Psychiatry* **2002**, *159*, 1752-1759.

70. Shida, K.; Nomoto, K., Probiotics as efficient immunopotentiators: translational role in cancer prevention. *Indian J. Med. Res.* **2013**, *138*, 808-814.

71. Cho, Y. J.; Son, H. J.; Kim, K. S., A 14-week randomized, placebo-controlled, double-blind clinical trial to evaluate the efficacy and safety of ginseng polysaccharide (Y-75). *J. Transl. Med.* **2014**, *12*, 283.

72. Santos, M. S.; Gaziano, J. M.; Leka, L. S.; Beharka, A. A.; Hennekens, C. H.; Meydani, S. N., Beta-carotene-induced enhancement of natural killer cell activity in elderly men: an investigation of the role of cytokines. *Am. J. Clin. Nutr.* **1998**, *68*, 164-170.

73. Lee, J. B.; Shin, Y. O., Oligonol supplementation affects leukocyte and immune cell counts after heat loading in humans. *Nutrients* **2014**, *6*, 2466-2477.

74. Goto, H.; Sagitani, A.; Ashida, N.; Kato, S.; Hirota, T.; Shinoda, T.; Yamamoto, N., Anti-influenza virus effects of both live and non-live *Lactobacillus acidophilus* L-92 accompanied by the activation of innate immunity. *Br. J. Nutr.* **2013**, *110*, 1810-1818.

75. Masuda, Y.; Murata, Y.; Hayashi, M.; Nanba, H., Inhibitory effect of MD-Fraction on tumor metastasis: involvement of NK cell activation and suppression of intercellular adhesion molecule (ICAM)-1 expression in lung vascular endothelial cells. *Biol. Pharm. Bull.* **2008**, *31*, 1104-1108.

76. Miyoshi, I.; Kubonishi, I.; Yoshimoto, S.; Akagi, T.; Ohtsuki, Y.; Shiraishi, Y.; Nagata, K.; Hinuma, Y., Type C virus particles in a cord T-cell line derived by co-cultivating normal human cord leukocytes and human leukaemic T cells. *Nature* **1981**, *294*, 770-771.

77. Nagahama, K.; Eto, N.; Yamamori, K.; Nishiyama, K.; Sakakibara, Y.; Iwata, T.; Uchida, A.; Yoshihara, I.; Suiko, M., Efficient approach for simultaneous estimation of multiple health-promoting effects of foods. *J. Agric. Food Chem.* **2011**, *59*, 8575-8588.

78. Tominaga, H.; Ishiyama, M.; Ohseto, F.; Sasamoto, K.; Hamamoto, T.; Suzuki, K.; Watanabe, M., A water-soluble tetrazolium salt useful for colorimetric cell viability assay. *Anal. Commun.* **1999**, *36*, 47-50.

79. Chodon, D.; Ramamurty, N.; Sakthisekaran, D., Preliminary studies on induction of apoptosis by genistein on HepG2 cell line. *Toxicol. In Vitro* **2007**, *21*, 887-891.

80. Frey, R.; Li, J.; Singletary, K., Effects of genistein on cell proliferation and cell cycle arrest in nonneoplastic human mammary epithelial cells: involvement of Cdc2, $p21^{waf/cip1}$, $p27^{kip1}$, and Cdc25C expression. *Biochem. Pharmacol.* **2001**, *61*, 979-989.

81. Chang, K.; Kung, M.; Chow, N.; Su, S., Genistein arrests hepatoma cells at G2/M phase: involvement of ATM activation and upregulation of $p21^{waf1/cip1}$ and Wee1. *Biochem. Pharmacol.* **2004**, *67*, 717-726.

82. Su, S.; Chow, N.; Kung, M.; Hung, T.; Chang, K., Effects of soy isoflavones on apoptosis induction and G2-M arrest in human hepatoma cells involvement of caspase-3 activation, Bcl-2 and Bcl-XL downregulation, and Cdc2 kinase activity. *Nutr. Cancer* **2003**, *45*, 113-123.

83. Raschke, M.; Rowland, I.; Magee, P.; Pool-Zobel, B., Genistein protects prostate cells against hydrogen peroxide-induced DNA damage and induces expression of genes involved in the defence against oxidative stress. *Carcinogenesis* **2006**, *27*, 2322-2330.

84. Sierens, J.; Hartley, J.; Campbell, M.; Leathem, A.; Woodside, J., Effect of phytoestrogen and antioxidant supplementation on oxidative DNA damage assessed using the comet assay. *Mutat. Res.* **2001**, *485*, 169-176.

85. Wu, H.; Chan, W., Genistein protects methylglyoxal-induced oxidative DNA damage and cell injury in human mononuclear cells. *Toxicol. In Vitro* **2007**, *21*, 335-342.

86. Chan, W.; Yu, J., Inhibition of UV irradiation-induced oxidative stress and apoptotic biochemical changes in human epidermal carcinoma A431 cells by genistein. *J. Cell Biochem.* **2000**, *78*, 73-84.

87. Foti, P.; Erba, D.; Riso, P.; Spadafranca, A.; Criscuoli, F.; Testolin, G., Comparison between daidzein and genistein antioxidant activity in primary and cancer lymphocytes. *Arch. Biochem. Biophys.* **2005**, *433*, 421-427.

88. Liang, H.; Qiu, S.; Shen, J.; Sun, L.; Wang, J.; Bruce, I.; Xia, Q., Genistein attenuates oxidative stress and neuronal damage following transient global cerebral ischemia in rat hippocampus. *Neurosci. Lett.* **2008**, *438*, 116-120.

89. Wei, H.; Zhang, X.; Wang, Y.; Lebwohl, M., Inhibition of ultraviolet light-induced oxidative events in the skin and internal organs of hairless mice by isoflavone genistein. *Cancer Lett.* **2002**, *185*, 21-29.

90. Satoh, T.; Izumi, M.; Inukai, Y.; Tsutsumi, Y.; Nakayama, N.; Kosaka, K.; Shimojo, Y.; Kitajima, C.; Itoh, K.; Yokoi, T.; Shirasawa, T., Carnosic acid protects neuronal HT22 Cells through activation of the antioxidant-responsive element in free carboxylic acid- and catechol hydroxyl moieties-dependent manners. *Neurosci. Lett.* **2008**, *434*, 260-265.

91. Satoh, T.; Kosaka, K.; Itoh, K.; Kobayashi, A.; Yamamoto, M.; Shimojo, Y.; Kitajima, C.; Cui, J.; Kamins, J.; Okamoto, S.; Izumi, M.; Shirasawa, T.; Lipton, S., Carnosic acid, a catechol-type electrophilic compound, protects neurons both *in vitro* and *in vivo* through activation of the Keap1/Nrf2 pathway via S-alkylation of targeted cysteines on Keap1. *J. Neurochem.* **2008**, *104*, 1116-1131.

92. Ikeda, M.; Kato, N., Life style-related diseases of the digestive system: cell culture system for the screening of anti-hepatitis C virus (HCV) reagents: suppression of HCV replication by statins and synergistic action with interferon. *J. Pharmacol. Sci.* **2007**, *105*, 145-150.

93. Kim, S.; Peng, L.; Lin, W.; Choe, W.; Sakamoto, N.; Kato, N.; Ikeda, M.; Schreiber, S.; Chung, R., A cell-based, high-throughput screen for small molecule regulators of hepatitis C virus replication. *Gastroenterology* **2007**, *132*, 311-320.

94. Kapadia, S.; Chisari, F., Hepatitis C virus RNA replication is regulated by host geranylgeranylation and fatty acids. *Proc. Natl. Acad. Sci. U. S. A.* **2005**, *102*, 2561-2566.

95. Ye, J.; Wang, C.; Sumpter, R. J.; Brown, M.; Goldstein, J.; Gale, M. J., Disruption of hepatitis C virus RNA replication through inhibition of host protein geranylgeranylation. *Proc. Natl. Acad. Sci. U. S. A.* **2003**, *100*, 15865-15870.

96. Rumelhart, D. E.; Hinton, G. E.; Williams, R. J., Learning representations by back-propagating errors. *Nature* **1986**, *323*, 533-536.

97. Arab Chamjangali, M.; Beglari, M.; Bagherian, G., Prediction of cytotoxicity data (CC_{50}) of anti-HIV 5-phenyl-1-phenylamino-1*H*-imidazole derivatives by artificial neural network trained with Levenberg-Marquardt algorithm. *J. Mol. Graph. Model.* **2007**, *26*, 360-367.

98. Lim, C.; Fujiwara, S.; Yamashita, F.; Hashida, M., Prediction of human skin permeability using a combination of molecular orbital calculations and artificial neural network. *Biol. Pharm. Bull.* **2002**, *25*, 361-366.

99. Jaiswal, K.; Naik, P., Distinguishing compounds with anticancer activity by ANN using inductive QSAR descriptors. *Bioinformation* **2008**, *2*, 441-451.

100. Lara, J.; Wohlhueter, R.; Dimitrova, Z.; Khudyakov, Y., Artificial neural network for prediction of antigenic activity for a major conformational epitope in the hepatitis C virus NS3 protein. *Bioinformatics* **2008**, *24*, 1858-1864.

101. Cohen, G., Caspases: the executioners of apoptosis. *Biochem. J.* **1997**, *326 (Pt 1)*, 1-16.

102. Haupt, S.; Berger, M.; Goldberg, Z.; Haupt, Y., Apoptosis - the p53 network. *J. Cell Sci.* **2003**, *116*, 4077-4085.

103. Balkwill, F.; Mantovani, A., Inflammation and cancer: back to Virchow? *Lancet* **2001**, *357*, 539-545.

104. Sethi, G.; Sung, B.; Aggarwal, B., TNF: a master switch for inflammation to cancer. *Front. Biosci.* **2008**, *13*, 5094-5107.

105. Rose-John, S.; Scheller, J.; Elson, G.; Jones, S., Interleukin-6 biology is coordinated by membrane-bound and soluble receptors: role in inflammation and cancer. *J. Leukoc. Biol.* **2006**, *80*, 227-236.

106. Catalona, W.; Smith, D.; Ratliff, T.; Basler, J., Detection of organ-confined prostate cancer is increased through prostate-specific antigen-based screening. *JAMA* **1993**, *270*, 948-954.

107. Catalona, W.; Smith, D.; Wolfert, R.; Wang, T.; Rittenhouse, H.; Ratliff, T.; Nadler, R., Evaluation of percentage of free serum prostate-specific antigen to improve specificity of prostate cancer screening. *JAMA* **1995**, *274*, 1214-1220.

108. Oh, J.; Lotan, Y.; Gurnani, P.; Rosenblatt, K.; Gao, J., Prostate cancer biomarker discovery using high performance mass spectral serum profiling. *Comput. Methods Programs Biomed.* **2009**, *96*, 33-41.

109. Johnson, J.; Syed, D.; Heren, C.; Suh, Y.; Adhami, V.; Mukhtar, H., Carnosol, a dietary diterpene, displays growth inhibitory effects in human prostate cancer PC3 cells leading to G2-phase cell cycle arrest and targets the 5'-AMP-activated protein kinase (AMPK) pathway. *Pharm. Res.* **2008**, *25*, 2125-2134.

110. Dohnal, V.; Kuca, K.; Jun, D., What are artificial neural networks and what they can do? *Biomed. Pap. Med. Fac. Univ. Palacky Olomouc Czech. Repub.* **2005**, *149*, 221-4.

111. Winkler, D., Neural networks as robust tools in drug lead discovery and development. *Mol. Biotechnol.* **2004**, *27*, 139-168.

112. Huang, Y.; Kangas, L.; Rasco, B., Applications of artificial neural networks (ANNs) in food science. *Crit. Rev. Food Sci. Nutr.* **2007**, *47*, 113-126.

113. Li, C.; Feng, J.; Huang, W. Y.; An, X. T., Composition of Polyphenols and Antioxidant Activity of Rabbiteye Blueberry (*Vaccinium ashei*) in Nanjing. *J. Agric. Food Chem.* **2013**, *61*, 523-531.

114. Matsuo, Y.; Fujita, Y.; Ohnishi, S.; Tanaka, T.; Hirabaru, H.; Kai, T.; Sakaida, H.; Nishizono, S.; Kouno, I., Chemical constituents of the leaves of rabbiteye blueberry (*Vaccinium ashei*) and characterisation of polymeric proanthocyanidins containing phenylpropanoid units and A-type linkages. *Food Chem.* **2010**, *121*, 1073-1079.

115. Takami, Y.; Uto, H.; Takeshita, M.; Kai, H.; Akamatsu, E.; Moriuchi, A.; Hasegawa, S.; Oketani, M.; Ido, A.; Kataoka, H.; Tsubouchi, H., Proanthocyanidin derived from the leaves of

Vaccinium virgatum suppresses platelet-derived growth factor-induced proliferation of the human hepatic stellate cell line LI90. *Hepatol. Res.* **2010**, *40*, 337-345.

116. Inoue, N.; Nagao, K.; Nomura, S.; Shirouchi, B.; Inafuku, M.; Hirabaru, H.; Nakahara, N.; Nishizono, S.; Tanaka, T.; Yanagita, T., Effect of *Vaccinium ashei* reade leaf extracts on lipid metabolism in obese OLETF rats. *Biosci. Biotechnol. Biochem.* **2011**, *75*, 2304-2308.

117. Agarwal, C.; Sharma, Y.; Zhao, J.; Agarwal, R., A polyphenolic fraction from grape seeds causes irreversible growth inhibition of breast carcinoma MDA-MB468 cells by inhibiting mitogen-activated protein kinases activation and inducing G_1 arrest and differentiation. *Clin. Cancer Res.* **2000**, *6*, 2921-2930.

118. Carnésecchi, S.; Schneider, Y.; Lazarus, S. A.; Coehlo, D.; Gossé, F.; Raul, F., Flavanols and procyanidins of cocoa and chocolate inhibit growth and polyamine biosynthesis of human colonic cancer cells. *Cancer Lett.* **2002**, *175*, 147-155.

119. Kuo, P. L.; Hsu, Y. L.; Lin, T. C.; Lin, C. C., The antiproliferative activity of prodelphinidin B-2 3'-O-gallate from green tea leaf is through cell cycle arrest and Fas-mediated apoptotic pathway in A549 cells. *Food Chem. Toxicol.* **2005**, *43*, 315-323.

120. Singh, T.; Sharma, S. D.; Katiyar, S. K., Grape proanthocyanidins induce apoptosis by loss of mitochondrial membrane potential of human non-small cell lung cancer cells *in vitro* and *in vivo*. *PLoS One* **2011**, *6*, e27444.

121. Nagahama, K.; Eto, N.; Sakakibara, Y.; Matsusita, Y. I.; Sugamoto, K.; Morishita, K.; Suiko, M., Oligomeric proanthocyanidins from rabbiteye blueberry leaves inhibits the proliferation of human T-cell lymphotropic virus type 1-associated cell lines via apoptosis and cell cycle arrest. *J. Funct. Foods* **2014**, *6*, 356-366.

122. Folin, O.; Denis, W., A colorimetric method for the determination of phenols (and phenol derivatives) in urine. *J. Biol. Chem.* **1915**, *22*, 305-308.

123. Poiesz, B. J.; Ruscetti, F. W.; Gazdar, A. F.; Bunn, P. A.; Minna, J. D.; Gallo, R. C., Detection and isolation of type C retrovirus particles from fresh and cultured lymphocytes of a patient with cutaneous T-cell lymphoma. *Proc. Natl. Acad. Sci. U. S. A.* **1980**, *77*, 7415-7419.

124. Arima, N.; Molitor, J. A.; Smith, M. R.; Kim, J. H.; Daitoku, Y.; Greene, W. C., Human T-cell leukemia virus type I Tax induces expression of the Rel-related family of kappa B enhancer-binding proteins: evidence for a pretranslational component of regulation. *J. Virol.* **1991**, *65*, 6892-6899.

125. Maeda, M.; Shimizu, A.; Ikuta, K.; Okamoto, H.; Kashihara, M.; Uchiyama, T.; Honjo, T.; Yodoi, J., Origin of human T-lymphotrophic virus I-positive T cell lines in adult T cell leukemia. Analysis of T cell receptor gene rearrangement. *J. Exp. Med.* **1985**, *162*, 2169-2174.

126. Naczk, M.; Grant, S.; Zadernowski, R.; Barre, E., Protein precipitating capacity of phenolics of wild blueberry leaves and fruits. *Food Chem.* **2006**, *96*, 640-647.

127. Pop, C.; Salvesen, G. S., Human caspases: activation, specificity, and regulation. *J. Biol. Chem.* **2009**, *284*, 21777-21781.

128. Scaffidi, C.; Fulda, S.; Srinivasan, A.; Friesen, C.; Li, F.; Tomaselli, K. J.; Debatin, K. M.; Krammer, P. H.; Peter, M. E., Two CD95 (APO-1/Fas) signaling pathways. *EMBO J.* **1998**, *17*, 1675-1687.

129. Abbas, T.; Dutta, A., p21 in cancer: intricate networks and multiple activities. *Nat. Rev. Cancer* **2009**, *9*, 400-414.

130. Nandakumar, V.; Singh, T.; Katiyar, S. K., Multi-targeted prevention and therapy of cancer by proanthocyanidins. *Cancer Lett.* **2008**, *269*, 378-387.

131. Lizarraga, D.; Lozano, C.; Briedé, J. J.; van Delft, J. H.; Touriño, S.; Centelles, J. J.; Torres, J. L.; Cascante, M., The importance of polymerization and galloylation for the antiproliferative properties of procyanidin-rich natural extracts. *FEBS J.* **2007**, *274*, 4802-4811.

132. Sun, J.; Hai Liu, R., Cranberry phytochemical extracts induce cell cycle arrest and apoptosis in human MCF-7 breast cancer cells. *Cancer Lett.* **2006**, *241*, 124-134.

133. Kozikowski, A. P.; Tückmantel, W.; Böttcher, G.; Romanczyk, L. J., Studies in polyphenol chemistry and bioactivity. 4.(1) Synthesis of trimeric, tetrameric, pentameric, and higher oligomeric epicatechin-derived procyanidins having all-4beta,8-interflavan connectivity and their inhibition of cancer cell growth through cell cycle arrest. *J. Org. Chem.* **2003**, *68*, 1641-1658.

134. Kresty, L. A.; Howell, A. B.; Baird, M., Cranberry proanthocyanidins induce apoptosis and inhibit acid-induced proliferation of human esophageal adenocarcinoma cells. *J. Agric. Food Chem.* **2008**, *56*, 676-680.

135. Pierini, R.; Kroon, P. A.; Guyot, S.; Ivory, K.; Johnson, I. T.; Belshaw, N. J., Procyanidin effects on oesophageal adenocarcinoma cells strongly depend on flavan-3-ol degree of polymerization. *Mol. Nutr. Food Res.* **2008**, *52*, 1399-1407.

136. Meeran, S. M.; Katiyar, S. K., Grape seed proanthocyanidins promote apoptosis in human epidermoid carcinoma A431 cells through alterations in Cdki-Cdk-cyclin cascade, and caspase-3 activation via loss of mitochondrial membrane potential. *Exp. Dermatol.* **2007**, *16*, 405-415.

137. Prasad, R.; Katiyar, S. K., Bioactive phytochemical proanthocyanidins inhibit growth of head and neck squamous cell carcinoma cells by targeting multiple signaling molecules. *PLoS One* **2012**, *7*, e46404.

138. Prasad, R.; Vaid, M.; Katiyar, S. K., Grape proanthocyanidin inhibit pancreatic cancer cell growth *in vitro* and *in vivo* through induction of apoptosis and by targeting the PI3K/Akt pathway. *PLoS One* **2012**, *7*, e43064.

139. Roninson, I. B., Oncogenic functions of tumour suppressor $p21^{Waf1/Cip1/Sdi1}$: association with cell senescence and tumour-promoting activities of stromal fibroblasts. *Cancer Lett.* **2002**, *179*, 1-14.

140. Cazzalini, O.; Scovassi, A. I.; Savio, M.; Stivala, L. A.; Prosperi, E., Multiple roles of the cell cycle inhibitor p21(CDKN1A) in the DNA damage response. *Mutat Res* **2010**, *704*, 12-20.

141. Watanabe, M.; Nakahata, S.; Hamasaki, M.; Saito, Y.; Kawano, Y.; Hidaka, T.; Yamashita, K.; Umeki, K.; Taki, T.; Taniwaki, M.; Okayama, A.; Morishita, K., Downregulation of CDKN1A in adult T-cell leukemia/lymphoma despite overexpression of CDKN1A in human T-lymphotropic virus 1-infected cell lines. *J. Virol.* **2010**, *84*, 6966-6977.

142. Sohn, D.; Essmann, F.; Schulze-Osthoff, K.; Jänicke, R. U., p21 blocks irradiation-induced apoptosis downstream of mitochondria by inhibition of cyclin-dependent kinase-mediated caspase-9 activation. *Cancer Res.* **2006**, *66*, 11254-11262.

143. Matsuoka, M.; Jeang, K. T., Human T-cell leukaemia virus type 1 (HTLV-1) infectivity and cellular transformation. *Nat. Rev. Cancer* **2007**, *7*, 270-280.

144. Silbermann, K.; Grassmann, R., Human T cell leukemia virus type 1 Tax-induced signals in cell survival, proliferation, and transformation. *Signal Transduction* **2007**, *7*, 34-52.

145. Nakamura, Y., Isolation of p53-target genes and their functional analysis. *Cancer Sci.* **2004**, *95*, 7-11.

146. Shin, S.; Sung, B. J.; Cho, Y. S.; Kim, H. J.; Ha, N. C.; Hwang, J. I.; Chung, C. W.; Jung, Y. K.; Oh, B. H., An anti-apoptotic protein human survivin is a direct inhibitor of caspase-3 and -7. *Biochemistry* **2001**, *40*, 1117-1123.

147. Zhou, M.; Gu, L.; Li, F.; Zhu, Y.; Woods, W. G.; Findley, H. W., DNA damage induces a novel p53-survivin signaling pathway regulating cell cycle and apoptosis in acute lymphoblastic leukemia cells. *J. Pharmacol. Exp. Ther.* **2002**, *303*, 124-131.

148. Brown, L.; Boswell, S.; Raj, L.; Lee, S. W., Transcriptional targets of p53 that regulate cellular proliferation. *Crit. Rev. Eukaryot. Gene Expr.* **2007**, *17*, 73-85.

149. Lanoue, L.; Green, K. K.; Kwik-Uribe, C.; Keen, C. L., Dietary factors and the risk for acute infant leukemia: evaluating the effects of cocoa-derived flavanols on DNA topoisomerase activity. *Exp. Biol. Med. (Maywood)* **2010**, *235*, 77-89.

150. Srivastava, R. K., TRAIL/Apo-2L: mechanisms and clinical applications in cancer. *Neoplasia* **2001**, *3*, 535-546.

151. Zhang, L.; Fang, B., Mechanisms of resistance to TRAIL-induced apoptosis in cancer. *Cancer Gene Ther.* **2005**, *12*, 228-237.

152. Psahoulia, F. H.; Drosopoulos, K. G.; Doubravska, L.; Andera, L.; Pintzas, A., Quercetin enhances TRAIL-mediated apoptosis in colon cancer cells by inducing the accumulation of death receptors in lipid rafts. *Mol. Cancer Ther.* **2007**, *6*, 2591-2599.

153. Kauntz, H.; Bousserouel, S.; Gossé, F.; Raul, F., The flavonolignan silibinin potentiates TRAIL-induced apoptosis in human colon adenocarcinoma and in derived TRAIL-resistant metastatic cells. *Apoptosis* **2012**, *17*, 797-809.

154. Maldonado, M. E.; Bousserouel, S.; Gossé, F.; Lobstein, A.; Raul, F., Implication of NF-κB and p53 in the expression of TRAIL-death receptors and apoptosis by apple procyanidins in human metastatic SW620 cells. *Biomedica* **2010**, *30*, 577-586.

155. Maldonado-Celis, M. E.; Bousserouel, S.; Gossé, F.; Lobstein, A.; Raul, F., Apple procyanidins activate apoptotic signaling pathway in human colon adenocarcinoma cells by a lipid-raft independent mechanism. *Biochem. Biophys. Res. Commun.* **2009**, *388*, 372-376.

156. Bleumink, M.; Köhler, R.; Giaisi, M.; Proksch, P.; Krammer, P. H.; Li-Weber, M., Rocaglamide breaks TRAIL resistance in HTLV-1-associated adult T-cell leukemia/lymphoma by translational suppression of c-FLIP expression. *Cell Death Differ.* **2011**, *18*, 362-370.

157. Ding, J.; Polier, G.; Köhler, R.; Giaisi, M.; Krammer, P. H.; Li-Weber, M., Wogonin and related natural flavones overcome tumor necrosis factor-related apoptosis-inducing ligand (TRAIL) protein resistance of tumors by down-regulation of c-FLIP protein and up-regulation of TRAIL receptor 2 expression. *J. Biol. Chem.* **2012**, *287*, 641-649.

158. Shoji, T.; Masumoto, S.; Moriichi, N.; Akiyama, H.; Kanda, T.; Ohtake, Y.; Goda, Y., Apple procyanidin oligomers absorption in rats after oral administration: analysis of procyanidins in plasma using the porter method and high-performance liquid chromatography/tandem mass spectrometry. *J. Agric. Food Chem.* **2006**, *54*, 884-892.

159. García-Ramírez, B.; Fernandez-Larrea, J.; Salvadó, M. J.; Ardèvol, A.; Arola, L.; Bladé, C., Tetramethylated dimeric procyanidins are detected in rat plasma and liver early after oral administration of synthetic oligomeric procyanidins. *J. Agric. Food Chem.* **2006**, *54*, 2543-2551.

160. Ou, K.; Gu, L., Absorption and metabolism of proanthocyanidins. *J. Funct. Foods* **2014**, *7*, 43-53.

161. Powell, N. D.; Tarr, A. J.; Sheridan, J. F., Psychosocial stress and inflammation in cancer. *Brain. Behav. Immun.* **2013**, *30 Suppl*, S41-S47.

162. Glaser, R.; Kiecolt-Glaser, J. K., Stress-induced immune dysfunction: implications for health. *Nat. Rev. Immunol.* **2005**, *5*, 243-251.

163. Segerstrom, S. C.; Miller, G. E., Psychological stress and the human immune system: a meta-analytic study of 30 years of inquiry. *Psychol. Bull.* **2004**, *130*, 601-630.

164. Franchimont, D.; Galon, J.; Gadina, M.; Visconti, R.; Zhou, Y.; Aringer, M.; Frucht, D. M.; Chrousos, G. P.; O'Shea, J. J., Inhibition of Th1 immune response by glucocorticoids: dexamethasone selectively inhibits IL-12-induced Stat4 phosphorylation in T lymphocytes. *J. Immunol.* **2000**, *164*, 1768-1774.

165. Inagaki, N.; Miura, T.; Nakajima, T.; Yoshida, K.; Nagai, H.; Koda, A., Studies on the anti-allergic mechanism of glucocorticoids in mice. *J. Pharmacobiodyn.* **1992**, *15*, 581-587.

166. Planey, S. L.; Litwack, G., Glucocorticoid-induced apoptosis in lymphocytes. *Biochem. Biophys. Res. Commun.* **2000**, *279*, 307-312.

167. Krukowski, K.; Eddy, J.; Kosik, K. L.; Konley, T.; Janusek, L. W.; Mathews, H. L., Glucocorticoid dysregulation of natural killer cell function through epigenetic modification. *Brain. Behav. Immun.* **2011**, *25*, 239-249.

168. Schirra, M.; Palma, A.; D'Aquino, S.; Angioni, A.; Minello, E. V.; Melis, M.; Cabras, P., Influence of postharvest hot water treatment on nutritional and functional properties of kumquat (*Fortunella japonica* Lour. Swingle Cv. Ovale) fruit. *J. Agric. Food Chem.* **2008**, *56*, 455-460.

169. Agócs, A.; Nagy, V.; Szabó, Z.; Márk, L.; Ohmacht, R.; Deli, J., Comparative study on the carotenoid composition of the peel and the pulp of different citrus species. *Innov. Food Sci. Emerg. Technol.* **2007**, *8*, 390-394.

170. Wang, Y. C.; Chuang, Y. C.; Ku, Y. H., Quantitation of bioactive compounds in citrus fruits cultivated in Taiwan. *Food Chem.* **2007**, *102*, 1163-1171.

171. Peng, L. W.; Sheu, M. J.; Lin, L. Y.; Wu, C. T.; Chiang, H. M.; Lin, W. H.; Lee, M. C.; Chen, H. C., Effect of heat treatments on the essential oils of kumquat (*Fortunella margarita* Swingle). *Food Chem.* **2013**, *136*, 532-537.

172. Jayaprakasha, G. K.; Chidambara Murthy, K. N.; Etlinger, M.; Mantur, S. M.; Patil, B. S., Radical scavenging capacities and inhibition of human prostate (LNCaP) cell proliferation by *Fortunella margarita*. *Food Chem.* **2012**, *131*, 184-191.

173. Sadek, E. S.; Makris, D. P.; Kefalas, P., Polyphenolic composition and antioxidant characteristics of kumquat (*Fortunella margarita*) peel fractions. *Plant Foods Hum. Nutr.* **2009**, *64*, 297-302.

174. Barreca, D.; Bellocco, E.; Caristi, C.; Leuzzi, U.; Gattuso, G., Kumquat (*Fortunella japonica* Swingle) juice: Flavonoid distribution and antioxidant properties. *Food Res. Int.* **2011**, *44*, 2190-2197.

175. Tan, S.; Li, M.; Ding, X.; Fan, S.; Guo, L.; Gu, M.; Zhang, Y.; Feng, L.; Jiang, D.; Li, Y.; Xi, W.; Huang, C.; Zhou, Z., Effects of *Fortunella margarita* fruit extract on metabolic disorders in high-fat diet-induced obese C57BL/6 mice. *PLoS One* **2014**, *9*, e93510.

176. Wang, Y. W.; Zeng, W. C.; Xu, P. Y.; Lan, Y. J.; Zhu, R. X.; Zhong, K.; Huang, Y. N.; Gao, H., Chemical Composition and Antimicrobial Activity of the Essential Oil of Kumquat (*Fortunella crassifolia* Swingle) Peel. *Int. J. Mol. Sci.* **2012**, *13*, 3382-3393.

177. Nagahama, K.; Eto, N.; Shimojo, T.; Kondoh, T.; Nakahara, K.; Sakakibara, Y.; Fukui, K.; Suiko, M., Effect of kumquat (*Fortunella crassifolia*) pericarp on natural killer cell activity *in vitro* and *in vivo*. *Biosci Biotechnol Biochem* **2015**, (http://dx.doi.org/10.1080/09168451.2015.1025033) (in press).

178. Iwakabe, K.; Shimada, M.; Ohta, A.; Yahata, T.; Ohmi, Y.; Habu, S.; Nishimura, T., The restraint stress drives a shift in Th1/Th2 balance toward Th2-dominant immunity in mice. *Immunol. Lett.* **1998**, *62*, 39-43.

179. Neri, S.; Mariani, E.; Meneghetti, A.; Cattini, L.; Facchini, A., Calcein-acetyoxymethyl cytotoxicity assay: standardization of a method allowing additional analyses on recovered effector cells and supernatants. *Clin. Diagn. Lab. Immunol.* **2001**, *8*, 1131-1135.

180. Bryant, J.; Day, R.; Whiteside, T. L.; Herberman, R. B., Calculation of lytic units for the expression of cell-mediated cytotoxicity. *J. Immunol. Methods* **1992**, *146*, 91-103.

181. Li, Q.; Nakadai, A.; Matsushima, H.; Miyazaki, Y.; Krensky, A. M.; Kawada, T.; Morimoto, K., Phytoncides (wood essential oils) induce human natural killer cell activity. *Immunopharmacol. Immunotoxicol.* **2006**, *28*, 319-333.

182. Lin, C. C.; Yu, C. S.; Yang, J. S.; Lu, C. C.; Chiang, J. H.; Lin, J. P.; Kuo, C. L.; Chung, J. G., Chrysin, a natural and biologically active flavonoid, influences a murine leukemia model in vivo through enhancing populations of T-and B-cells, and promoting macrophage phagocytosis and NK cell cytotoxicity. *In Vivo* **2012**, *26*, 665-670.

183. Nishi, K.; Muranaka, A.; Nishimoto, S.; Kadota, A.; Sugahara, T., Immunostimulatory effect of β-cryptoxanthin *in vitro* and *in vivo*. *J. Funct. Foods* **2012**, *4*, 618-625.

184. Nishimoto, S.; Muranaka, A.; Nishi, K.; Kadota, A.; Sugahara, T., Immunomodulatory effects of citrus fruit auraptene *in vitro* and *in vivo*. *J. Funct. Foods* **2012**, *4*, 883-890.

185. Nishino, H.; Murakoshi, M.; Tokuda, H.; Satomi, Y., Cancer prevention by carotenoids. *Arch. Biochem. Biophys.* **2009**, *483*, 165-168.

186. Mannisto, S.; Smith-Warner, S. A.; Spiegelman, D.; Albanes, D.; Anderson, K.; van den Brandt, P. A.; Cerhan, J. R.; Colditz, G.; Feskanich, D.; Freudenheim, J. L.; Giovannucci, E.; Goldbohm, R. A.; Graham, S.; Miller, A. B.; Rohan, T. E.; Virtamo, J.; Willett, W. C.; Hunter, D.

J., Dietary carotenoids and risk of lung cancer in a pooled analysis of seven cohort studies. *Cancer Epidemiol. Biomarkers Prev.* **2004**, *13*, 40-48.

187. Boon, C. S.; McClements, D. J.; Weiss, J.; Decker, E. A., Factors influencing the chemical stability of carotenoids in foods. *Crit. Rev. Food Sci. Nutr.* **2010**, *50*, 515-532.

188. Leong, S. Y.; Oey, I., Effects of processing on anthocyanins, carotenoids and vitamin C in summer fruits and vegetables. *Food Chem.* **2012**, *133*, 1577-1587.

189. Li, Y. F.; He, R. R.; Tsoi, B.; Li, X. D.; Li, W. X.; Abe, K.; Kurihara, H., Anti-stress effects of carnosine on restraint-evoked immunocompromise in mice through spleen lymphocyte number maintenance. *PLoS One* **2012**, *7*, e33190.

190. Mellqvist, U. H.; Hansson, M.; Brune, M.; Dahlgren, C.; Hermodsson, S.; Hellstrand, K., Natural killer cell dysfunction and apoptosis induced by chronic myelogenous leukemia cells: role of reactive oxygen species and regulation by histamine. *Blood* **2000**, *96*, 1961-1968.

191. He, R. R.; Wang, M.; Wang, C. Z.; Chen, B. T.; Lu, C. N.; Yao, X. S.; Chen, J. X.; Kurihara, H., Protective effect of apple polyphenols against stress-provoked influenza viral infection in restraint mice. *J. Agric. Food Chem.* **2011**, *59*, 3730-3737.

192. Kurihara, H.; Koda, H.; Asami, S.; Kiso, Y.; Tanaka, T., Contribution of the antioxidative property of astaxanthin to its protective effect on the promotion of cancer metastasis in mice treated with restraint stress. *Life Sci.* **2002**, *70*, 2509-2520.

193. Tachibana, H.; Koga, K.; Fujimura, Y.; Yamada, K., A receptor for green tea polyphenol EGCG. *Nat. Struct. Mol. Biol.* **2004**, *11*, 380-381.

194. Fujimura, Y.; Umeda, D.; Yamada, K.; Tachibana, H., The impact of the 67kDa laminin receptor on both cell-surface binding and anti-allergic action of tea catechins. *Arch. Biochem. Biophys.* **2008**, *476*, 133-138.

195. Hong Byun, E.; Fujimura, Y.; Yamada, K.; Tachibana, H., TLR4 signaling inhibitory pathway induced by green tea polyphenol epigallocatechin-3-gallate through 67-kDa laminin receptor. *J. Immunol.* **2010**, *185*, 33-45.

196. Kamiie, J.; Ohtsuki, S.; Iwase, R.; Ohmine, K.; Katsukura, Y.; Yanai, K.; Sekine, Y.; Uchida, Y.; Ito, S.; Terasaki, T., Quantitative atlas of membrane transporter proteins: development and application of a highly sensitive simultaneous LC/MS/MS method combined with novel in-silico peptide selection criteria. *Pharm. Res.* **2008**, *25*, 1469-1483.

197. Fukushima, T.; Yamamori, K.; Yoshihara, I.; Nagahama, K., Feature extraction of protein expression levels based on classification of functional foods with SOM. *Artif. Life Robot.* **2009**, *13*, 543-546.